

Laboratory Evaluation to Increase Effectiveness of Field-Scale Soil Flushing in the Hanford 100 Areas

September 2021

JE Szecsody
NP Qafoku
AR Lawter
RD Mackley
HP Emerson
CT Resch

DISCLAIMER

This report was prepared as an account of work sponsored by an agency of the United States Government. Neither the United States Government nor any agency thereof, nor Battelle Memorial Institute, nor any of their employees, makes **any warranty, express or implied, or assumes any legal liability or responsibility for the accuracy, completeness, or usefulness of any information, apparatus, product, or process disclosed, or represents that its use would not infringe privately owned rights.** Reference herein to any specific commercial product, process, or service by trade name, trademark, manufacturer, or otherwise does not necessarily constitute or imply its endorsement, recommendation, or favoring by the United States Government or any agency thereof, or Battelle Memorial Institute. The views and opinions of authors expressed herein do not necessarily state or reflect those of the United States Government or any agency thereof.

PACIFIC NORTHWEST NATIONAL LABORATORY
operated by
BATTELLE
for the
UNITED STATES DEPARTMENT OF ENERGY
under Contract DE-AC05-76RL01830

Printed in the United States of America

Available to DOE and DOE contractors from the
Office of Scientific and Technical Information,
P.O. Box 62, Oak Ridge, TN 37831-0062;
ph: (865) 576-8401
fax: (865) 576-5728
email: reports@adonis.osti.gov

Available to the public from the National Technical Information Service
5301 Shawnee Rd., Alexandria, VA 22312
ph: (800) 553-NTIS (6847)
email: orders@ntis.gov <<https://www.ntis.gov/about>>
Online ordering: <http://www.ntis.gov>

Laboratory Evaluation to Increase Effectiveness of Field- Scale Soil Flushing in the Hanford 100 Areas

September 2021

JE Szecsody
NP Qafoku
AR Lawter
RD Mackley
HP Emerson
CT Resch

Prepared for
the U.S. Department of Energy
under Contract DE-AC05-76RL01830

Pacific Northwest National Laboratory
Richland, Washington 99354

Abstract

This laboratory study was initiated to develop an improved technical understanding of the key controlling geochemical and physical processes of mobilizing residual Cr(VI) in Hanford sediments to provide increased effectiveness in soil flushing activities planned for Hanford 100 Areas. This was accomplished by (1) quantifying Cr mass, release rate, and surface phase changes as Cr is leached from different Hanford sediments; (2) maximizing Cr leaching during soil flushing by evaluating different leach solutions and leach strategies; and (3) minimizing leaching of remaining residual Cr after soil flushing ends. To quantify geochemical controls on Cr leaching from sediments, sequential liquid extractions were used to identify aqueous, adsorbed, and solid Cr surface phases (precipitates or Cr incorporated into other phases) before and after water-saturated and unsaturated leach experiments with pH 8 artificial groundwater and with other amendment solutions. Changes in the Cr release rate from sediments were also correlated to changes in Cr surface phases. During unsaturated infiltration, water advection occurs primarily through larger pores, with less movement through smaller grain layers leading to a slower release of Cr trapped in smaller pores next to smaller grains. To quantify these physical controls on Cr leaching from sediments, 10-ft-high 1-D infiltration experiments were conducted at differing leach solution application rates, and Cr leaching during application and subsequent residual water flow was quantified. Qualitative 2-D experiments were also conducted to evaluate surfactant addition to increase flow in low-permeability zones.

Cr-contaminated Hanford sediments from the 100-H, 100-K, 100-D, and 200 East Areas exhibited a wide variety of leach behavior from rapid release of a small amount of Cr to fast (i.e., minutes) and slow (i.e., hours or more) release of high Cr. Sediments with low labile Cr ($< 0.2 \mu\text{g/g}$) exhibited fast Cr release but less overall release, and most ($>95\%$) leached from the sediments within a few pore volumes in water-saturated columns. With nearly no sorption of chromate, aqueous and sorbed Cr (as chromate) were released quickly from sediment within the first few pore volumes, resulting in high leach concentrations, fast initial Cr release rates, and changes in pre- and post-leach extractions. In contrast, sediments with high labile Cr (0.2 to $20 \mu\text{g/g}$) exhibited a combination of fast and slow Cr release due to multiple Cr surface phases contributing to Cr release from the sediment at different rates with greater overall release. This resulted in elevated Cr effluent concentrations even after dozens of pore volumes were leached. In addition, the Cr release rate decreased with increasing time during leaching. A decrease in labile Cr (aqueous Cr, adsorbed Cr, pH 5 acetate dissolved precipitates) in post-leach extractions compared to pre-leach extractions showed initial aqueous and adsorbed Cr release, followed by dissolution of high-solubility precipitates such as CaCrO_4 (if present), then slow dissolution of calcite that may contain some chromate and possibly BaCrO_4 . The labile Cr in all sediments correlated well with the Cr release rate ($r^2 = 0.81$). Labile Cr also correlated well with the leached mass in water-saturated columns ($r^2 = 0.98$), and therefore can be used for prediction of potential removal with flushing applications.

Leaching under unsaturated conditions was less efficient, with 21 to 64% Cr leached in the same time (or pore volumes) as water-saturated columns. Slower infiltration rates of the leach water resulted in greater mass of leached Cr. The sediments that contained low labile Cr and exhibited fast Cr release in water-saturated experiments required additional pore volumes to leach the Cr in unsaturated conditions. After water application stopped, residual water flow in the 10-ft-high columns had an increasingly smaller Cr flux for these sediments. In contrast, sediments with high labile Cr and both fast and slow Cr release were less efficiently leached in unsaturated conditions with just artificial groundwater. After the infiltrating leach water stopped, residual leaching at increasingly slower water flow rates also resulted in increasing Cr concentrations (by as much as 15x) because the longer sediment-water contact times allowed for greater Cr release from sediments, as shown by Cr release rates calculated from stop-flow events in water-saturated experiments. In the field, this would result in significant Cr flux to groundwater over an extended period of time after injection compared to sediments that exhibited only fast Cr release.

For the sediments that exhibited fast and slow Cr release, different leach solutions were evaluated to alter the Cr leach behavior. A weak acid solution (pH 6 or 5), which should dissolve calcite that may contain some chromate, was marginally effective at increasing Cr leaching during solution injection. Alternatively, the addition of an aqueous reductant, which should reduce and precipitate Cr, was highly effective at decreasing Cr leaching during residual water movement in infiltration experiments. However, both the acidic leach and the reductant leach solutions would be significantly less efficient at field scale as solutions would react with all of the sediment in the vadose zone prior to reaching the targeted zone, depending on the depth of contamination. The use of a surfactant to increase water flow in low-permeability layers was qualitatively demonstrated in 2-D infiltration experiments. Overall, experiments showed that characterization of the Cr mass and release rate differences between sediments could be used to design an efficient leach strategy at field scale. Homogeneous sediments that exhibited only fast Cr release could likely be efficiently leached with a single leach solution at a slow infiltration rate, with the treatment volume based on field scale simulations. In contrast, sediments that exhibited fast and slow Cr release would require either a different infiltration strategy such as multiple infiltration pulses over long periods of time or different leach solutions to increase Cr release rate during leach water infiltration and/or a reductant to decrease Cr release during the residual water flow times. The slow advection of water through low permeability layers that contain Cr would add additional slow Cr release. Field scale Cr leaching in these heterogeneous sediments would be increased with the use a surfactant, depending on the permeability of matrix and fine-grained layers. Simulation of the Cr flux in the 10-ft infiltration experiments with differing solutions and infiltration strategies to obtain water flux and Cr release rates over time can be used by site contractors to test different leach strategies at field scale in the 80- to 100-ft vadose zone to increase the efficiency of Cr leaching, adjust leach solution(s) used, and determine the time scale of pumping needed.

Future direction of this work includes expanding physical and chemical methods to increase Cr leaching efficiency by evaluating the following:

- Periodic flushing to increase short-term removal of residual Cr
- Different reductants, including Ca-polysulfide, to minimize long-term residual Cr leaching
- Use of different surfactants to increase water flow and Cr leaching in low-permeability zones
- Generic field-scale simulations to evaluate the time scale of residual Cr leaching for sediments that have only fast Cr release and sediments that have fast and slow Cr release
- effectiveness of using electrical resistivity methods to monitor chromate advection in unsaturated sediments

Acknowledgments

Funding for this work was provided by the U.S. Department of Energy Richland Operations Office under the Deep Vadose Zone – Applied Field Research Initiative. The Pacific Northwest National Laboratory is operated by Battelle Memorial Institute for the Department of Energy under Contract DE-AC05-76RL01830.

Acronyms and Abbreviations

AGW	artificial groundwater
chromate	CrO_4^{2-} , the predominant Cr(VI) aqueous species in oxic groundwater at $\text{pH} > 3$
Cr(III)	chromium species in the +3 valence state
Cr(VI)	chromium species in the +6 valence state
DOE	U.S. Department of Energy
HEIS	Hanford Environmental Information System
ICP-OES	inductively coupled plasma-optical emission spectrometry
NQAP	Nuclear Quality Assurance Program
P&T	pump and treat
PTFE	polytetrafluoroethylene
PVC	polyvinyl chloride

Contents

Abstract.....	iii
Acknowledgments.....	v
Acronyms and Abbreviations	vi
Contents	vii
1.0 Introduction.....	1.1
1.1 Current Chromium Concentrations at 100 Areas.....	1.2
1.2 100 Area Remedial Actions.....	1.2
1.3 Approach.....	1.3
2.0 Experimental.....	2.1
2.1 Sediments.....	2.1
2.2 Sequential Liquid Extractions for Total Cr and Cr(VI).....	2.2
2.3 1-D Water-Saturated Leach Experiments	2.3
2.4 1-D Unsaturated Leach Experiments.....	2.4
2.5 2-D Unsaturated Leach Experiments with Sediment Heterogeneities.....	2.7
2.6 Chromium and Metals Analysis.....	2.8
3.0 Results.....	3.1
3.1 Water-Saturated Cr Leaching from Hanford Sediments.....	3.3
3.2 Cr Leaching in Unsaturated Columns.....	3.7
3.2.1 Comparing Cr Leaching in Saturated and Unsaturated Systems.....	3.7
3.2.2 Residual Cr Flux to Groundwater.....	3.7
3.2.3 Influence of Water Application Rate on Unsaturated Cr Leaching.....	3.9
3.3 Influence of Amendments on Cr Leaching.....	3.9
3.3.1 Acidic Water to Increase Cr Leaching.....	3.9
3.3.2 Surfactant to Increase Cr Leaching through Low-K Lenses	3.12
3.3.3 Aqueous Reductant to Decrease Residual Chromate Leaching.....	3.13
3.4 Influence of Surfactant Addition on Unsaturated Cr Leaching in 2-D Heterogeneous Sediment Systems	3.16
4.0 Discussion.....	4.1
4.1 Cr Leached Mass in Different Solutions and Application Rates	4.1
4.2 Cr Surface Phases and Relationship to Leached Mass	4.3
4.3 Cr Release Rate from Sediments	4.5
5.0 Conclusions.....	5.1
6.0 Quality Assurance.....	6.1
7.0 References.....	7.1
Appendix A – Cr Water-Saturated Leaching by Groundwater.....	A.1
Appendix B – Cr Water-Saturated Leaching with Amendments.....	B.1
Appendix C – Cr Sequential Extractions of Sediments: Pre- and Post-Leach.....	C.1

Appendix D – Cr Unsaturated Leaching in Infiltration Experiments D.1
 Appendix E – 2-D Infiltration Experiments.....E.1

Figures

Figure 1.1. Chromate contamination in groundwater in the Hanford River Corridor. 1.1
 Figure 2.1. 10-ft high 1-D infiltration columns with effluent at bottom leading into fraction collectors located in vacuum chambers (left), and enlargement of the bottom of the column showing infiltration front (right). 2.6
 Figure 2.2. Infiltration column with low-conductivity rectangular inclusions. Artificial groundwater was dripped in the upper left and artificial groundwater with a surfactant was dripped into the sediment in the upper right. 2.7
 Figure 3.1. Chromate leaching in 1-D water-saturated column experiments and corresponding pre- and post-leach sequential extractions for sediments that exhibited mainly fast chromate release. 3.4
 Figure 3.2. Chromate leaching in 1-D water saturated column experiments and corresponding pre- and post-leach sequential extractions for sediments that exhibited fast and slow Cr release. 3.5
 Figure 3.3. Chromate leached mass and release rate for sediments leached with artificial groundwater. 3.6
 Figure 3.4. Chromate leaching in 1-D infiltration columns for sediment R28 (a and b) and sediment R25 (c)..... 3.8
 Figure 3.5. Change in chromate leach mass at different infiltration rates. 3.9
 Figure 3.6. Chromate leaching in 1-D water-saturated column experiments with acidic injection solutions. 3.11
 Figure 3.7. Change in chromate leach rate and mass with differing acidic treatments..... 3.11
 Figure 3.8. Change in chromate leach rate with the addition of a surfactant..... 3.12
 Figure 3.9. Chromate water-saturated leaching without and with a surfactant for sediment R17 (a) and sediment R5 (b)..... 3.13
 Figure 3.10. Chromate in unsaturated infiltration without and with a surfactant. 3.14
 Figure 3.11. Change in chromate leach rate with the addition of a reductant..... 3.15
 Figure 3.12. Chromate water-saturated leaching without and with a reductant for sediment R5..... 3.15
 Figure 3.13. Change in chromate leach mass with the addition of a reductant..... 3.16
 Figure 3.14. Comparison of groundwater infiltration (in upper left of each experiment) to groundwater with a surfactant (in upper right). 2-D systems had a medium to coarse Hanford sand matrix with inclusions composed of (a) fine (#70) sand, (b) thin silt lens, (c) thick silt lens, and (d) multiple inclusions of 70% silt, 30% clay (dark inclusions), and fine sand (light inclusions). 3.17
 Figure 4.1. Chromium flux out of the bottom of the 290-cm infiltration columns. 4.2
 Figure 4.2. Leachable chromium observed in water-saturated and unsaturated experiments for field-contaminated Hanford sediments. 4.3
 Figure 4.3. Relationship of leached Cr to (a) total extracted Cr, (b) labile Cr, and (c) extraction 3..... 4.4

Figure 4.4. Labile Cr extractions for pre- and post-leach sediments that received different treatments..... 4.5

Figure 4.5. Cr release rate from sediments leached with pH 8 groundwater as a function of (a) total Cr, and (b) labile Cr. 4.6

Tables

Table 2.1. Cr-contaminated sediments used in this study..... 2.1

Table 2.2. Artificial groundwater used in extraction 1 and in experiments. 2.2

Table 2.3. Sequential extraction solutions. 2.2

Table 2.4. Water-saturated and infiltration experiments..... 2.4

Table 2.5. 2-D infiltration experiments..... 2.8

Table 3.1. Cr sequential extractions on sediments before and after leach experiments..... 3.2

Table 3.2. Cr release rate change during water-saturated leaching calculated from stop flow..... 3.3

Table 3.3. Cr leached mass in water saturated and unsaturated systems. 3.7

Table 3.4. Change in chromate leach mass at different infiltration rate. 3.9

Table 3.5. Change in chromate leach mass using different weak acid solutions. 3.10

Table 3.6. Change in chromate leach mass with the addition of a surfactant. 3.12

Table 3.7. Change in chromate leach mass with the addition of a reductant. 3.14

1.0 Introduction

At the Hanford Site, in southeastern Washington State, multiple chromium (Cr) groundwater plumes exist in the 100 Areas adjacent to the Columbia River due to releases from historical corrosion inhibition use in nuclear reactors (Figure 1.1). The majority of the Cr exists in its oxidized [i.e., Cr(VI)] and a highly mobile form of chromate (CrO_4^{2-}) as Cr(VI), which has a higher toxicity than the reduced, mostly immobile, trivalent form of Cr(III). Although aqueous CrO_4^{2-} exhibits nearly no adsorption at neutral and alkaline pH in aquifers (Zachara et al. 1989; Qafoku et al. 2009), considerable chromate adsorption has been observed under acidic conditions (Dresel et al. 2008; Qafoku et al. 2010; Stanin 2005). Since high concentrations of dichromate were released under acidic conditions, chromate may have initially adsorbed to subsurface sediments, but as the acid was neutralized by reactions with sediments, chromate either precipitated with calcium or barium (Arcon et al. 2005; Palmer and Willbrodt 1991), coprecipitated with calcium carbonate (Robles-Camacho and Armenta 2000; Tang et al. 2007), or adsorbed to Mn, Al, and Fe oxides and clay minerals (Rai et al. 1989; Vermeul et al. 2004; Zachara et al. 1987).

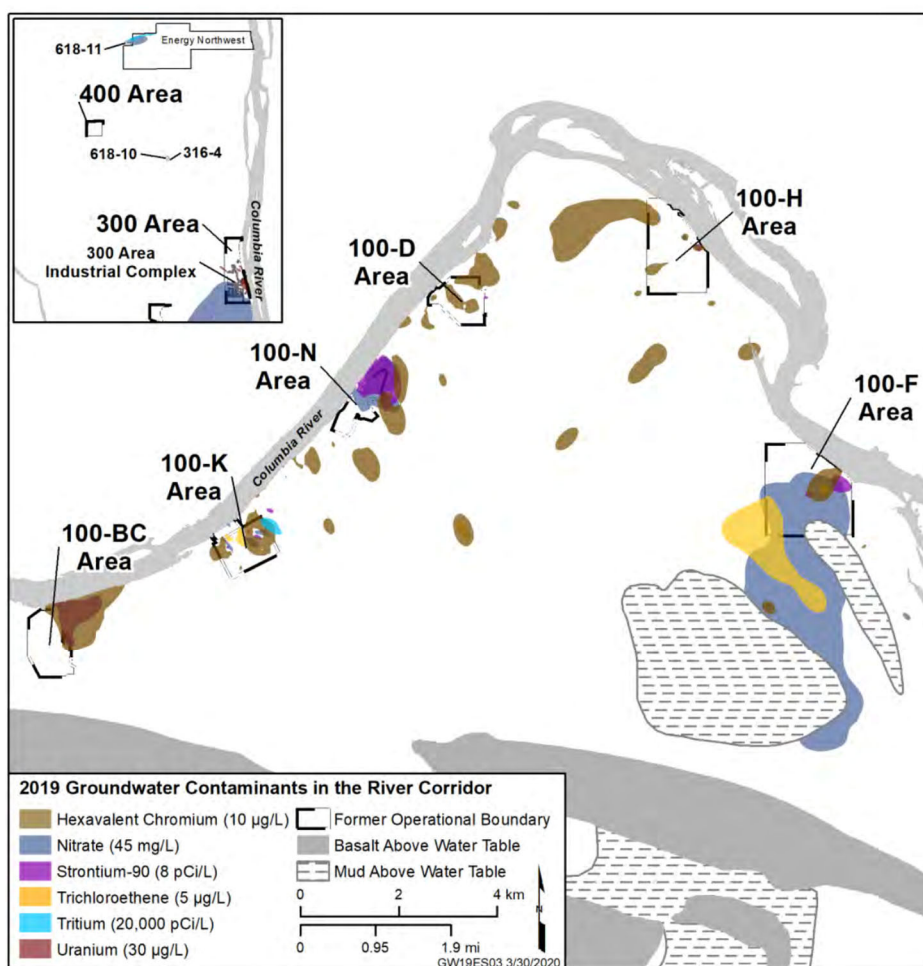


Figure 1.1. Chromate contamination in groundwater in the Hanford River Corridor.

1.1 Current Chromium Concentrations at 100 Areas

Given the slightly alkaline pH (7.7 to 8.3) and oxic conditions at Hanford, chromate is expected to move rapidly in the vadose zone and groundwater with minimal adsorption or geochemical reduction (Ginder-Vogel et al. 2005; Hu et al. 2007). Sites within the Columbia River Corridor can contain Cr concentrations as high as 230 µg/g (Qafoku et al. 2011), but the mobile, leachable Cr is correlated to specific high-solubility precipitates. Although natural Cr is present in sediments, it is a small fraction of the total immobile Cr. Sediment from the Hanford and Ringold formations are a combination of both basaltic and granitic rocks, with an average solid phase Cr concentration of 18.5 µg/g (DOE 1993) and only a small fraction (< 5%) of mobile Cr associated with high-solubility precipitates (Szecsody et al. 2017, 2019; Truex et al. 2017).

By contrast, anthropogenic Cr is present in higher fractions of the mobile phases than naturally occurring Cr. For example, vadose zone sediment samples have been collected in (1) near-surface contaminated sediments to 5-m depth exposed during remedial activities (100-C Area), (2) borehole sediments during characterization of deeper contamination in the 100-B Area (boreholes C5671 and C5674), and (3) shallow and deep contaminated sediments near contaminated areas in the 100-D Area (Dresel et al. 2008). A similar distribution of solid phase Cr was observed in all Cr release areas and was not related to Cr concentration or depth of collection. Solid phase Cr was associated with secondary mineral phases and clay inclusions within the sediment matrix, with Cr association with iron oxides [most likely magnetite, a redox sensitive mineral with structural Fe(II)] and as insoluble barium chromate (BaCrO₄). Chromium was also present in areas rich in aluminosilicates and/or iron-rich aluminosilicates (most likely ferroan, clinocllore, or biotite). The authors also hypothesized that surface iron may have reduced small quantities of Cr(VI), subsequently forming precipitates of Cr(III)-bearing minerals. However, Cr(VI) reduction to insoluble Cr(III) was neither significant nor complete, even in localized areas. The bulk solid phase associated Cr mass in all sediments was present as Cr(VI).

In another Hanford study, most of the Cr(VI) mass in the vadose zone sediments (>90%) was readily leached in laboratory columns, resulting in concentrations up to 187 mg/L Cr(VI) in column effluent (Szecsody et al. 2019). The highly soluble dissolving phase was most likely calcium chromate. Other relatively insoluble Cr(VI)-bearing phases may have contributed to slow Cr(VI) release over hundreds of hours. The source of Ca and Ba for the Cr(VI) precipitates was from mineral dissolution associated with the historical surface spills of Cr(VI) as an acidic dichromate solution. The mineral dissolution may have also triggered the release of Fe(II) from the Fe(II)-bearing minerals. This was observed in other studies conducted with simulated waste liquids that were highly alkaline or acidic (Qafoku et al. 2003, 2010, 2011). In acidic conditions, CrO₄²⁻ reduction occurs from Fe(II) in illite, montmorillonite (Szecsody et al. 2013), and iron oxides (Dong et al. 2003). Both the Hanford 100-B and 100-D studies emphasized that the persistence of Cr(VI) in the sediments and the large differences in released mass from different sediments were caused by dissolution of multiple Cr(VI)-bearing solids.

1.2 100 Area Remedial Actions

Current remediation efforts to address chromium include application of pump-and-treat (P&T) at the 100-D, 100-H, and 100-K Areas and monitored natural attenuation at the 100-F/IU Area, while remedy selection is still underway at the other 100 Areas (Truex et al. 2015). Whereas the P&T systems focus on mass removal, permeable reactive barriers have been used to reduce Cr flux to the river. This was accomplished by creating reducing environments to transform Cr(VI) to Cr(III). At 100-D, a combination of Na-dithionite and nano-ZVI abiotically reduced chromium, whereas Ca-polysulfide and polylactate reduced chromium abiotically and biotically, respectively (Patterson and Fendorf 1997). Although the P&T systems continue to remove Cr mass from the aquifer and the barriers reduced Cr flux to the river,

Cr(VI) contamination still persists, largely due to a dynamic water table driven by changes in river stage, coupled with a slow release of Cr from sediments in the vadose zone (Zachara et al. 2004; Truex et al. 2015; Szecsody et al. 2019).

Soil flushing is a technology that has the potential to remove Cr from sediments in the vadose zone. Soil flushing operates through the addition of water, and if necessary, an appropriate mobilizing agent to increase Cr mobilization in the vadose zone toward groundwater so it can be treated with a P&T system. Soil flushing is currently planned for the 100-K Area, but there are several uncertainties associated with its application, including quantifying geochemical controls of Cr transport behavior and the physical mechanisms controlling water migration through the vadose zone. Even in homogeneous sediment, infiltration of water occurs primarily through larger pores, and Cr trapped in smaller pores next to smaller grains migrates more slowly due to decreased flow. Low-permeability lenses that typically have a higher water content and greater aqueous Cr are more difficult to flush, as capillary forces tend to limit water migration through the lenses because infiltrating water tends to flow around low-permeability lenses. Efficient soil flushing of Cr out of the vadose zone needs to consider the infiltration rate and duration for Cr trapped in high-permeability sediments and possible amendments to better advect water through low-permeability zones.

Increased effectiveness and success in soil flushing activities will likely be achieved when field designs and operational approaches are based on an improved technical understanding of the key controlling geochemical and physical factors and processes of removing residual Cr(VI) in the aqueous, adsorbed, and solid phases from sediments. For example, Cr in 100-D sediments is known to be associated with carbonates, which leach Cr more slowly relative to 100-K area vadose sediments containing mainly aqueous and adsorbed Cr. Therefore, the purpose of this laboratory study is to develop an improved technical understanding of the key controlling geochemical and physical processes of mobilizing residual Cr(VI) in Hanford sediments by (1) characterizing solid phase associated Cr and leach rates from different Hanford sediments; (2) maximizing Cr leaching during soil flushing by evaluating the effects of leach rate, volume, and addition of amendments to increase leaching in homogeneous and heterogeneous sediments; and (3) minimizing leaching of remaining residual Cr after soil flushing ends.

1.3 Approach

The Cr association with different solid phases of vadose and saturated zone sediments is characterized by sequential liquid extractions and through water-saturated leach experiments to identify the rate at which Cr leaches from the sediment and the volume of flushing water needed to leach most of the Cr mass from the sediment. A chemical amendment (weak acid; pH 5 and pH 6 artificial groundwater) is also evaluated as a method to increase the efficiency of Cr soil flushing in homogeneous sediment by increasing the dissolution rate of calcite (or other carbonates), which likely contains some chromate.

The efficiency of Cr leaching in hydrologically unsaturated vs. saturated sediments is quantified by comparing 1-D water-saturated leach experiments to 1-D unsaturated leach experiments. Differing water leach rates applied to unsaturated leach experiments are used to quantify the Cr leach for different unsaturated flow rates. In previous studies, slower unsaturated water infiltration rates resulted in greater leaching of Cr (Qafoku et al. 2011) and uranium (Szecsody et al. 2012). Finally, 1-D and 2-D unsaturated leach experiments in heterogeneous systems containing Cr-laden low-permeability zones are conducted with and without the addition of a surfactant in the leach water to reduce the water surface tension and increase flow (and Cr flushing) through the low-permeability zones. Overall, these experiments provide a basis for correlating Cr present in different surface phases in the sediments (i.e., adsorbed, incorporated in calcite, iron oxides, or other precipitates) and the rate at which Cr is released from the sediment to be able to increase effectiveness of soil flushing at field scale.

Finally, to minimize Cr leaching from unsaturated sediments during residual water flow, the addition of a reductant (Na dithionite) was evaluated as a method to decrease Cr downward migration after soil flushing has ceased by reducing chromate to Cr(III)(OH)₃ or (Cr, Fe)(OH)₃ precipitates (Eary and Rai 1988; Loyaux-Lawniczak et al. 2000).

2.0 Experimental

2.1 Sediments

Cr-contaminated sediments used in this study were collected from previous studies from the vadose zone and saturated zones in the Hanford 100-H, 100-D, 100-K, and 200 East Areas (Table 2.1). Previous Cr characterization of the sediments, when available, was compared to sequential extractions and leaching conducted in this study. The mass of these sediments varied from 24 to 1400 g, so some sediments could be only used for a single water-saturated leach experiment and extractions. In addition, sediments that had high Cr mass were more extensively used. One synthetic sediment was also used (R30; Table 2.1). This sediment was made using roughly 40% gravel and 60% < 2-mm material from background (uncontaminated) boreholes in the Hanford 300 Area. Chromium in the sediment totaled 11.62 µg/g, with labile Cr of 0.013 µg/g. Additional chromium was added to the sediment in multiple Cr phases, including BaCrO₄ (Alfa Aesar; 14.43 µg/g Cr), CaCrO₄ (Alfa Aesar; 4.79 µg/g Cr), and laboratory-produced Cr-substituted calcite (0.42 µg/g Cr) for a total of 31.26 µg/g Cr. Sediments R17 through R21 previous characterization showed in sequential extractions that aqueous, adsorbed, pH 5 acetate, and pH 2.3 acetic acid extractable Cr was Cr(VI), and the 8 mol/L extractable Cr was nearly all Cr(III) (Szecsody et al., 2020a). X-ray adsorption near edge structure (XANES) analysis of a 100-K area vadose zone sediment (C9973, 85.2') showed mostly Cr(III), consistent with Cr in Fe oxides, with a small fraction Cr(VI), which is consistent with CaCrO₄ and chromate-substituted calcite (Szecsody et al., 2020b).

Table 2.1. Cr-contaminated sediments used in this study.

#	Area	Borehole/Depth	HEIS
R1	100H VZ	C9989 33-33.5	B3MPL5
R2	100H VZ	C9924 39-39.5'	B3MP10
R3	100H VZ	C9989 43-43.5'	B3MPM1
R4	100H VZ	C9987 32.5-33'	B3MP81
R28	100D VZ	100-D-104, 20', drain of 183-D yellow YS, YS2	
R29	100D VZ	100-D-104, 20', drain of 183-D brown, BS	
R5	100D Sat	C8953 82'	B2WL47
R6	100D Sat	C8954 109.6 - 111.2'	B2WLL3
R7	100D Sat	C8955 90.5 - 91	B2WKD2
R8	100D Sat	C8954 83.4'	B2WL32
R12	100D Sat	C8953 89.7 - 90.2'	B2WL47
R13	100D Sat	C8955 90.5 - 91'	B2WKD2
R17	100K VZ	D0090 92.5'	B3TDH6
R18	100K VZ	D0090 95'	B3TDJ2
R19	100K VZ	D0090 97.5'	B3TDJ3
R20	100K Sat	D0090 100'	B3TDJ4
R21	100K Sat	D0090 100-105'	B3TDD4
R22	200E T, S	C9507 94.1 - 95.1'. T19 14C	B361N1
R23	200E T, S	C9507 104.4 - 105.4' T19 16C	B35434
R24	200E T, S	C9507 137.1 - 138.1. T19 138'	B35461
R25	200 VZ S-13	C9513 131.5'	B3DCJ7
R26	200 VZ S-13	C9513 90.5'	B3DCJ2
R27	200 sat	C9602 375.8-376.5'	B37CD4
R30		Artificial sediment, multiple Cr phases	

2.2 Sequential Liquid Extractions for Total Cr and Cr(VI)

Sequential extractions were used to identify the aqueous, adsorbed, and differing precipitated Cr phases in the untreated and post-leach sediments. Other metals were also characterized in some extractions, including Ca, Mg, and Ba, which are associated with Cr precipitates including Cr-substituted calcite and Ba-chromate. Sequential liquid extractions have been used to evaluate contaminants present in different aqueous, adsorbed, and solid precipitates for metals including U, Ca, Cr, Cu, P, Fe, Mn, Al, and Si (Chao and Zao et al. 1983; Hall et al. 1996; Gleyzes et al. 2002; Sutherland and Tack 2002; Mossop and Davison 2003; Lerner et al. 2006). For most of the sediments evaluated, the total chromium phases were below the detection limits of X-ray diffraction (~0.5% of each mineral) and most other surface phase techniques, so sequential liquid extractions were used to operationally define changes in solid phases during leaching.

Table 2.2. Artificial groundwater used in extraction 1 and in experiments.

Constituent	Conc. (mg/L)	Mass for 1 L (g)
H ₂ SiO ₃ *nH ₂ O, silicic acid	15.3	0.0153
KCl, potassium chloride	8.20	0.0082
MgCO ₃ , magnesium carbonate	13.0	0.0130
NaCl, sodium chloride	15.0	0.0150
CaSO ₄ , calcium sulfate	67.0	0.0670
CaCO ₃ , calcium carbonate	150	0.1500

The six increasingly acidic sequential extractions were used for identifying Cr in different phases (Table 2.3) under the following conditions: extraction 1 for 1 h (aqueous Cr), extraction 2 for 1 h (adsorbed Cr fraction), extraction 3 for 1 h (rind-carbonate Cr fraction), extraction 4 for 5 days (total carbonate Cr fraction), extraction 5 for 1 h (Fe-oxide Cr fraction), and extraction 6 at 95°C for 3 h (hard-to-extract Cr fraction) (Truex et al. 2017). The first extraction consisted of mixing the sediment (1:2 sediment:water ratio in a 45-mL PTFE Teflon tube) with artificial groundwater (Table 2.2) for 1.0 h at 25°C. The sediment-water solution was then centrifuged at 3000 rpm for 10 min, and the liquid was drawn off the top of the sediment and filtered (0.45-µm nylon/PVDF) for analysis. The process was repeated for the second and third extractions. The fourth extraction consisted of mixing the sediment with extraction 4 solution for 5.0 days at 25°C, then centrifuging and filtering. The fifth extraction was reacted with the sediment for 1 h. Finally, the nitric acid extraction consisted of mixing the sediment for 3.0 h at 95°C, then centrifuging and filtering (0.45-µm PTFE). Extractions consisted of 3 to 5 g of pre- or post-leach sediment and 6 to 10 mL of extraction solution placed in 45-mL PTFE centrifuge tubes.

Table 2.3. Sequential extraction solutions.

Extraction #	Solution	Extraction Phases
1	Artificial groundwater	Aqueous Cr
2	0.5 mol/L Mg(NO ₃) ₂	Adsorbed Cr
3	0.5 mol/L Na-acetate (pH 5)	Rind-carbonate Cr
4	0.44 mol/L acetic acid, 0.20 mol/L Ca(NO ₃) ₂ (pH 2.3)	Total carbonate Cr
5	0.1 mol/L ammonium oxalate, 0.1 mol/L oxalic acid	Fe-oxide Cr
6	8 mol/L HNO ₃	Hard-to-extract Cr

2.3 1-D Water-Saturated Leach Experiments

Small water-saturated column experiments (1.6 cm diameter by 20 cm length) were used to identify the total mass of Cr leaching from the sediment and the rate of Cr release from the sediment (Table 2.3). These column experiments consisted of injecting artificial groundwater (Table 2.2) or other amendments into one end of the column at a constant flow rate to achieve a 2-h residence time for a total of 7.7 to 12 pore volumes. The residence time is defined as the time it takes for 1 pore volume of water to travel through the column, as measured by effluent volume. At the effluent end of the column, liquid samples were collected in sufficient number and frequency to measure the change in contaminant concentration (i.e., 30 for these experiments). Samples were automatically collected using a timed fraction collector (Isco Foxy 200), which contained 5-mL falcon tubes to collect effluent. Chromate (and other co-contaminants) typically leaches from the sediment at a high initial rate (i.e., at a high initial concentration, which decreases over time), then at a slower rate at later pore volumes. Because of this general breakthrough curve behavior, more effluent samples are collected in the first 2 pore volumes, with less frequent sample collection for subsequent pore volumes.

Some leach experiments also included the injection of 80 mg/L bromide as a conservative tracer. Other amendment solutions injected into the sediment columns to change the rate at which chromate leached included: (1) reductant solution, (2) weak acidic solutions (i.e., pH 6.0 and pH 5.0), and (3) a surfactant solution. The reductant solution consisted of 0.03 mol/L sodium dithionite and 0.12 mol/L potassium carbonate (pH 12) and was injected from 1.0 to 2.5 pore volumes (labeled “part reductant” in Table 2.3) or over all pore volumes (labeled “full reductant”). The weak acidic solutions consisted of artificial groundwater that was equilibrated to pH 6.0 or 5.0 over several days using a small addition of nitric acid. The surfactant solution consisted of 500 mg/L sodium lauryl sulfate $[\text{CH}_3(\text{CH}_2)_{11}(\text{OCH}_2\text{CH}_2)_n \text{OSO}_3\text{Na}]$.

Stop-flow events were additionally used in the 1-D leach experiments with durations ranging from 16 to 450 h without flow, providing time for chromate to dissolve from one or more surface phases into pore water (i.e., from diffusion from intraparticle pore space or time-dependent dissolution of precipitate phases or slow desorption). The stop-flow events were conducted for approximately 16 h (at 1 pore volume), 150 h (at 2.5 pore volumes), and 500 h (at 10 to 50 pore volumes). The different times were selected to target leaching of different chromate phases. Initially, aqueous and sorbed chromate was leached (i.e., < 1 pore volume), so the release rate from the sediment was relatively rapid (so a 16-h stop-flow is used). Over a larger number of pore volumes, chromate was released from dissolution of calcite, iron oxide, and potentially other phases, so longer stop-flow times were used. Operationally, initiating a stop-flow event involves turning off the pump, plugging both ends of the column (to prevent water movement out of the sediment column), and turning off the fraction collector. Ending a stop-flow event involved reconnecting the column to the pump, turning on the fraction collector, and then turning on the pump. The calculation of the contaminant release rate from sediment (μg contaminant/g of sediment/day) uses the change in contaminant effluent concentration before and after the stop-flow event, and the length of time of the stop-flow event. Sequential extractions were also conducted on the post-leach sediments to obtain mass balance on the Cr in the sediment.

Table 2.4. Water-saturated and infiltration experiments.

Sediment	Exp. #	Experiment Type	Injection Solution	Initial $v^{(a)}$ (cm/h)	Final $v^{(b)}$ (cm/h)
R18	S10	Water-sat. leach	pH 8 AGW	6.26	
	S14	Water-sat. leach	pH 6 AGW	4.99	
	S15	Water-sat. leach	Part reductant	6.57	
R1	S1	Water-sat. leach	pH 8 AGW	5.47	
R3	S9	Water-sat. leach	pH 8 AGW	5.73	
R22	S4	Water-sat. leach	pH 8 AGW	4.57	
R5	S2	Water-sat. leach	pH 8 AGW	5.61	
	S12	Water-sat. leach	pH 6 AGW	5.14	
	S13	Water-sat. leach	Part reductant ^(c)	4.71	
	S20	Water-sat. leach	Surfactant	4.61	
	S21	Water-sat. leach	Full reductant	4.66	
	J3	Unsat. infiltration	pH 8 AGW	12.2	0.042
R28	S18	Water-sat. leach	pH 8 AGW	5.19	
	J4	Unsat. infiltration	pH 8 AGW	10.05	0.0401
	J6	Unsat. infiltration	pH 8 AGW	47.41	0.00751
	J7	Unsat. infiltration	pH 8 AGW	5.26	0.0287
	J8	Unsat. infiltration	pH 8 AGW	16.51	0.0245
	J9	Unsat. infiltration	Full reductant ^(d)	55.76	0.00176
	J10	Unsat. infiltration	Surfactant	38.7	0.0043
R17	S3	Water-sat. leach	pH 8 AGW	5.04	
	S5	Water-sat. leach	pH 6 AGW	4.71	
	S6	Water-sat. leach	Surfactant	4.52	
	S7	Water-sat. leach	Part reductant ^(c)	5.16	
	S8	Water-sat. leach	pH 5 leach	3.93	
R25	S11	Water-sat. leach	pH 8 AGW	4.61	
	S16	Water-sat. leach	pH 6 AGW	4.4	
	S17	Water-sat. leach	Part reductant ^(c)	4.62	
	J5	Unsat. infiltration	pH 8 AGW	56.35	0.00102
R8	S19	Water-sat. leach	pH 8 AGW	6.05	
R30	S22	Water-sat. leach	pH 8 AGW	5.15	

(a) v = initial interstitial velocity (constant for water-saturated experiments)
 (b) v = final interstitial velocity during residual draining of infiltration experiment
 (c) 0.03 mol/L Na-dithionite + 0.12 mol/L K_2CO_3 injected at 1.0 to 2.5 pore volumes only
 (d) 0.03 mol/L Na-dithionite + 0.12 mol/L K_2CO_3 injected for all 10 pore volumes
 AGW = artificial groundwater

2.4 1-D Unsaturated Leach Experiments

Cr flushing in 1-D unsaturated leach experiments were used to approximate the soil flushing that occurs at field scale at less than saturated conditions. This unsaturated Cr flushing was compared to Cr flushing under water-saturated conditions. These leach experiments consist of infiltration of artificial groundwater or other amendments into a 9.5- to 10-ft-high by 1-in. inner diameter column filled with Cr-contaminated and uncontaminated Hanford formation sediments (Figure 2.1). At field scale, Cr contamination is typically at a specific depth interval and the remainder of the 80 to 100 ft of sediment in the vadose zone is not Cr contaminated. To approximate these conditions, the lowest 1.0 ft of the sediment column was packed with Cr-contaminated sediment and the remaining 8.5 to 9 ft of the column was filled with uncontaminated sediment. Because the grain size distribution of most Hanford formation sediments at field scale consisted of sandy gravel or gravely sand (with some silt), sediments used in these unsaturated

leach experiments were modified to include the gravel fraction. The uncontaminated Hanford formation sediment used in all experiments consisted of 44% gravel (2 mm to 12 mm), 39% sand, and 17% silt/clay from the Pasco gravel pit. The Cr-contaminated sediments consisted of selected < 2-mm sediments (Table 2.1) with 50% peak gravel added by weight. The upper size limit of the gravel added was 12 mm (1/2 in.) in order to fit in the 1.03-in. inner diameter schedule 40 clear PVC columns. Sediments had artificial groundwater initially added at 4% water content (g/g), which is an average field water content. The bottom of the sediment column contains a 30-micron woven nylon screen, a layer of coarse #16 sand, and a layer of #30 fine sand (Accusand, Utica, IL) next to the Cr-contaminated sediment. The sand layers enable water to drip out of the bottom of the column into a fraction collector.

The 1-D unsaturated leach experiments consisted of dripping artificial groundwater (or other amendments) at the top of the sediment column at a flow rate of 0.1 to 1.5 mL/min using a high performance liquid chromatography (HPLC) pump (Figure 2.1, blue HPLC pumps in upper left) for 5 to 50 h, and drip collection of water samples at the bottom of the sediment column was conducted for 100 to 600 h. The flow rate for collected samples was calculated from the weight of each sample collected and time of sampling. Sample times ranged from 4 min (for high infiltration rates of 1.0 mL/min) to 990 min after hundreds of hours of residual water dripping out of the column, as shown by the interstitial velocity change for these infiltration experiments in Table 2.3. Early 1-D experiments had a fraction collector mounted in a vacuum chamber and there was a porous plate with a 1-bar air entry value at the bottom of the column (Figure 2.1). Although liquid samples were collected by maintaining 0.5 bars of suction for the fraction collector chamber, the flow rate through the porous plate was too slow for the 1.0-mL/min infiltration rate, so collection of samples for the remaining tests was done by gravity dripping. The chromate concentration in effluent samples was measured by inductively coupled plasma-optical emission spectrometry (ICP-OES; Section 2.6). After all effluent samples were collected from the infiltration experiment, the column was sectioned and 10 samples were taken at differing depths to measure the final water content. Sequential extractions were also conducted on the post-leach Cr-contaminated sediment to obtain mass balance on the Cr in the sediment.

Given the change in volumetric flow rate of water at the bottom of the infiltration column over time and the chromate concentration, the chromate flux rate was calculated (i.e., in $\mu\text{g Cr h}^{-1} \text{cm}^{-2}$). This is the scalable chromate flux to groundwater at field scale, so the time it takes for the chromate flux to be insignificant is useful for field scale P&T operations. As shown in Section 3.0, sediments that exhibited both fast and slow Cr release from the sediment maintained significantly more Cr flux to groundwater over time than sediments that exhibited only fast Cr release. Although this 10-ft-high column showed residual water leaching for hundreds of hours, it is likely that field-scale soil leaching with 80- to 100-ft of vadose zone would take considerably longer. Simulations of the laboratory-scale water flux and Cr transport could be used in the future to approximate the time scale of water drainage and Cr flux to groundwater at field scale.



Figure 2.1. 10-ft high 1-D infiltration columns with effluent at bottom leading into fraction collectors located in vacuum chambers (left), and enlargement of the bottom of the column showing infiltration front (right).

2.5 2-D Unsaturated Leach Experiments with Sediment Heterogeneities

Two-dimensional infiltration experiments in systems with low-conductivity inclusions were conducted to demonstrate the change in water flow rate through inclusions with the addition of a surfactant. The rectangular inclusions varied in grain size from a medium sand to a clayey silt within a matrix sediment of coarse sand. The experiments were designed such that water would rapidly infiltrate through the coarse matrix sediment, then infiltrate slowly through or around fine-grained inclusions. The surfactant reduces the surface tension of the infiltrating water and should result in more rapid infiltration through inclusions. The purpose of these visual demonstrations is to illustrate whether surfactant addition would increase flow through low-conductivity inclusions, which may contain higher chromate concentrations, thus increasing soil flushing efficiency.

These infiltration experiments were conducted in a clear polycarbonate flow system that was 115 cm (45 in.) tall by 54 cm (21 in.) wide by 1.9 cm (3/4 in.) thick (Figure 2.2). Five 2-D infiltration experiments were conducted with differing inclusions, but all with a matrix of Hanford formation sediment that was a coarse sand (2 to 5 mm) with some silt and clay (Table 2.5). Inclusion porous media for these 2-D experiments varied from a medium sand (#20/30, Table 2.5) to silt with 23% clay. The details of inclusion size and depth are in Appendix E. Inclusion sediment for the fourth and fifth 2-D experiment was Hanford formation < 53- μ m size fraction with 20% vermiculite added. For the fifth experiment, the top half of the flow cell was packed with random-size lenses of low-conductivity sediment (< 53 μ m Hanford formation and #40-60 sand), and the bottom half of the flow cell was packed with rectangular inclusions. Water was dripped in the upper two corners of the flow cell at a rate of 10 mL/min and images were taken to show the differences in infiltration patterns of groundwater versus groundwater containing 500 mg/L surfactant (sodium laurel sulfate).



Figure 2.2. Infiltration column with low-conductivity rectangular inclusions. Artificial groundwater was dripped in the upper left and artificial groundwater with a surfactant was dripped into the sediment in the upper right.

Table 2.5. 2-D infiltration experiments

Exp #	Inclusion Sediment	Matrix Sediment
1	(2) #20/30 sand, (2) 30/40 sand, (2) 40/60 sand	Hanford Fm coarse sand
2	(2) #70 sand, (2) #7020 sand	Hanford Fm coarse sand
3	(8) Hanford formation silt with 3% clay	Hanford Fm coarse sand
4	(8) Hanford formation silt with 23% clay	Hanford Fm coarse sand
5	(4) Hanford formation silt with 23% clay	Hanford Fm coarse sand

2.6 Chromium and Metals Analysis

The chromium concentrations in the sequential extractions, water-saturated, and unsaturated leach experiments were analyzed for total Cr by ICP-OES with a detection limit of 0.2 µg /L (undiluted). For some amendments such as the Na-dithionite solution, dilution was necessary, so the detection limit was higher. Although inductively coupled plasma mass spectrometry has lower undiluted detection limits (~0.02 µg /L), all samples including groundwater need at least 100x dilution, which results in an actual detection limit higher than undiluted samples run by ICP-OES. A few other metals (Ba, Ca) were also analyzed in some extractions and leach experiments, as these metals complex with chromate in precipitates. The bromide tracer in leach experiments was quantified with ion chromatography. Bromide had a detection limit of 0.1 mg/L. As part of the ion chromatography analysis, other anions were also measured, which proved useful for some leach experiments containing elevated sulfate and nitrate concentrations.

3.0 Results

Key geochemical and physical processes controlling chromate leaching behavior in field-contaminated Hanford sediments were evaluated by (1) quantifying Cr mass, release rate, and surface phase changes as Cr is leached from different Hanford sediments; (2) maximizing Cr leaching during soil flushing by evaluating different leach solutions and leach strategies; and (3) minimizing leaching of remaining residual Cr after soil flushing ends. These objectives were accomplished with a series of 22 water-saturated experiments and 10 unsaturated infiltration experiments (Table 2.4), with a mass balance of Cr in the sediment from pre-leach sequential extractions, column leached mass, and post-leach sequential extractions (Table 3.1).

Chromate leaching mass was first evaluated in water-saturated columns using artificial groundwater injection (Section 0). Stop-flow events during these experiments were used to calculate the Cr release rate at different times during the leach experiments (Table 3.2). Unsaturated sediment columns (10 ft high) were then used to compare Cr leaching behavior at low water saturation with artificial groundwater (Section 3.2) to water-saturated behavior. Water-saturated and unsaturated experiments were then used as a baseline for comparison of Cr leaching behavior with differing amendments in the injection water (Section 3.3). Finally, 2-D experiments were conducted to evaluate the use of a surfactant to increase infiltrating water into and through low-permeability zones (Section 3.4).

Table 3.1. Cr sequential extractions on sediments before and after leach experiments.

Sed.	Experiment before Extr.	Extr. 1 (µg/g)	Extr. 2 (µg/g)	Extr. 3 (µg/g)	Extr. 4 (µg/g)	Extr. 5 (µg/g)	Extr. 6 (µg/g)	Total (µg/g)	Extr. 1-3 (µg/g)	Leached (µg/g)
R18	None	0.00739	0.00874	0.0255	2.512	1.782	11.89	16.22	0.0417	
	None	0.00746	0.00781	0.0327	1.792	1.283	12.02	15.15	0.0480	
	S10 pH 8 leach	0.000	0.00830	0.0273	1.429	1.386	12.33	15.18	0.0356	0.00033
	S14 pH 6 leach	0.000	0.00929	0.0302	2.267	1.489	12.26	16.06	0.0395	0.00110
	S15 red. leach	0.00290	0.00794	0.0874	3.480	1.392	10.08	15.05	0.0982	0.00394
R27	None	0.0206	0.0287	0.0334	0.119	0.045	5.674	5.922	0.0828	
	None	0.0215	0.0239	0.0414	0.178	0.060	5.384	5.709	0.0867	
	Leach ^(a)	0.0219	0.0129	0.0262	0.088	0.017	5.914	6.079	0.0609	0.0416
R1	None	0.00149	0.000	0.0644	0.504	0.668	10.38	11.61	0.0659	
	S1 pH 8 leach	0.00832	0.00890	0.0210	0.852	0.240	6.503	7.633	0.0382	0.00077
R3	None	0.00260	0.0114	0.0478	0.290	0.369	7.245	7.966	0.0618	
	S9 pH 8 leach	0.00938	0.0121	0.0257	0.672	0.123	5.910	6.753	0.0472	0.00237
R22	None	0.03890	0.000	0.000	0.000	0.000	2.976	3.014	0.0389	
	S4 pH 8 leach	0.00758	0.00896	0.0265	0.0852	0.0273	9.50	9.65	0.0430	0.00114
R5	None	0.217	1.20	0.857	2.919	1.373	11.40	17.96	2.271	
	S2 pH 8 leach	0.0711	0.0518	0.134	2.26	0.553	7.31	10.38	0.257	1.395
	S12 pH 6 leach	0.0430	0.0533	0.125	2.48	0.534	8.37	11.60	0.221	1.025
	S13 red. leach	0.0242	0.0218	0.188	2.15	0.448	7.25	10.09	0.234	0.977
	S20 surfact. leach	0.0084	0.150	0.216	0.493	0.319	2.76	3.95	0.374	0.495
	S21 red. leach	0.0000	0.0374	0.164	0.527	0.454	2.60	3.78	0.201	0.0982
	J3 pH 8 infiltrate	0.0603	0.0506	0.241	2.674	1.11	15.98	20.11	0.351	0.423
R28	None	0.0093	0.0135	0.0532	8.150	1.41	214.7	224.3	0.0760	
	None	0.0070	0.0133	0.0336	7.907	1.73	219.1	228.7	0.0539	
	S18 pH 8 leach	0.149	0.0250	0.139	2.872	3.67	215.2	222.0	0.314	0.0373
	J4 pH 8 infiltrate	0.108	0.0288	0.150	6.846	2.15	272.7	282.0	0.286	0.0331
	J6 pH 8 infiltrate	0.118	0.0252	0.127	2.159	2.58	178.3	183.3	0.270	0.0238
	J7 pH 8 infiltrate	0.168	0.0310	0.175	2.894	6.66	198.2	208.1	0.374	0.0338
	J8 pH 8 infiltrate	0.204	0.0286	0.184	2.025	8.15	231.8	242.4	0.416	0.0301
	J9 red. infiltrate	0.0118	0.0252	0.0599	6.17	1.41	175.9	183.5	0.0969	0.0050
	J10 surf. infiltrate	0.0195	0.0201	0.0455	4.92	4.98	143.0	153.0	0.0851	0.0400
		None	0.000	0.000	0.212	12.59	0.00	8.63	21.43	0.212
R17	S3 pH 8 leach	0.0093	0.0111	0.0265	1.602	1.21	14.13	16.99	0.0469	0.00083
	S5 pH 6 leach	0.0085	0.0113	0.0284	2.661	1.41	10.96	15.08	0.0483	0.00050
	S6 surfact. leach	0.0080	0.0099	0.0236	4.214	1.93	11.80	17.98	0.0415	0.0017
	S7 red. leach	0.0088	0.0080	0.0546	13.13	5.54	11.59	30.33	0.0714	0.00039
	S8 pH 5 leach	0.0077	0.0087	0.0265	9.667	2.41	10.69	22.81	0.0429	0.0019
R7	None	0.351	0.651	0.576	2.439	1.16	12.87	18.05	1.578	1.757 ^(b)
	None	0.240	0.509	0.845	5.410	4.380	31.73	43.11	1.594	
R25	S11 pH 8 leach	0.00659	0.0187	0.157	3.79	1.084	26.47	31.53	0.182	1.609
	S16 pH 6 leach	0.00947	0.0192	0.195	3.79	1.135	26.38	31.53	0.224	1.565
	S17 red. leach	0.0206	0.0086	0.187	5.49	1.304	24.18	31.19	0.216	1.072
	J5 pH 8 infiltrate	0.0316	0.0325	0.110	1.33	0.468	13.52	15.49	0.174	0.331
R8	None	0.6368	0.4802	0.2056	0.704	1.060	25.85	28.94	1.323	
	S19 pH 8 leach	0.179	0.0618	0.0928	0.0730	0.343	24.64	25.39	0.3340	1.114
R30	None	4.895	11.40	2.785	0.875	0.401	5.139	25.49	19.07	
	None	4.841	11.87	3.280	0.462	2.880	5.564	28.90	19.99	
	S22 pH 8 leach	0.202	0.976	0.821	0.989	0.257	5.577	8.821	1.998	16.61
R31	None	0.0034	0.0064	0.0030	2.205	1.488	8.284	11.61	0.013	

(a) Leach mass from Lee et al. 2017.

(b) Leach mass from Szecsody et al. 2019.

Table 3.2. Cr release rate change during water-saturated leaching calculated from stop flow.

Sed.	Exp. #	Inj. Solution	Cr Rel.			Cr Rel.			Pore Vol.	Cr Rel. Rate ³	Cum. Cr
			Pore Vol.	Rate ¹	Cum. Cr	Pore Vol.	Rate ²	Cum. Cr			
R1	S1	pH 8 AGW	1.12	1.40 x 10 ⁻²	5.37E-04	2.62	-3.35E-02	7.14E-04	9.56	6.56E-03	7.71E-04
R3	S9	pH 8 AGW	1.28	5.50 x 10 ⁻¹	1.76E-03	2.87	1.80E-01	2.24E-03	10.11	5.37E-02	2.37E-03
	S2	pH 8 AGW	1.01	3.88 x 10 ¹	1.16x10 ⁻¹	2.51	9.99E+01	7.80E-01	9.64	7.38E+00	1.35E+00
	S12	pH6 AGW	1.10	3.28 x 10 ²	4.15E-01	2.45	1.01E+02	9.48E-01	8.81	2.96E+00	1.02E+00
R5	S13	Part reductant	1.06	4.77 x 10 ²	3.39E-01	2.21	-2.58E+00	9.75E-01	9.35	9.20E-02	9.77E-01
	S21	Full reductant	0.97	-5.86	8.62E-02	2.23	-1.15E-01	9.82E-02	7.68	1.34E+00	9.98E-02
	S20	Surfactant	0.95	1.92 x 10 ²	2.91E-01	2.27	7.91E+00	4.85E-01	8.2	3.26E-01	4.95E-01
R8	S19	pH 8 AGW	1.29	9.97 x 10 ¹	5.23E-01	3.02	4.89E+01	9.66E-01	10.67	1.56E+01	1.11E+00
	S3	pH 8 AGW	1.04	7.63 x 10 ⁻²	6.18E-04	2.35	-7.10E-03	7.98E-04	8.74	6.36E-03	8.31E-04
	S5	pH 6 AGW	0.98	-7.43 x 10 ⁻²	5.01E-04	2.34	0.00E+00	5.01E-03	9.34	0.00E+00	5.01E-03
R17	S8	pH 5 AGW	0.82	6.24 x 10 ⁻¹	1.55E-03	2.11	-8.01E-03	1.87E-03	8.82	0.00E+00	1.87E-03
	S6	Surfactant	0.98	6.18 x 10 ⁻¹	1.51E-03	2.34	0.00E+00	1.65E-03	8.91	0.00E+00	1.65E-03
	S7	Part reductant	1.05	-7.89 x 10 ⁻²	2.38E-04	2.70	4.34E-02	3.86E-04	9.78	0.00E+00	3.86E-04
	S10	pH 8 AGW	1.38	0.00	2.80E-04	3.17	2.29E-03	2.85E-04	11.13	1.96E-02	3.26E-04
R18	S14	pH 6 AGW	1.20	-1.91 x 10 ⁻¹	8.48E-04	2.67	2.26E-03	1.01E-03	9.87	9.71E-04	1.10E-03
	S15	Part reductant	1.48	4.89 x 10 ⁻²	1.08E-03	2.98	7.34E-02	2.28E-03	12.11	9.72E-02	3.95E-03
R22	S4	pH 8 AGW	1.28	2.47 x 10 ⁻²	9.77E-04	2.56	-2.90E-03	1.10E-03	8.36	8.54E-03	1.11E-03
	S11	pH 8 AGW	1.01	4.80 x 10 ¹	1.46E+00	2.30	1.04E+01	1.59E+00	8.16	1.60E+00	1.61E+00
R25	S16	pH 6 AGW	0.93	5.76 x 10 ¹	1.36E+00	2.22	1.76E+01	1.54E+00	8.45	2.08E+00	1.57E+00
	S17	Part reductant	0.87	6.02 x 10 ¹	9.90E-01	1.98	1.25E+00	1.06E+00	7.82	1.11E-01	1.07E+00
R28	S18	pH 8 AGW	1.08	-7.57	2.02E-02	2.39	-1.22E+00	2.84E-02	8.91	-1.55E-02	3.73E-02
R30	S22	pH 8 AGW	1.08	1.39 x 10 ²	4.56E+00	2.48	6.58E+01	9.30E+00	8.87	2.85E+01	1.39E+01

¹ stop flow times at 1 pore volume ranged from 38 to 89 h

² stop flow times at 2.5 pore volumes ranged from 96 to 186 h

³ stop flow times at 10 pore volumes ranged from 280 to 523 h

3.1 Water-Saturated Cr Leaching from Hanford Sediments

Most of the Cr leach experiments showed the maximum peak concentration (and bulk of mass) released within the first pore volume of water injected. Sediments that had Cr in phases that were quickly released (i.e., aqueous Cr, adsorbed Cr, in high-solubility precipitates such as CaCrO₄) showed little additional Cr released after 2 pore volumes and also showed no increase in Cr concentration after stop-flow events. In contrast, sediments that had additional Cr in phases that slowly dissolved (CrO₄-substituted calcite, BaCrO₄) showed elevated Cr concentrations over most pore volumes and had elevated Cr concentrations after stop-flow events. Water-saturated leach results for all sediments are shown in Appendix A and Table 2.4, and sequential extractions (pre- and post-leach) in Appendix C. Examples of sediments that leached chromate rapidly within the first few pore volumes were mainly the result of chromate present primarily in aqueous and adsorbed phases (Figure 3.1). For the three sediments shown, chromate leached from the sediment only within the first 2.5 pore volumes, with low or background Cr from 2.5 to 10 pore volumes. Stop-flow events (shown with red arrows) also showed none to low Cr concentration increase after the stop flow, which indicates after the initial high aqueous and adsorbed Cr flushing, there is very little additional release of Cr from the sediment. Most sediments contained significant natural Cr (shown in the the next section), but leaching generally showed that natural Cr did not leach. Sequential extractions in some cases, showed that the first three extractions (i.e., aqueous, adsorbed, pH 5 dissolvable) was roughly equivalent to the leached Cr mass after 10 pore volumes (shown in Figure 3.1a and b).

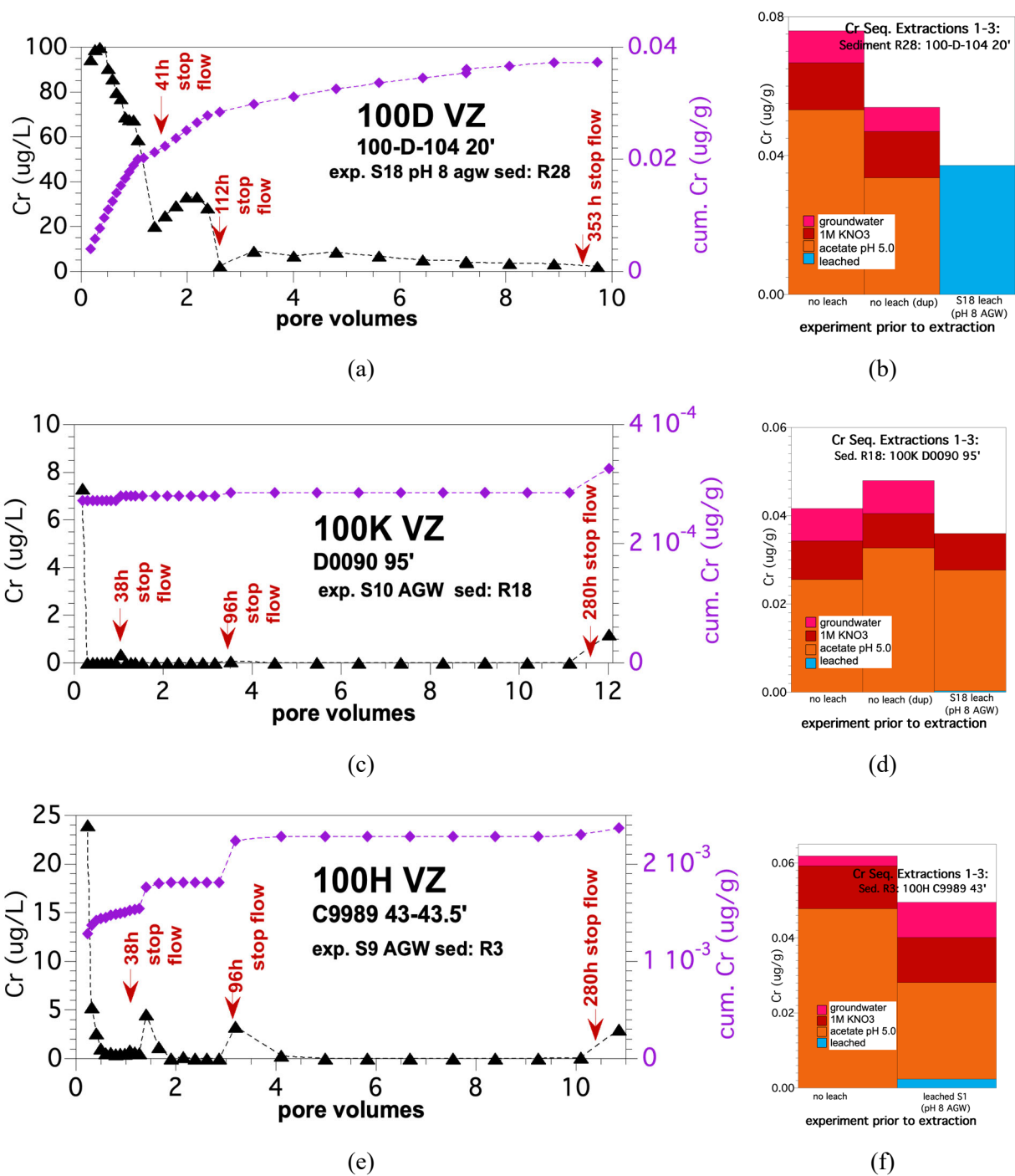


Figure 3.1. Chromate leaching in 1-D water-saturated column experiments and corresponding pre- and post-leach sequential extractions for sediments that exhibited mainly fast chromate release.

Examples of three sediments that exhibited both fast and slow Cr release had initial peak concentrations of 1000 to 10,000 $\mu\text{g/L}$ (Figure 3.2) and all had additional high-concentration peaks after stop-flow events. Sequential extractions before leaching showed that the first three extractions (aqueous, adsorbed, and pH 5 dissolvable) correlated with the mass of Cr leached within the 10 pore volumes [i.e., leached fraction (blue) in the second and third bars of each] were equivalent to the total of the three extractions in

the first bar of each]. For the first and third leach experiments (sediments R8 and R25, Figure 3.3), the initial concentration was the highest Cr concentration leached. In contrast, sediment R5's initial peak concentration of 1000 $\mu\text{g/L}$ was exceeded by a second Cr peak of 3900 $\mu\text{g/L}$ at 1.5 pore volumes, which followed a stop-flow event. There were also additional co-contaminants nitrate and sulfate that eluted at this time (Appendix A), so dissolution of co-contaminant phases might have contributed to the slow Cr release by coating some Cr surface phases.

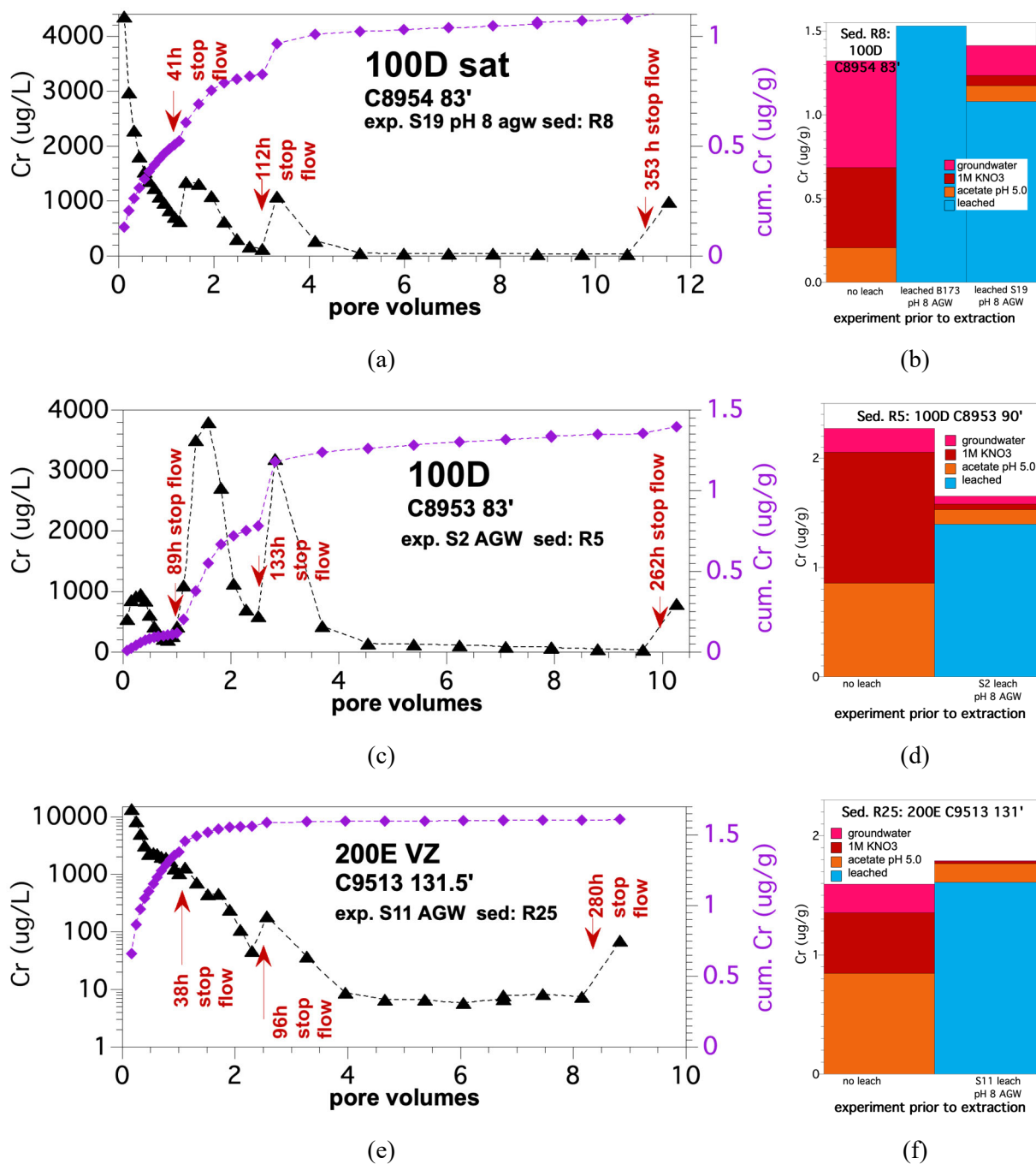


Figure 3.2. Chromate leaching in 1-D water saturated column experiments and corresponding pre- and post-leach sequential extractions for sediments that exhibited fast and slow Cr release.

Although a total of nine different field-contaminated sediments were evaluated for Cr release rate and mass, trends showed that sediments with low labile Cr released the Cr quickly, so a simple 10 pore volume leach would flush Cr from these sediments. But these sediments are unlikely to release Cr at field scale due to concentrations of leachable Cr, which were only slightly above natural Cr. Sediments with high Cr mass exhibited more complex behavior as the Cr was present in multiple surface phases, which resulted in the bulk of Cr releasing quickly but continued to leach for many pore volumes. Although only 10 to 12 pore volumes were used in this study, Szecsody et al. (2019) demonstrated that this sediment was leached for 100 pore volumes and continued to show slow Cr release after a stop-flow event (Figure 3.3). The sediments with significant Cr mass are likely to be leached and release Cr at field scale, but results showed a simple 10 pore volume leach is insufficient to remove most of the labile Cr mass. Therefore, differing amendments were evaluated for their efficiency at either increasing the Cr release rate or reducing/precipitating Cr(III) phases to decrease leaching, as described in the following sections.

Chromate leached from Hanford sediments at different rates that indicated chromate was present in different surface phases included (1) aqueous chromate, (2) adsorbed chromate, and (3) one or more precipitate phases. For nine field-contaminated Hanford sediments, leaching using artificial groundwater at pH 8 showed that the Cr leached mass and rate varied by 4 to 5 orders of magnitude. There was a correlation between sediment-Cr released mass and rate, where sediments with higher Cr mass released it at more rapid rates (Figure 3.3), likely due to sediments with higher Cr concentrations having a greater fraction of anthropogenic Cr mass, which is in more easily released phases. The three Hanford sediments with high Cr mass (R5 in exp. S2, R8 in S19, R25 in exp. S11, Table 2.4) released > 1 µg/g of Cr at rates that were 1 to 5 orders of magnitude greater than sediments with low Cr mass. Sediment R30 (leach experiment S22) is a synthetic sediment composed of Hanford formation sediment with additions of CaCrO₄, Cr-substituted calcite, and BaCrO₄. This sediment showed similar Cr release rates to the other field-contaminated sediment, but with greater leached mass.

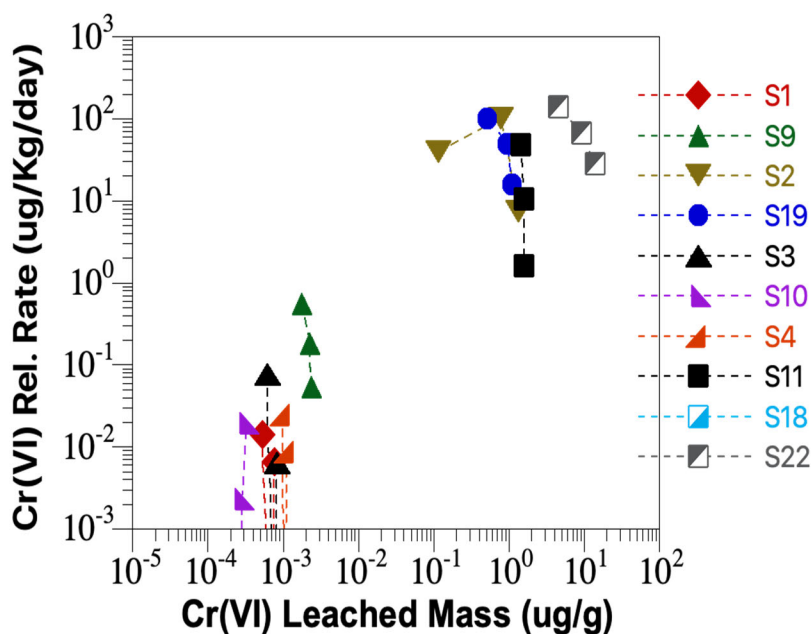


Figure 3.3. Chromate leached mass and release rate for sediments leached with artificial groundwater.

3.2 Cr Leaching in Unsaturated Columns

3.2.1 Comparing Cr Leaching in Saturated and Unsaturated Systems

Water infiltration through sediments at less than water-saturated conditions typically advects through larger pores, although capillary forces can move water into smaller pores. In contrast, water advects through most pores under water-saturated pressure-driven conditions. Therefore, because only grain surfaces of larger pores are in contact with infiltrating water, leaching of contaminants through unsaturated sediments tends to be less efficient than under water-saturated conditions. For three sediments (R5, R25, R28), unsaturated leach experiments resulted in 30%, 21%, and 64% leached Cr mass relative to water-saturated leaching (respectively, Table 3.3). There were differences between water-saturated and unsaturated columns, but sediment-leach water contact times were approximately the same (i.e., ~500 h including stop-flow events for saturated columns and ~430 h for unsaturated infiltration experiments). This is consistent with the hypothesis that leaching contaminants from sediment surfaces is less efficient in unsaturated conditions.

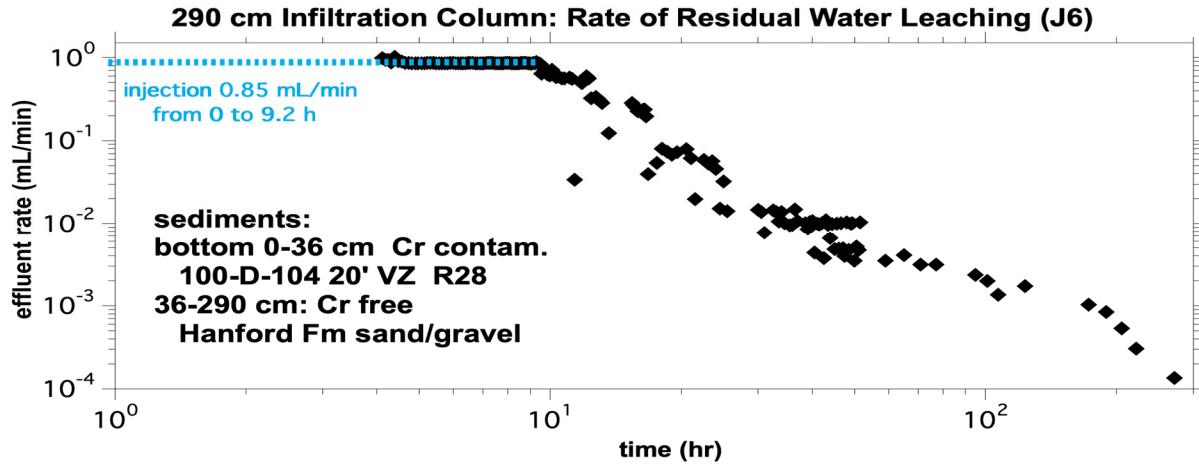
Table 3.3. Cr leached mass in water saturated and unsaturated systems.

Sed.	Exp. #	Solution	Leached (µg/g)
R5	S2	pH 8 AGW	1.395
	J3 infil.	pH 8 AGW	0.423
R25	S11	pH 8 AGW	1.61
	J5 infil.	pH 8 AGW	0.331
R28	S18	pH 8 AGW	0.0373
	J6 infil.	pH 8 AGW	0.0238

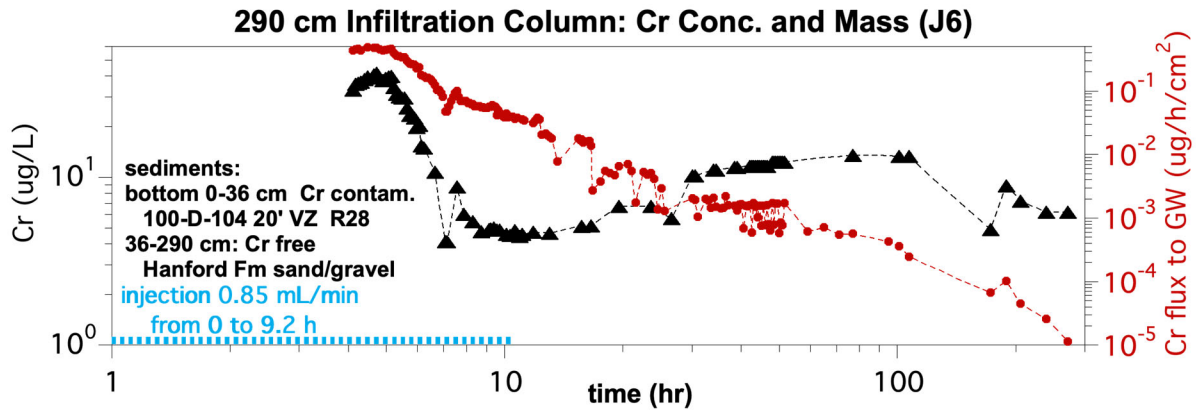
3.2.2 Residual Cr Flux to Groundwater

Water flow in these infiltration experiments was constant only during the times in which water was injected at the sediment surface. For example, an infiltration experiment (J6) had water injected at 0.85 mL/min for the first 8.5 h (blue dashed line in Figure 3.4a), but then during the following 300 h (with no additional water injection at the surface), water continued to leach from the column bottom at a slower rate over time. This represents the water flux to groundwater at field scale. The Cr concentration was initially high, peaking at 5 h (Figure 3.4b, black triangles), then decreased by 10-20 h. However, at the increasingly slower water flow rates (i.e., higher sediment-water contact times), the chromate concentration increased slightly, from 4 µg/L to 15 µg/L. The resulting Cr flux to groundwater decreased by orders of magnitude over time (red circles, Figure 3.4b). In this case, Cr in the residual leaching is inconsequential in this 10-ft-high laboratory column, so it is likely to be minimal at field scale. In contrast, for a sediment that exhibits both fast and slow Cr release (sediment R25), during residual water leaching, the chromate concentration increased considerably from 3.5 µg/L at 10 h to 43 µg/L by 200 h (Figure 3.4c). In this case, the Cr flux to groundwater from 10 to 80 h decreases only slightly, as the increasing Cr concentration is nearly offsetting the decrease in water flux.

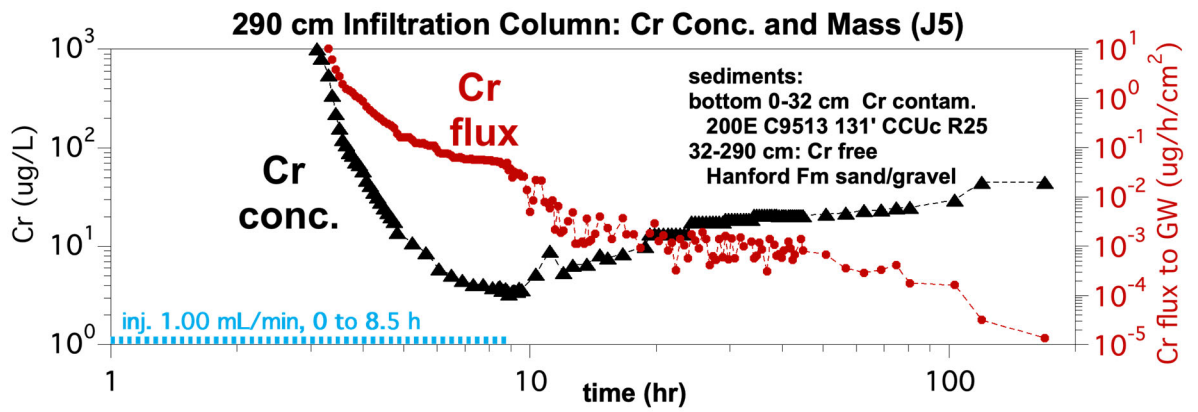
Overall, all eight infiltration experiments showed differences in the Cr flux because of the difference in Cr release rate of the sediment, infiltration rate, and amendments added (Appendix C). Sediments with higher sustained flux during residual water flow exhibited fast and slow Cr release from sediments. It is likely, however, that residual Cr would continue to leach to groundwater for months, and sediments that exhibit slow Cr release would require a different leach strategy such as a reductant addition, as described in Section 3.3.3.



(a)



(b)



(c)

Figure 3.4. Chromate leaching in 1-D infiltration columns for sediment R28 (a and b) and sediment R25 (c)

3.2.3 Influence of Water Application Rate on Unsaturated Cr Leaching

As described earlier, water advection in unsaturated flow conditions occurs through larger pores, and water diffuses into smaller pores driven by capillary forces. Experiments were conducted to evaluate the influence of the infiltration rate on Cr leaching, as slower infiltration rates should access a greater fraction of pores. Four infiltration experiments were conducted at different infiltration rates with a single sediment (Table 3.4). For comparison, the water-saturated sediment leached 0.0373 $\mu\text{g/g}$, and all unsaturated infiltration experiments leached less Cr mass. The leached mass was a function of the infiltration rate, with the slowest infiltration rate (experiment J7) leaching 91% of the water-saturated leach Cr mass (experiment S18). In contrast, at the most rapid infiltration rate leaching 64% of the water saturated leached Cr mass. A plot of the cumulative leached Cr mass for the different infiltration rates shows the systematic increase in Cr leaching at slower infiltration rates (Figure 3.5). Based on these results, slower infiltration is recommended at field scale, although the maximum infiltration rate is likely controlled by the uptake rate of the surface sediment. Effluent samples were filtered, so any colloidal Cr transport effects that might occur at faster flow rates was not observed.

Table 3.4. Change in chromate leach mass at different infiltration rate.

Sed.	Exp. #	Initial Vel. (cm/h)	Leached ($\mu\text{g/g}$)
	S18 sat.	12.5	0.0373
	J7 infil.	5.26	0.0338
R28	J4 infil.	10.05	0.0331
	J8 infil.	16.51	0.0301
	J6 infil.	47.41	0.0238

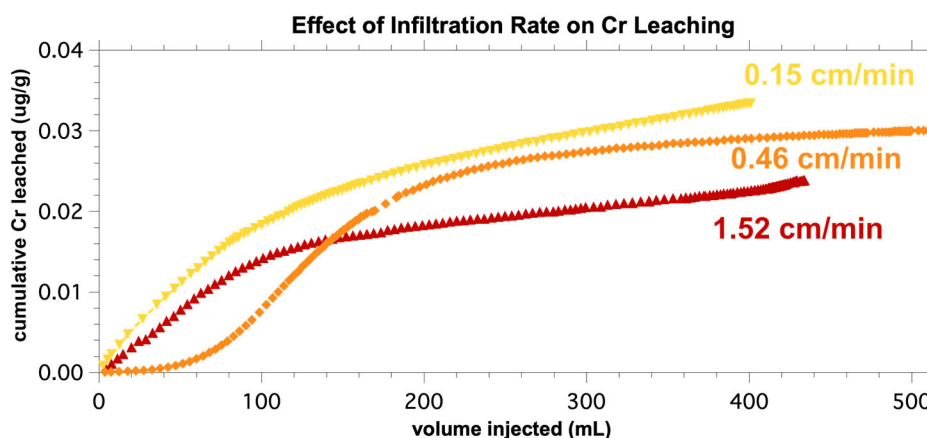


Figure 3.5. Change in chromate leach mass at different infiltration rates.

3.3 Influence of Amendments on Cr Leaching

3.3.1 Acidic Water to Increase Cr Leaching

Because significant chromate can be incorporated into calcite and Fe-oxides and acids dissolve both minerals, leach experiments using weak acids were investigated to increase the rate of Cr release from sediments. A previous evaluation of acid dissolution of Hanford, Cold Creek, and Ringold sediments showed that considerable calcite can be relatively quickly dissolved, followed by the slow dissolution of clays such as montmorillonite. To dissolve all the calcite in Hanford or Ringold formation sediments (at a

porosity of 35% and dry bulk density of 1.64 g/cm³), a total of 825 or 600 pore volumes of pH 3 water or 82,500 and 60,000 pore volumes of pH 5 water is needed, based on the acid neutralization capacity previously measured (Szecsody et al. 2012). However, because only a fraction of the calcite likely contains chromate substitution, partial dissolution of calcite may be sufficient to sufficiently increase Cr leaching.

An example of weak acid dissolution of a portion of calcite was evaluated in 2015 at the 100-K Area in well K166. Injection water after treatment was acidified to pH 6, and calcite dissolution occurred in down gradient wells as shown by elevated carbonate and calcite in groundwater. Based on the increase in calcium, it was calculated that about 0.6% of the calcite in the sediment (averaging 2.0% by weight) would be dissolved to supply the aqueous carbonate and calcite. This corresponded to 2.4 pore volumes of pH 5 or 240 pore volumes of pH 6 water needed to dissolve 0.6% of the calcite in Hanford formation sediment. Based on these results, leaching of Cr was compared in four different sediments between baseline groundwater at pH 8.0 and pH 6 groundwater or pH 5 groundwater (Table 2.3, sediments R18, R5, R17, and R25). For one sediment (R18), the pH 6 solution resulted in 2.3 times greater leached Cr mass, whereas for the three other sediments, the pH 6 solution experiments showed a lesser amount of leached Cr mass. The single pH 5 solution experiment showed about 30% more leached Cr mass compared to the pH 8 leach experiment for sediment R17 (Table 3.3). The chromate leach profiles and cumulative mass for pH 5, 6, and 8 injections for sediment R17 illustrate that the difference in Cr leaching for the weak acid solution mainly influences the first few pore volumes (Figure 3.6). The rate of Cr release from sediment (rate calculated at each stop-flow event) increased with the addition of acidic solutions (Figure 3.7, data in Table 2.4), which implies the weak acid solution resulted in more rapid dissolution of some Cr-containing precipitate phases.

Although these experiments show that weak acid leach solutions are somewhat effective at increasing Cr leaching from sediment, application of these laboratory results to field scale offers significant challenges. Generally, chromate contamination in the vadose zone of differing 100 Areas occurs at specific depths, but application of the weak acid to the surface would mainly be consumed by calcite dissolution in shallow sediments, greatly decreasing the efficiency. If the weak acid solutions could be applied at depth near the Cr-contaminated sediment, Cr leaching would likely be increased.

Table 3.5. Change in chromate leach mass using different weak acid solutions.

Sed.	Exp. #	Solution	Leached (µg/g)
R18	S10	pH 8 AGW	0.00033
	S14	pH 6 AGW	0.0011
R5	S2	pH 8 AGW	1.395
	S12	pH 6 AGW	1.025
R17	S3	pH 8 AGW	0.00083
	S5	pH 6 AGW	0.0005
	S8	pH 5 AGW	0.0019
R25	S11	pH 8 AGW	1.61
	S16	pH 6 AGW	1.565

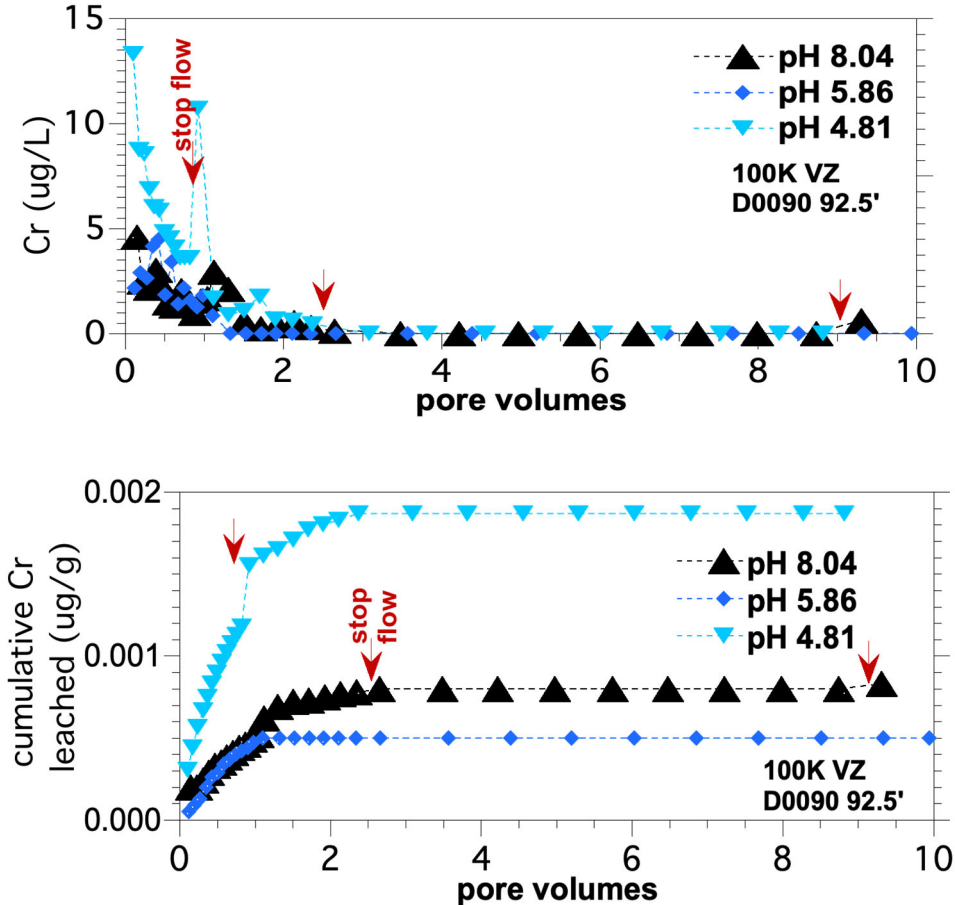


Figure 3.6. Chromate leaching in 1-D water-saturated column experiments with acidic injection solutions.

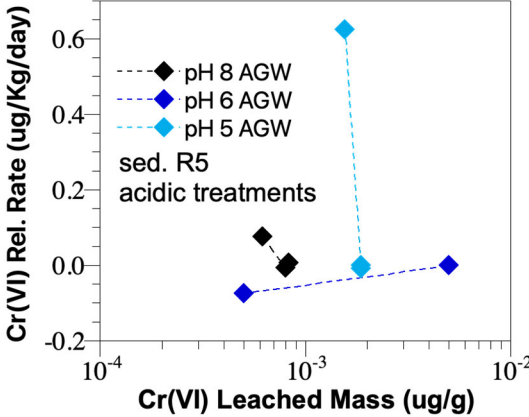


Figure 3.7. Change in chromate leach rate and mass with differing acidic treatments.

3.3.2 Surfactant to Increase Cr Leaching through Low-K Lenses

Modification of the infiltration solution with a surfactant was evaluated to decrease the surface tension of water to increase water flow through low-permeability lenses in the vadose zone, as described in Section 3.4. As a baseline, Cr leaching was compared using artificial groundwater (pH 8) with and without a surfactant in homogeneous water-saturated columns and infiltration experiments. The critical micelle concentration of sodium lauryl sulfate for low ionic strength water is 330 mg/L (Williams et al. 1955), so a concentration of 500 mg/L was used in the injection/infiltrating solutions. For water-saturated experiments, a sediment with low Cr showed an increase in Cr leaching, but a sediment with high Cr showed a large decrease in Cr leaching (Table 3.6 and leached mass in Figure 3.8, breakthrough curves in Figure 3.9). The Cr release rates did not change because of the surfactant addition, as expected, because mineral dissolution rates did not change (Figure 3.8). The infiltration leach experiment with the surfactant showed about 70% more Cr leached compared to the infiltration experiment without surfactant (Figure 3.10) at the same infiltration rate. Overall, it is unclear what a surfactant addition has on Cr leaching in homogeneous water-saturated sediment experiments, given the inconsistent results. The greater Cr leaching observed in one experiment during unsaturated flow is consistent with the hypothesis that reducing the water surface tension may result in additional flow through smaller pores, even in homogeneous sediments.

Table 3.6. Change in chromate leach mass with the addition of a surfactant.

Sed.	Exp. #	Solution	Leached (μg/g)
R5	S2	pH 8 AGW	1.395
	S20	Surfactant	0.495
R17	S3	pH 8 AGW	0.00083
	S6	Surfactant	0.0017
R28	S18 sat.	pH 8 AGW	0.0373
	J6 infil.	pH 8 AGW	0.0238
	J10 infil.	Surfactant	0.0400

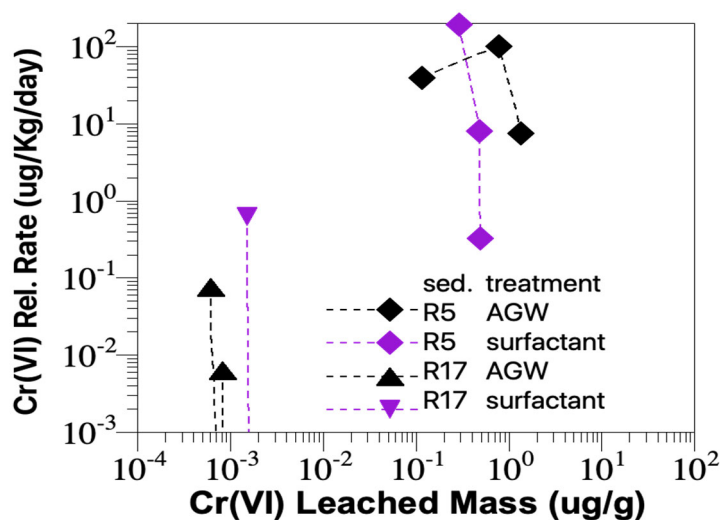


Figure 3.8. Change in chromate leach rate with the addition of a surfactant.

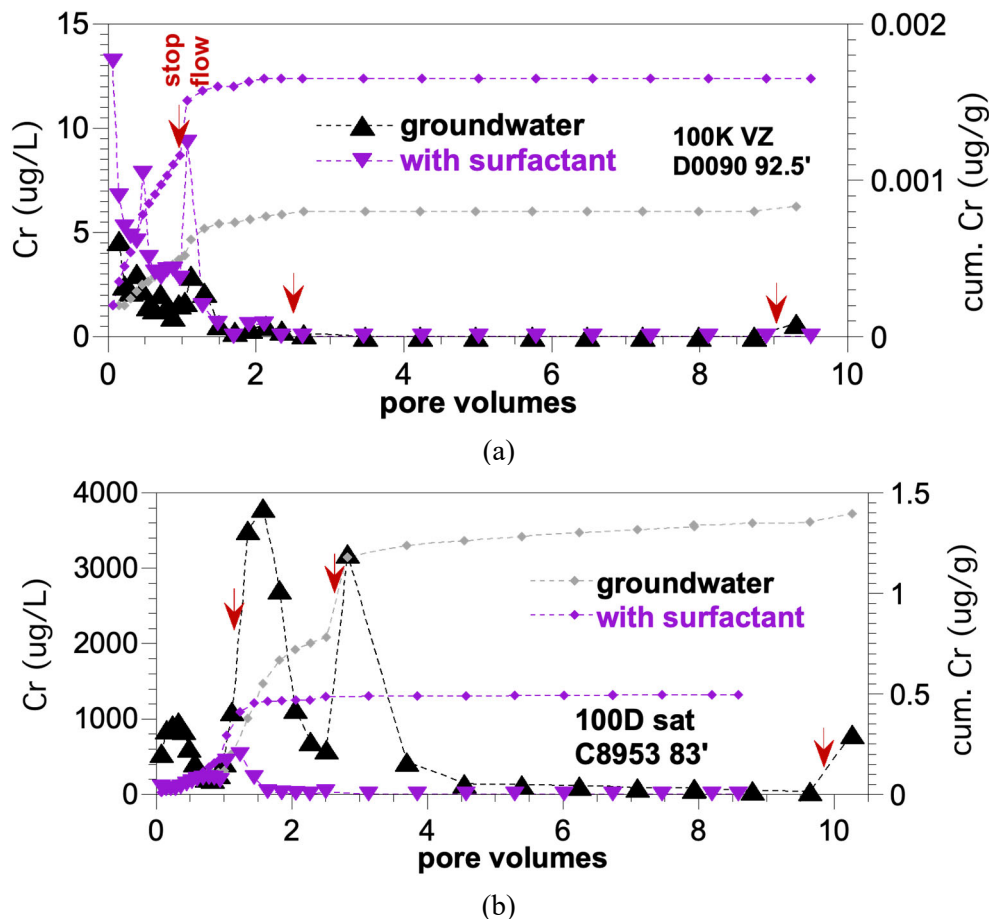


Figure 3.9. Chromate water-saturated leaching without and with a surfactant for sediment R17 (a) and sediment R5 (b).

3.3.3 Aqueous Reductant to Decrease Residual Chromate Leaching

Field-scale soil flushing operations intend to use water being flushed through the vadose zone to advect highly soluble chromate phases in the vadose zone to groundwater, which is captured in a P&T system. Several factors result in more complex chromate leaching behavior through the vadose zone, including (1) slow chemical release of Cr from moderate solubility precipitates, (2) slow physical release of Cr in sediments in low-permeability zones (which water advects slowly or only diffuses through); and (3) residual water flow through the vadose zone to groundwater after surface application stops (as described in Section 3.2).

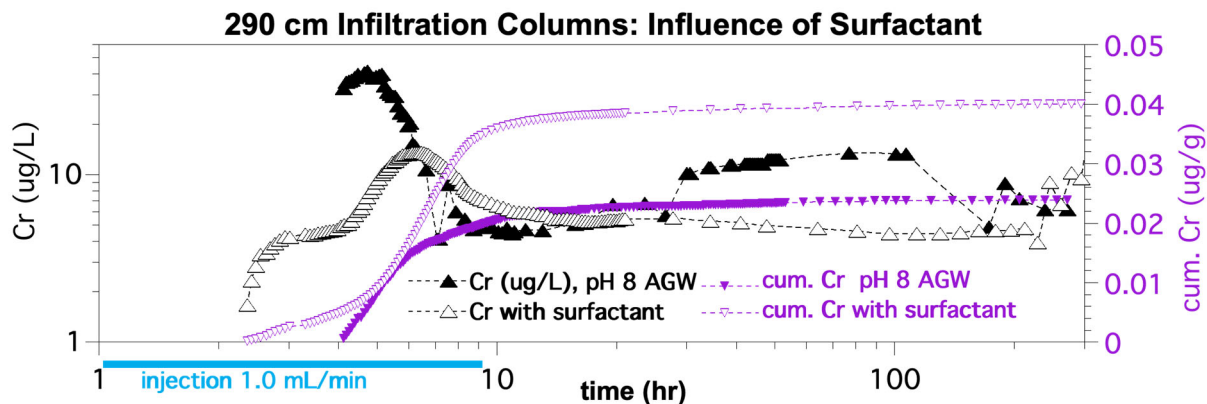


Figure 3.10. Chromate in unsaturated infiltration without and with a surfactant.

For sediments that exhibit slow release of Cr, experiments were conducted to evaluate the use of addition of an aqueous reductant to decrease Cr leaching during the residual water flow stage of leaching. Most experiments were conducted in small water-saturated columns, although one experiment was conducted in an unsaturated leach column. Three out of four water-saturated experiments showed a 49% decrease in Cr leached mass with reductant addition in only a part of the injection solution (i.e., from 1.0 to 2.5 pore volumes of a 10-pore volume injection; Table 3.7). Cr leached mass decreased significantly with greater reductant treatment (Figure 3.11). One sediment (R18) showed an increase in Cr leaching with the reductant addition, although leached mass for the pH 8 and reductant leach experiments is very small. For the addition of a reductant for all 10 pore volumes, chromate leaching decreased 93% (sediment R5, shown in Figure 3.12 in dark green). In general, addition of the reductant resulted in a large decrease in the Cr release rates (Figure 3.11).

Table 3.7. Change in chromate leach mass with the addition of a reductant.

Sed.	Exp. #	Solution	Leached (µg/g)
R18	S10	pH 8 AGW	0.00033
	S15	Part. reduct.	0.00394
R5	S2	pH 8 AGW	1.395
	S13	Part reduct.	0.977
	S21	full reduct.	0.0982
R17	S3	pH 8 AGW	0.00083
	S7	part reduct.	0.00039
R25	S11	pH 8 AGW	1.61
	S17	Part reduct.	1.072
R28	J6 infil.	pH 8 AGW	0.0238
	J9 infil.	Full reduct.	0.0050

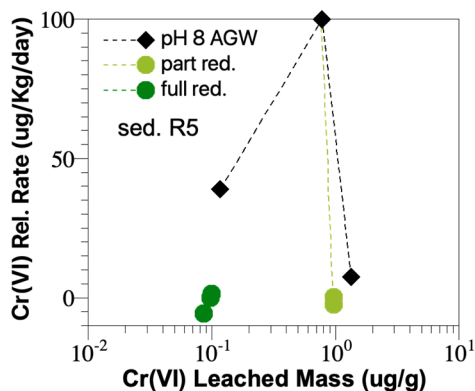


Figure 3.11. Change in chromate leach rate with the addition of a reductant.

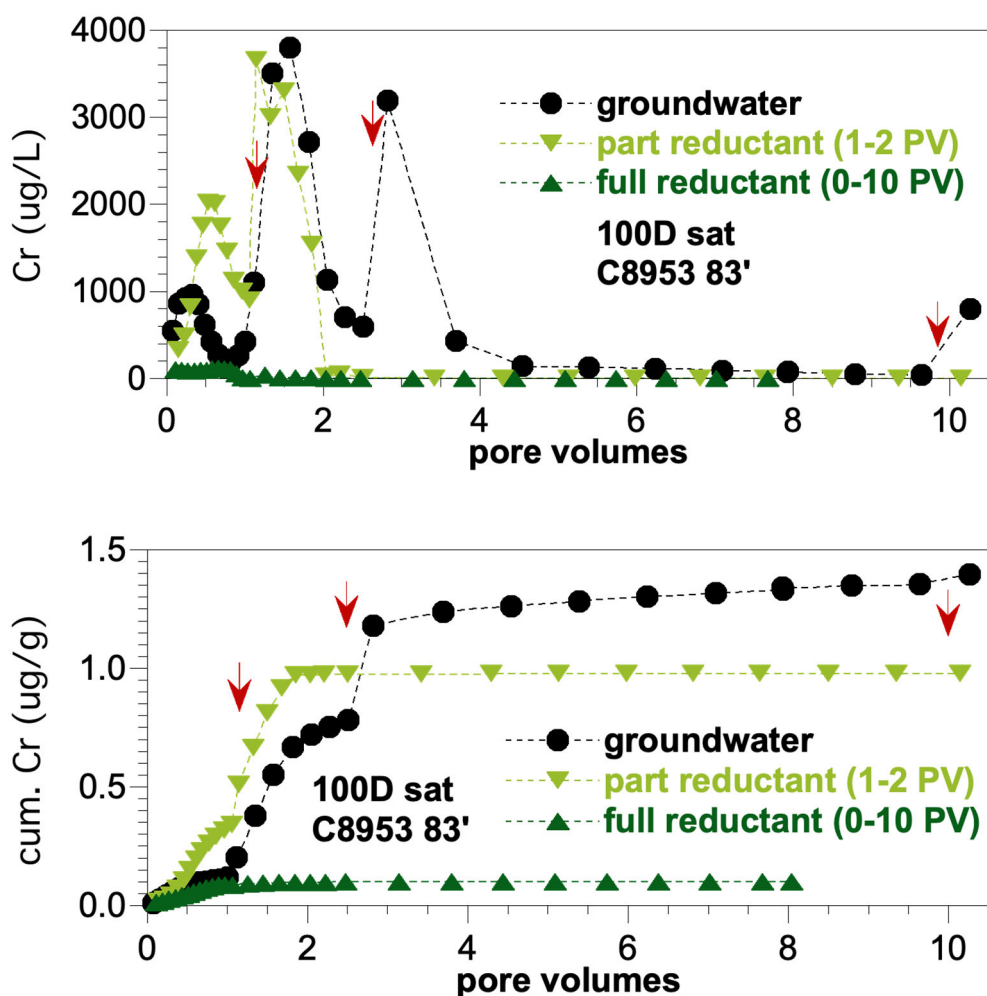


Figure 3.12. Chromate water-saturated leaching without and with a reductant for sediment R5.

Calculated negative release rates (Table 2.5 and in Figure 3.11 for partially and fully reduced sediments) mean net Cr uptake during the stop-flow event. This results from the Cr release rate from the sediment being smaller than the Cr^{VI} reduction rate (and precipitation of Cr(OH)₃ by the Na-dithionite).

Because the reductant solution is in contact with air during infiltration (i.e., sediment is not fully water-saturated), some of the reductant will be oxidized by oxygen in air. Therefore, reductant addition under these conditions is not as efficient as under water-saturated conditions. A comparison of chromate leaching with just pH 8 artificial groundwater to groundwater with a reductant still shows a 79% decrease in Cr leaching (Figure 3.13), which is somewhat less than the 93% less Cr leaching for the reductant addition over all 10 pore volumes in water-saturated columns (Figure 3.13, comparison of black to dark green symbols). Previous studies have shown that when chromate is reduced, the $(Cr, Fe)(OH)_3$ precipitates created remain immobile even after the system reoxidizes (Loyaux-Lawniczak et al., 2000). However, infiltration of a reductant solution through tens of feet of unsaturated sediment over days to weeks will be even less efficient than the 10-ft infiltration experimental comparison shown here, as the reductant used (Na-dithionite) hydrolyzes with a half-life of 27 h (Szecsody et al. 2004), rendering it less redox reactive after a few days. Although the general idea of using a reductant to decrease residual vadose zone Cr leaching to groundwater by removing all Cr(VI) from solution is promising, a less-reactive reductant such as calcium polysulfide (or other reductants) may be better suited for the vadose zone application.

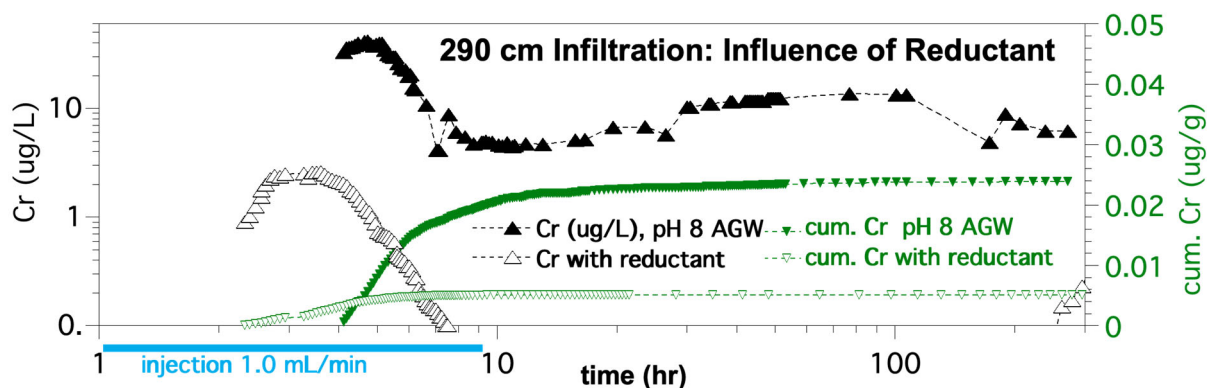


Figure 3.13. Change in chromate leach mass with the addition of a reductant.

3.4 Influence of Surfactant Addition on Unsaturated Cr Leaching in 2-D Heterogeneous Sediment Systems

To simulate field conditions, 2-D infiltration experiments were conducted to quantify the extent to which surfactant addition to the infiltration water increases water flow into and through low-conductivity zones. The surfactant reduces the surface tension of the infiltrating water, resulting in more rapid infiltration through inclusions. At field scale, low-conductivity inclusions are likely at higher water content, and therefore may contain greater aqueous and adsorbed Cr. In addition, these finer grained inclusions also have higher surface area, so they may also contain higher concentrations of Cr in precipitates. Because the effect of a surfactant addition is dependent on the hydraulic conductivity of the inclusions relative to the matrix sediment, five 2-D experiments were conducted with differing hydraulic conductivity ratios. The 2-D infiltration experiments conducted are qualitative experiments illustrating the influence of a surfactant addition. Inclusions did not contain Cr, so a change in actual Cr leaching is only implied from the increased water flow through inclusions with a surfactant relative to infiltration with just groundwater.

Even with a medium to coarse matrix sediment (average grain size 2.2 mm), fine sand inclusions showed little difference between groundwater (Figure 3.14a, infiltration on left) and surfactant (infiltration on right), as in both cases, water was mainly migrating downward through a portion of inclusions with little lateral movement. Fine-grained inclusions that were thin did have increased lateral water movement due to higher capillary forces (Figure 3.14b), but there was still little difference in vertical movement between

groundwater and the surfactant because the layer was thin. Thicker silt/clay inclusions illustrated the difference between groundwater moving around the inclusions (Figure 3.14c, left) and the surfactant moving through the inclusion (right). This resulted in a greater flushing of water containing the surfactant through inclusions (Figure 3.14d, right side). Additional images are in Appendix D.

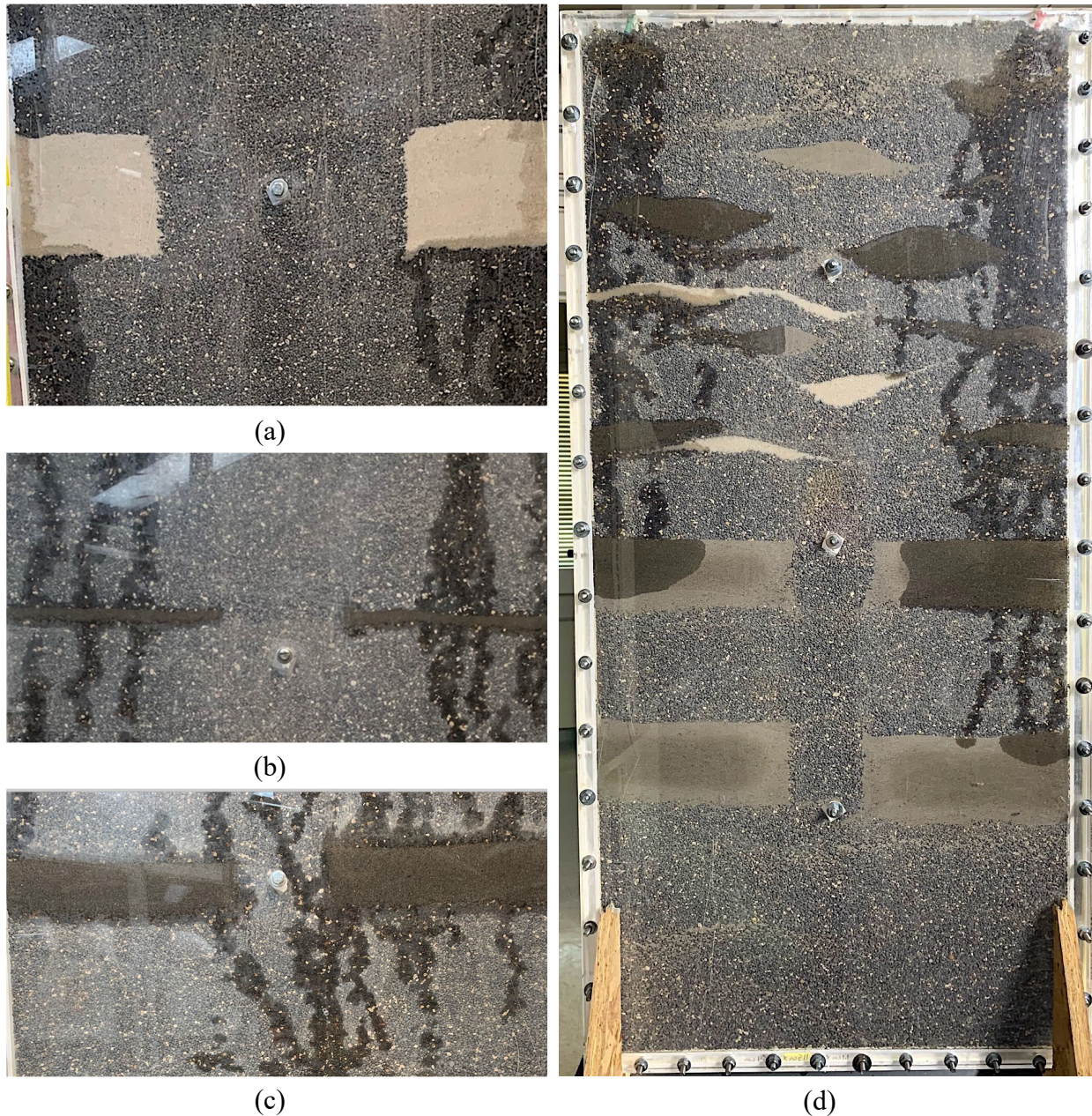


Figure 3.14. Comparison of groundwater infiltration (in upper left of each experiment) to groundwater with a surfactant (in upper right). 2-D systems had a medium to coarse Hanford sand matrix with inclusions composed of (a) fine (#70) sand, (b) thin silt lens, (c) thick silt lens, and (d) multiple inclusions of 70% silt, 30% clay (dark inclusions), and fine sand (light inclusions).

4.0 Discussion

Chromium is present in sediments in multiple phases that differ in leachability characteristics. The purpose of this study was to quantify key geochemical and physical processes controlling which Cr surface phases in field-contaminated sediments are leachable, the rate at which these phases release Cr, and opportunities to increase effectiveness of Cr leaching. Chromium, present as chromate in aqueous and adsorbed phases, is highly mobile and advects from sediment within a few pore volumes (assuming no physical diffusion limiting release from low-permeability layers, for example), and results in high leach concentrations and high Cr release rates from sediment. Natural and anthropogenic chromium is also present as Cr(VI) precipitates such as high-solubility CaCrO_4 , moderate-solubility chromate-substituted calcite, and low-solubility BaCrO_4 . Finally, natural chromium is also present primarily in Cr(III) phases such as magnetite and other iron oxides, substitution in clays and mafic minerals (forsterite). Sequential liquid extractions were used to quantify aqueous and adsorbed Cr and operationally define solid phases, as the mass of Cr precipitates in most of the sediments (except 100-D-104 sediment with a total of 224 $\mu\text{g/g}$) was below detection limits of most surface phase techniques.

As described in the Section 0, sediments with low or no Cr contamination had small amounts of aqueous and adsorbed Cr ($< 0.1 \mu\text{g/g}$) that were readily leachable and moderate amounts of low-solubility precipitates (10 to 40 $\mu\text{g/g}$) that were not leachable. These sediments typically released chromate within the first few pore volumes, with little additional release at later times or during stop-flow events, which indicated no slow contributions from Cr dissolution from precipitates. In contrast, sediments with moderate to high Cr contamination had varying aqueous and adsorbed Cr ($< 0.5 \mu\text{g/g}$) that was readily released, as well as additional Cr present in high- and moderate-solubility phases that was slowly released.

4.1 Cr Leached Mass in Different Solutions and Application Rates

Water-saturated and unsaturated leach experiments on sediments using artificial groundwater (pH 8.0), weak acidic solutions (pH 6.0 or 5.0), a reductant (Na-dithionite), and a surfactant resulted in differences in the leached Cr mass. Sediments with high anthropogenic Cr released significant Cr at high concentrations during initial leaching and lower concentrations over many pore volumes. Water-saturated leaching using pH 8 artificial groundwater released more Cr than unsaturated infiltration experiments (Figure 4.1, infiltration experiments indicated in blue), likely due to water advected mainly in larger pores during infiltration. As described in Section 3.2.1, the rate of infiltration was also correlated to the Cr mass released, as slower infiltration resulted in more pores and sediment surfaces accessed (Section 3.2.3). For infiltration experiments, the chromium flux out of the bottom of the column was calculated from the water flow rate and Cr concentration. Water was infiltrated into these columns for 10 to 50 h, then residual water advected out of the bottom of the column for the next 500 h. Sediments that exhibited both fast and slow Cr release from the sediment (Figure 4.1, sediment R25 in black triangles) sustained a higher Cr flux at slower flow rates, and the Cr concentration increased significantly. Treatment of a sediment with a reductant resulted in the lowest Cr flux rate (tan triangles, Figure 4.1). Although this residual Cr flux occurred over 450 h in the 10-ft-high laboratory columns, simulation of this data can be used to approximate the Cr flux rate and length of time needed to continue P&T operations at field scale with an 80- to 100-ft-thick vadose zone.

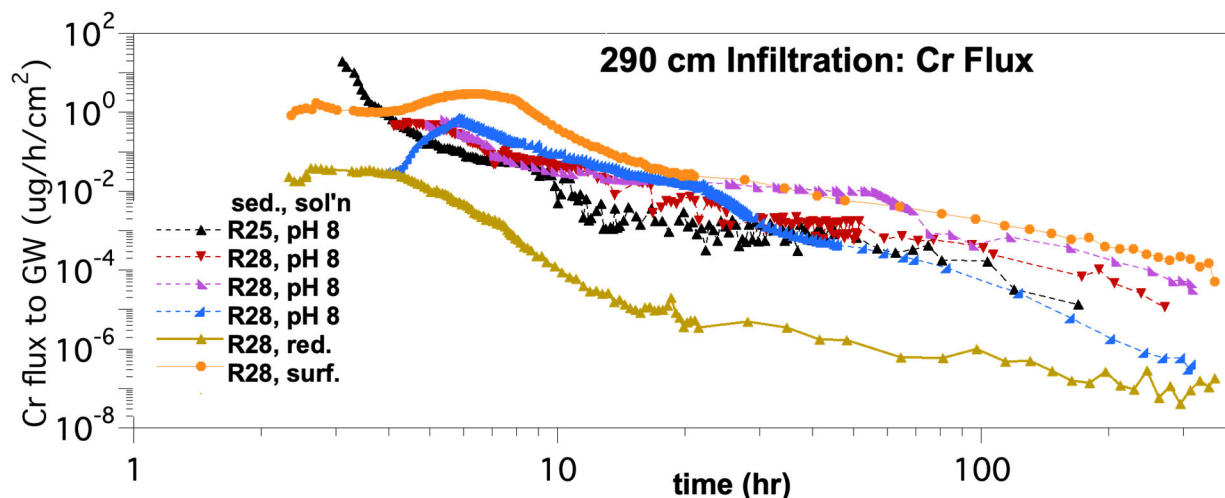


Figure 4.1. Chromium flux out of the bottom of the 290-cm infiltration columns.

Use of a reductant in the injection or infiltration water decreased the leached Cr mass and was more effective when the reductant was injected throughout the entire leach experiment (“full reductant” in Figure 4.2b) compared to when the reductant was injected in a portion of the leach experiment. This result was expected, as chromate is readily reduced by a variety of abiotic reductants and stays reduced/precipitated even after the system is oxidized. However, as described in Section 3.3.3, use of a reductant at field scale will be less efficient than in these laboratory columns. Use of a weak acid in the injection water did accelerate dissolution of calcite, which contained some chromate (Section 3.3.1). This effect was minimal to ineffective with injection of the pH 6 artificial groundwater but more effective for pH 5 artificial groundwater and resulted in greater Cr leaching than the pH 8 artificial groundwater leach (sediment D0090, 92' in Figure 4.2a). The addition of a surfactant in the leach solution had minimal effect on Cr leaching in these homogeneous experiments, as expected (Section 3.3.2). The surfactant was evaluated for increasing water flow in low-permeability zones, some of which may contain higher Cr concentrations, thus increasing leach efficiency (Section 3.4). The high Cr found in the 100-D-30 pit at a 60 ft (18 m) depth was in a low-permeability layer that was at a higher water content (Szecsody et al. 2019). Although leachable Cr mass in different solutions provide some information about leachable Cr phases, a comparison of the leached Cr to sequential extractions provides additional evidence as to changes in the Cr surface phases, as described in the following section.

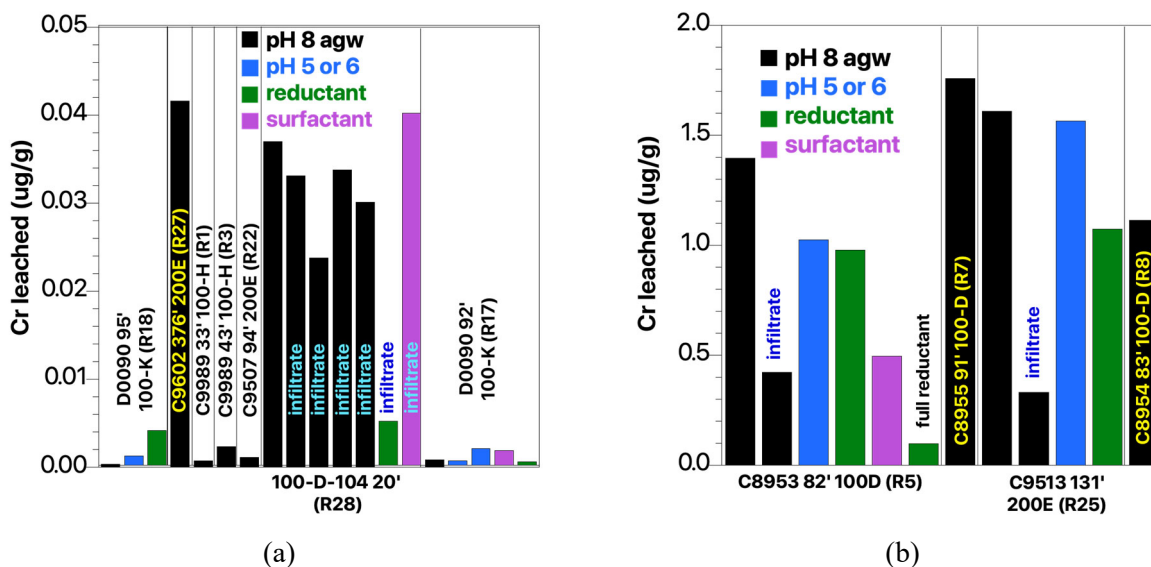


Figure 4.2. Leachable chromium observed in water-saturated and unsaturated experiments for field-contaminated Hanford sediments.

4.2 Cr Surface Phases and Relationship to Leached Mass

Sequential extractions on pre- and post-leach sediments were used to quantify Cr surface phases that were leached. For sediments that were leached with the pH 8 artificial groundwater, the comparison of the leached Cr to total extracted Cr showed no correlation (Figure 4.3a). In contrast, the sum of the first three extractions for pre-leach sediments (i.e., aqueous Cr, adsorbed Cr, pH 5 extractable Cr) correlated well with the leached Cr (Figure 4.3b). The largest contributor to leached Cr was extraction 3 (pH 5 acetate dissolved precipitates), so there still was a correlation between extraction 3 and leached Cr (Figure 4.3c). Not all sediments had the largest mass fraction in extraction 3, so this correlation with leached Cr ($r^2 = 0.81$) was not as high as with labile Cr ($r^2 = 0.98$). This implies that these phases were leached, so masses should decrease significantly when analyzed in post-leach sediments. This was generally the case for sediments that leached significant Cr (Figure 4.4b), where pre-leach labile Cr extractions for sediments R5, R17, R25, and R8 were about equal to the sum of the leached Cr and post-leach labile extractions. The post-leach labile Cr extractions decreased 80% to 90% relative to pre-leach labile extractions. However, for sediments that had low pre-leach labile Cr (i.e., $< 0.1 \mu\text{g/g}$ in Figure 4.4a), the leached Cr was much smaller (i.e., $\sim 0.001 \mu\text{g/g}$). This strong correlation for high leachable Cr and weak correlation for low leachable Cr is also shown in Figure 4.3b.

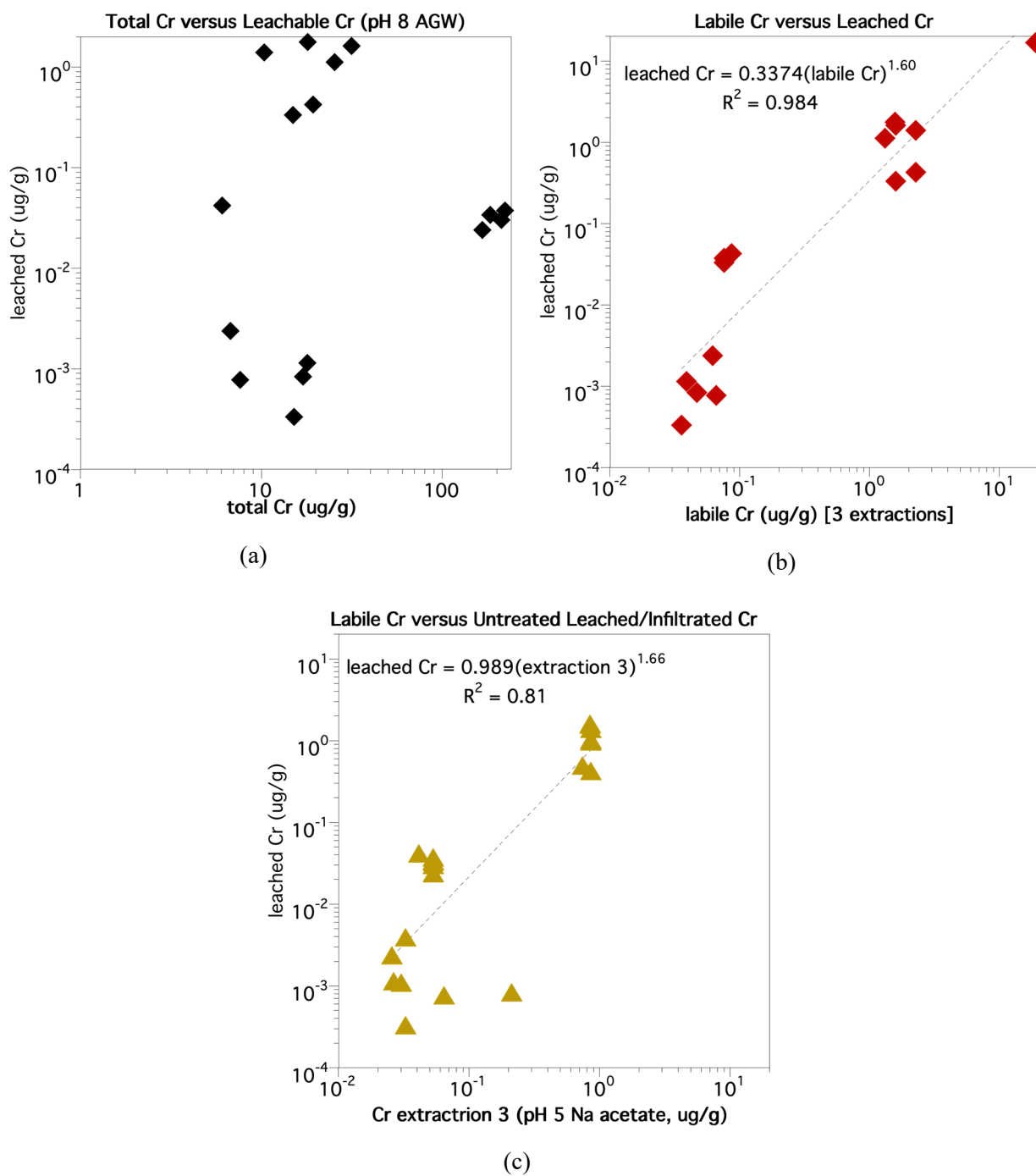


Figure 4.3. Relationship of leached Cr to (a) total extracted Cr, (b) labile Cr, and (c) extraction 3.

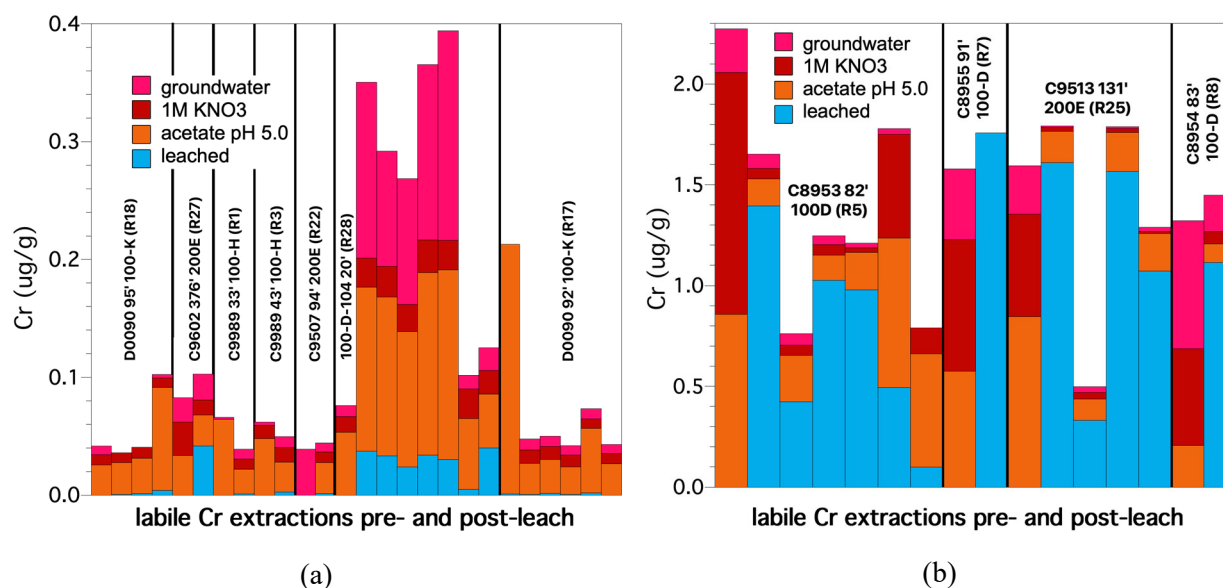


Figure 4.4. Labile Cr extractions for pre- and post-leach sediments that received different treatments.

4.3 Cr Release Rate from Sediments

As Cr leaches from sediment, the general observation of high initial leach concentrations followed by low concentrations at later times is caused by initial advection of aqueous, then adsorbed, Cr, then dissolution of high-solubility Cr precipitates (CaCrO_4), then some dissolution of moderate-solubility Cr precipitates (i.e., possibly chromate-substituted calcite). Therefore, the rate of Cr release from sediments calculated from stop-flow events at 1.0, 2.5, and 10 pore volumes should correlate with the release of adsorbed Cr at ~ 1.0 pore volumes, high-solubility precipitates at ~ 2.5 pore volumes, and slow dissolution of moderate-solubility precipitates at ~ 10 pore volumes. For sediments leached with pH 8 artificial groundwater, the initial Cr release rates at 1.0 pore volumes were high (black diamonds, Figure 4.2a and b) and correlated well (i.e., $r^2 = 0.81$) with the labile Cr mass (Figure 4.5b), but not the total Cr (Figure 4.5a). The Cr release rates at 2.5 pore volumes, in all cases, were smaller by approximately half than the release rates at 1.0 pore volumes (brown diamonds, Figure 4.5). These Cr release rates at 2.5 pore volumes had only a fair correlation with the labile Cr ($r^2 = 0.64$). The Cr release rates calculated third at 10 pore volumes were about 10 times smaller than release rates at 1 pore volume and were moderately correlated with the labile Cr (small tan diamonds, $r^2 = 0.72$). Some Cr release rates, particularly the rates at 10 pore volumes, were negative, which suggests there was a net decrease in the Cr aqueous concentration after the stop flow. This indicated Cr precipitation or incorporation. Fast initial rates and subsequent slow (or negative) release rates indicate that nearly all the mobile Cr has been leached. This was generally the case for sediments that had low leachable Cr and mainly just fast Cr release.

For rates calculated on leach experiments with a reductant, the Cr release rates were negative (Table 2.4), because residual aqueous dithionite (or ferrous iron reduced by dithionite) was reducing and precipitating chromate. This was the desired outcome (i.e., less leached Cr and continued decrease in Cr leaching), as reductant addition is targeted at for use in the final flushing water to decrease residual Cr leaching.

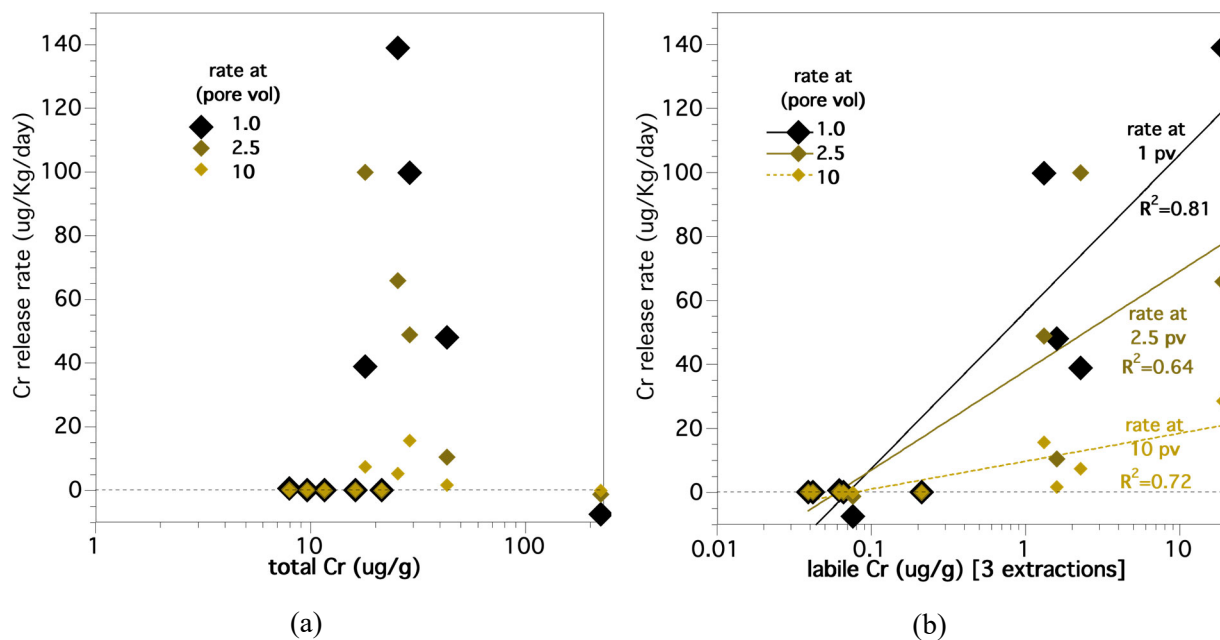


Figure 4.5. Cr release rate from sediments leached with pH 8 groundwater as a function of (a) total Cr, and (b) labile Cr.

5.0 Conclusions

The purpose of this laboratory study was to quantify key geochemical and physical processes controlling Cr leaching in Hanford sediments by (1) identifying Cr surface phases and quantify corresponding leach rates from Hanford sediments; (2) maximizing Cr leaching during soil flushing by evaluating the effects of leach rate, volume, and addition of amendments; (3) minimizing Cr leaching after soil flushing ends (i.e., during residual water leaching). Results of this study provide the basis to increase effectiveness of soil flushing in the field. Cr-contaminated Hanford sediments exhibited a wide variety of leach behavior, from rapid release of a small amount of Cr to fast and slow release of high Cr from sediments. Sediments that had Cr in phases that were quickly released (i.e., aqueous Cr, adsorbed Cr, in high-solubility precipitates such as CaCrO_4) showed little additional Cr released after two pore volumes. In contrast, sediments that had additional Cr in phases that slowly dissolved (CrO_4 -substituted calcite, BaCrO_4) showed elevated Cr concentrations over most pore volumes and had elevated Cr concentrations after stop-flow events.

The difference in Cr release rate from sediment is caused by the mobilization (or partial mobilization) of different aqueous and solid Cr phases in the sediment, which was quantified by sequential liquid extractions before and after leaching. The six sequential extractions quantified aqueous Cr, adsorbed Cr, and Cr in different precipitate phases through four extractions that used progressively stronger acids targeting dissolution of specific minerals. Sequential extractions proved useful as the first three extractions (aqueous Cr, adsorbed Cr, and pH 5 acetate) correlated well with the Cr leached mass, and so could be used to estimate leachable Cr. The total extracted Cr in the sediment was not correlated with leachable Cr. A previous study showed that the labile Cr extractions were predominantly Cr(VI), whereas the remaining three acidic extractions were predominantly Cr(III) precipitates of low solubility (Szecsody et al., 2020b).

In general, sediments with low labile Cr ($< 0.2 \mu\text{g/g}$) exhibited fast Cr release, and most ($> 95\%$) leached from the sediments within a few pore volumes in water-saturated columns. Leaching under unsaturated conditions was less efficient (i.e., 21% to 64% Cr leached in the same amount of pore volumes as water-saturated columns), as water advected through larger pores. Slower infiltration rates of the leach water resulted in greater mass of leached Cr. These sediments that had low labile Cr and exhibited fast Cr release could likely be efficiently leached in the field with a single slow leach solution at a slow infiltration rate.

In contrast, most sediments with high labile Cr (0.2 to $20 \mu\text{g/g}$) exhibited a combination of fast and slow Cr release due to multiple Cr surface phases being released from the sediment at different rates. Given nearly no sorption of chromate, aqueous and sorbed Cr (chromate) are released quickly from sediment and are advected within the first few pore volumes. High-solubility precipitates such as CaCrO_4 (if present) then dissolve into solution followed by the slow dissolution of calcite that may contain some chromate. For some of these sediments, even after 100 pore volumes of water-saturated leaching there was still significant Cr leaching from the sediment, so a single pH 8 artificial groundwater leaching would not be sufficient because at field scale Cr would be a continued source to groundwater. This progression of fast Cr release followed by slow Cr release from sediments was characterized by stop-flow events at different times during leach experiments. The calculated release rates from stop-flow events correlated well with the labile Cr mass. This effect was demonstrated in the 10-ft-high unsaturated leach experiments, where after infiltrating leach water stopped, residual leaching at increasingly slower water flow rates also had increasing Cr concentrations (as much as 15x) because longer sediment-water contact times allowed for greater Cr release from sediments. This resulted in significant Cr flux to groundwater over an extended period of time compared to sediments that exhibited only a fast Cr release.

Efficient leaching of sediments that exhibited fast and slow Cr release would require either a different infiltration strategy (i.e., multiple infiltration pulses over long periods of time) or different solutions to (a) increase Cr release rate during leach water infiltration and (b) decrease Cr release during the residual water flow times, which lasted hundreds of hours in lab experiments and likely months or longer at field scale. A weak acid solution (pH 6 or 5) was marginally effective at increasing Cr leaching during solution infiltration. Alternatively, the addition of an aqueous reductant was highly effective at decreasing Cr leaching during residual water movement. However, both the acidic leach and reductant leach solutions would be significantly less efficient at field scale as solutions would react with all of the non-Cr-containing sediment in the vadose zone, leaving less for Cr-contaminated sediment. The use of a surfactant to increase water flow in low-permeability layers was qualitatively demonstrated in 2-D infiltration experiments in cases where low-permeability layers had significantly lower permeability (i.e., silt or clay) than the matrix sediment composed of coarse sand. The slow advection of water through low permeability layers that contain Cr would add additional slow Cr release. Field scale Cr leaching in these heterogeneous sediments would be increased with the use a surfactant, depending on the permeability of matrix and fine-grained layers. Simulation of the Cr flux from the bottom of the 10-ft infiltration experiments with differing solutions and infiltration strategies to obtain water flux and Cr release rates over time can be used by site contractors to test different leach strategies at field scale in the 80- to 100-ft vadose zone to optimize infiltration strategy, leach solution(s) used, and time scale of pumping needed.

Future direction includes expanding physical and chemical methods to increase Cr leaching efficiency in laboratory experiments including the following:

- Evaluate periodic flushing to increase short-term removal of residual Cr.
- Evaluate different reductants including Ca-polysulfide to minimize long-term residual Cr leaching.
- Evaluate use of different surfactants to increase water flow and Cr leaching in low-permeability zones.
- Conduct generic field-scale simulations to evaluate the time scale of residual Cr leaching for sediments that have only fast Cr release and sediments that have fast and slow Cr release.
- Evaluate the sensitivity of electrical resistivity methods (DC electrical resistivity and spectral induced polarization) to monitor advection of chromate in unsaturated sediments.

6.0 Quality Assurance

This work was performed in accordance with the Pacific Northwest National Laboratory Nuclear Quality Assurance Program (NQAP). The NQAP complies with DOE Order 414.1D, *Quality Assurance*. The NQAP uses NQA-1-2012, *Quality Assurance Requirements for Nuclear Facility Application*, as its consensus standard and NQA-1-2012 Subpart 4.2.1 as the basis for its graded approach to quality. Reviews of calculations in this paper study were conducted for this work in accordance with the NQAP.

7.0 References

- Arcon I, B Mirtic, and A Kodre. 2005. "Determination of valence states of chromium in calcium chromates using X-ray adsorption near-edge structure (XANES) spectroscopy." *Journal of the American Ceramic Society* 81(1):222-224.
- ASME NQA-1-2012, *Quality Assurance Requirements for Nuclear Facility Application*. American Society of Mechanical Engineers, New York, NY.
- Chao T and L Zhou. 1983. "Extraction techniques for selective dissolution of amorphous iron oxides from soils and sediments." *Soil Science Society of America Journal* 47(2):225-232.
- DOE. 1993. *Hanford Site Background: Part 1, Soil background for nonradioactive analytes*. DOE/RL-92-94, Rev. 1, U.S. Department of Energy, Richland Operations Office, Richland, WA.
- DOE Order 414.1D, *Quality Assurance*. U.S. Department of Energy, Washington, D.C.
- Dong H, RK Kukkadapu, JK Fredrickson, JM Zachara, DW Kennedy, and HM Kostandarithes. 2003. "Microbial reduction of structural Fe(III) in illite and goethite." *Environmental Science & Technology* 37:1268-1276.
- Dresel PE, NP Qafoku, JP McKinley, JS Fruchter, CC Ainsworth, C Liu, ES Ilton, and JL Phillips. 2008. *Geochemical Characterization of Chromate Contamination in the 100Area Vadose Zone at the Hanford Site*. PNNL-17674, Pacific Northwest National Laboratory, Richland, WA.
- Eary LE and D Rai. 1988. "Chromate removal from aqueous wastes by reduction with ferrous iron." *Environmental Science and Technology* 22(8):972-977.
- Ginder-Vogel M, T Borch, MA Mayes, PM Jardine, and S Fendorf. 2005. "Chromate reduction and retention processes within arid subsurface environments." *Environmental Science & Technology* 39:7833-7839.
- Gleyzes C, S Tellier, and M Astruc. 2002. "Fractionation studies of trace elements in contaminated soils and sediments: a review of sequential extraction procedures." *Trends in Analytical Chemistry* 21(6 & 7):451-467.
- Hall G, J Vaive, R Beer, and N Hoashi. 1996. "Selective leaches revisited, with emphasis on the amorphous Fe oxyhydroxide phase extraction." *Journal of Geochemical Exploration* 56:59-78.
- Hu J, I Lo, and G Chen. 2007. "Performance and mechanism of chromate (VI) adsorption by FeOOH-coated maghemite (Fe₂O₃) nanoparticles." *Separation and Purification Technology* 58:76-82.
- Larner B, A Seen, and A Townsend. 2006. "Comparative study of optimized BCR sequential extraction scheme and acid leaching of elements in certified reference material NIST 2711." *Analytica Chimica Acta* 556:444-449.
- Lee, B., J. Szecsody, N. Qafoku, E. McElroy, S. Baum, M. Snyder, A. Lawter, M. Truex, B. Gartman, L. Zhong, D. Saunders, B. Williams, J. Horner, I. Leavy, C. Resch, B. Christiansen, R. Clayton, and K. Johnson, 2017. Contaminant attenuation and transport characterization of 200-UP-1 operable unit sediment samples, Pacific Northwest National Laboratory, PNNL-26208.

- Loyaux-Lawniczak S, P Refait, J Ehrhardt, P Lacomte, and J Genin. 2000. "Trapping of Cr by formation of ferrihydrite during the reduction of chromate ions by Fe(II)-Fe(III) hydroxysalt green rusts." *Environmental Science & Technology* 34(3):438-443.
- Mossop K and C Davison. 2003. "Comparison of original and modified BCR sequential extraction procedures for the fractionation of copper, iron, lead, manganese, and zinc in soils and sediments." *Analytica Chimica Acta* 478:111-118.
- Palmer CD and PR Willbrodt. 1991. "Processes affecting the remediation of chromium-contaminated sites." *Environmental Health Perspectives* 92:25-40.
- Qafoku NP, CC Ainsworth, JE Szecsody, OS Qafoku, and SM Heald. 2003. "Effect of coupled dissolution and redox reactions on Cr(VI)aq attenuation during transport in the sediments under hyperalkaline conditions." *Environmental Science & Technology* 37:3640-3646.
- Qafoku NP, CC Ainsworth, JE Szecsody, and OS Qafoku. 2004. "Transport-controlled kinetics of dissolution and precipitation in the sediments under alkaline and saline conditions." *Geochimica et Cosmochimica Acta* 68(14):2981-2995.
- Qafoku NP, PE Dresel, E Ilton, JP McKinley, and CT Resch. 2010. "Chromium transport in an acidic waste contaminated subsurface medium: The role of reduction." *Chemosphere* 81(11):1492-1500.
- Qafoku NP, PE Dresel, JP McKinley, C Liu, SM Heald, CC Ainsworth, JL Phillips, and JS Fruchter. 2009. "Pathways of aqueous Cr (VI) attenuation in a slightly alkaline oxic subsurface." *Environmental Science & Technology* 43(4):1071-1077.
- Qafoku NP, EP Dresel, JP Mckinley, ES Ilton, W Um, CT Resch, RK Kukkadapu, and SW Petersen. 2011. *Geochemical characterization of chromate contamination in the 100 Area vadose zone at the Hanford site*. PNNL-17865, Pacific Northwest National Laboratory, Richland, WA.
- Patterson R and S Fendorf. 1997. "Reduction of hexavalent chromium by amorphous iron sulfide." *Environmental Science & Technology* 31:2039-2044.
- Rai D, L Eary, and J Zachara. 1989. "Environmental chemistry of chromium." *Science of the Total Environment* 86(1):15-23.
- Robles-Camacho J and MA Armienta. 2000. "Natural chromium contamination in groundwater at Leon Valley, Mexico." *Journal of Geochemical Exploration* 68(3):167-181.
- Stanin FT. 2005. "The transport and fate of chromium(VI) in the environment." In: J Guertin, J Jacobs, C Avakian (eds.), *Chromium(VI) Handbook*. CRC Press, Boca Raton, FL 165-207.
- Sutherland R and F Tack. 2002. "Determination of Al, Cu, Fe, Mn, Pb, and Zn in certified reference materials using the optimized BCR sequential extraction procedure." *Analytica Chimica Acta* 454:249-257.
- Szecsody, J., H. Emerson, R. Mackley, C. Resch, and S. Baum. 2020a. Identification of chromium mass and release rate from 100-KR-4 sediments. Pacific Northwest National Laboratory, Richland, WA, PNNL-30385.

Szecsody, J., C. Resch, O. Oafoku, H. Emerson, and B. Gartman. 2020b. 100-KR-4 sediment analysis for identification of chromium surface phases. Pacific Northwest National Laboratory, Richland, WA. PNNL-28775 Rev 1.0.

Szecsody J, L Zhong, M Oostrom, V Vermeul, J Fruchter, and M Williams 2012. *Use of polyphosphate to decrease uranium leaching in Hanford 300 area smear zone sediment*. PNNL-21733, Pacific Northwest National Laboratory, Richland, WA.

Szecsody J, M Truex, N Qafoku, D Wellman, T Resch, and L Zhong. 2013. "Influence of acidic and alkaline co-contaminants on uranium migration in vadose zone sediments." *Journal of Contaminant Hydrology* 151:155-175.

Szecsody J, M Truex, N Qafoku, J McKinley, K Ivarson, and S Di Pietro. 2019. "Persistence of chromate in vadose zone and aquifer sediments in Hanford, Washington." *Science of the Total Environment* 676:482-492.

Szecsody J, M Truex, B Lee, C Strickland, J Moran, M Snyder, C Resch, L Zhong, B Gartman, D Saunders, S Baum, I Leavy, J Horner, B Williams, B Christiansen, E McElroy, M Nims, R Clayton, and D Appriou. 2017. *Geochemical, Microbial, and Physical characterization of 200-DV-1 Operable Unit B-Complex Cores from Boreholes C9552, C9487, and C9488 on the Hanford Site Central Plateau*. PNNL-26266, Pacific Northwest National Laboratory, Richland, WA.

Szecsody, J., Williams, M., J. Fruchter, V Vermeul, D. Sklarew, 2004, In Situ Reduction of Aquifer Sediments: Enhancement of Reactive Iron Phases and TCE Dechlorination, *Environmental Science and Technology*, 38: 4656-4663.

Tang Y, E Elzinga, Y Lee, and R Reeder. 2007. "Coprecipitation of chromate with calcite: batch experiments and X-ray absorption spectroscopy." *Geochimica et Cosmochimica Acta* 71:1480-1493.

Truex M, J Szecsody, N Qafoku, C Strickland, J Moran, B Lee, M Snyder, A Lawter, C Resch, B Gartman, L Zhong, M Nims, D Saunders, B Williams, J Horner, I Leavy, S Baum, B Christiansen, R Clayton, E McElroy, D Appriou, K Tyrell, and M Striluk. 2017. *Contaminant Attenuation and Transport Characterization of 200-DV-1 Operable Unit Sediment Samples*. PNNL-26208, Pacific Northwest National Laboratory, Richland, WA.

Truex M, J Szecsody, N Qafoku, R Sahajpal, L Zhong, A Lawter, and B Lee. 2015. *Assessment of hexavalent chromium natural attenuation for the Hanford site 100 area*. PNNL-24705, Pacific Northwest National Laboratory, Richland, Washington.

Vermeul VR, BN Bjornstad, CJ Murray, DR Newcomer, ML Rockhold, JE Szecsody, MD Williams, and YL Xie. 2004. *In Situ Redox Manipulation Permeable Reactive Barrier Emplacement: Final Report Frontier Hard Chrome Superfund Site*. PNWD-3361, Battelle-Pacific Northwest Division, Richland, WA.

Williams, R., J. Phillips, and K. Mysels. 1955. The critical micelle concentration of sodium lauryl sulphate at 25C. *Transactions of the Faraday Society*, 51, 728-737.

Zachara JM, C Ainsworth, G Brown, J Catalano, J McKinley, O Qafoku, S Smith, J Szecsody, S Traina, and J Warner. 2004. "Chromium speciation and mobility in a high-level nuclear waste vadose zone plume." *Geochimica et Cosmochimica Acta* 68:13-30.

Zachara J, D Girvin, R Schmidt, and C Resch. 1987. "Chromate adsorption on amorphous iron oxyhydroxide in the presence of major groundwater ions." *Environmental Science & Technology* 21:589-594.

Zachara J, C Ainsworth, C Cowan, and C Resch. 1989. "Adsorption of chromate by subsurface soil horizons." *Soil Science Society of America Journal* 53:418-428.

Appendix A – Cr Water-Saturated Leaching by Groundwater

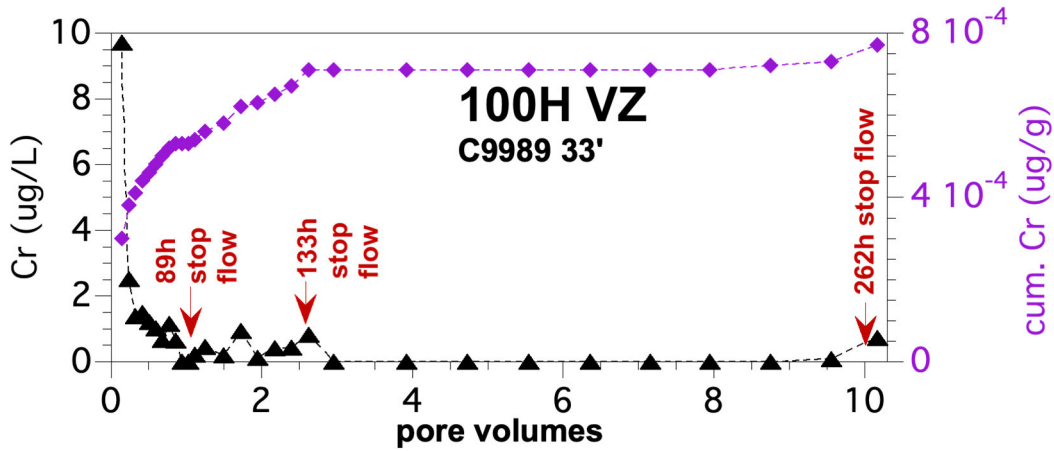


Figure A.1. Water-saturated Cr leach (S1) using artificial groundwater for sediment R1.

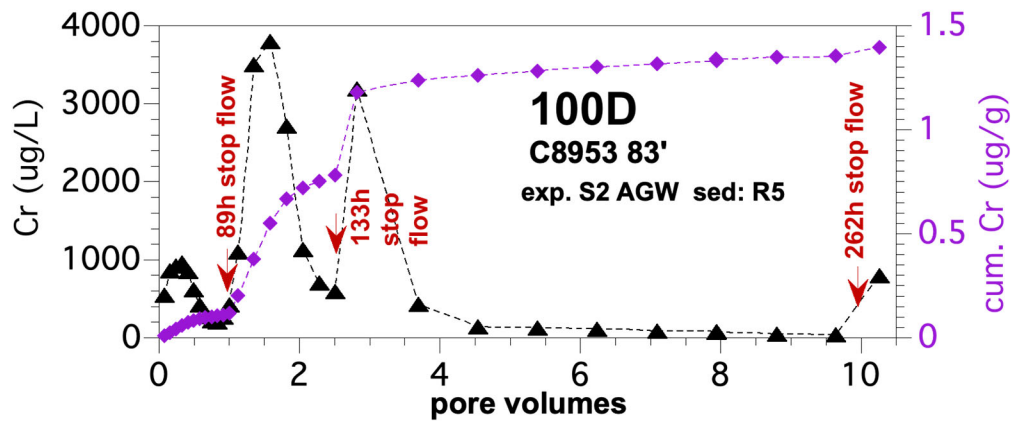


Figure A.2. Water-saturated Cr leach (S2) using artificial groundwater for sediment R5.

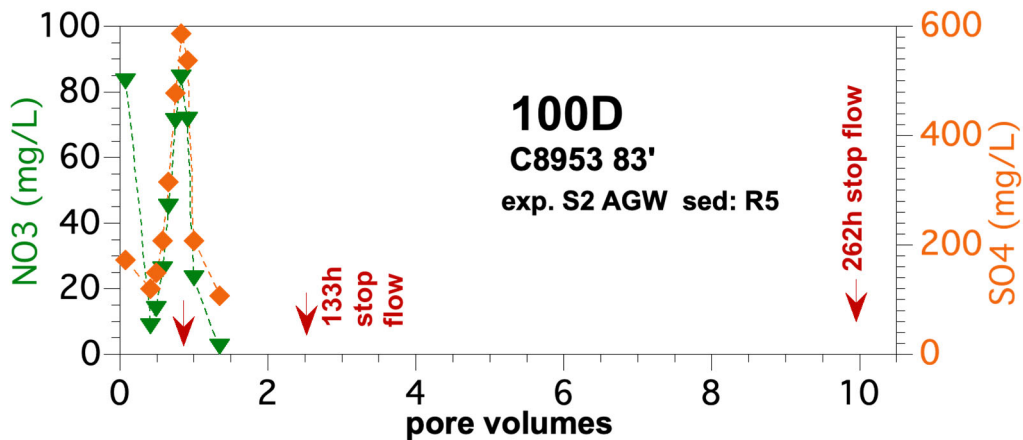


Figure A.3. Water-saturated Cr leach (S2) co-contaminants for sediment R5.

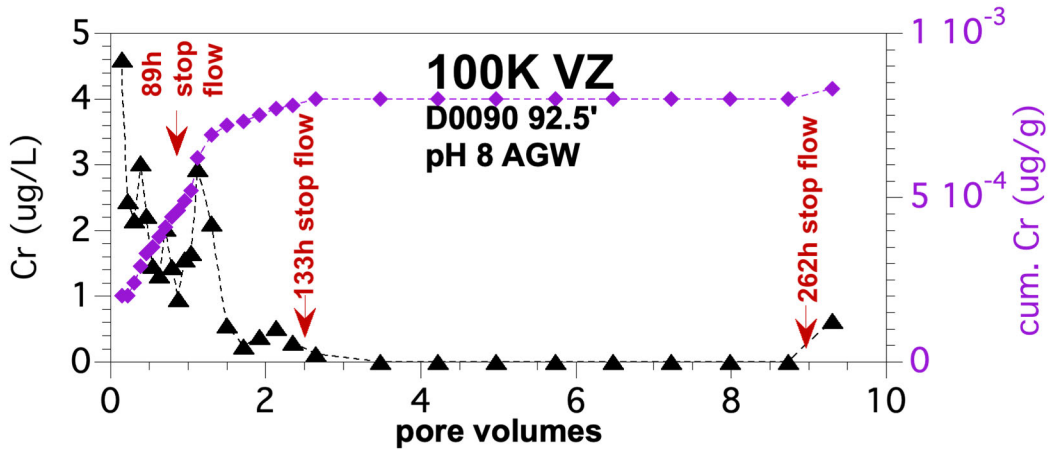


Figure A.4. Water-saturated Cr leach (S3) using artificial groundwater for sediment R17.

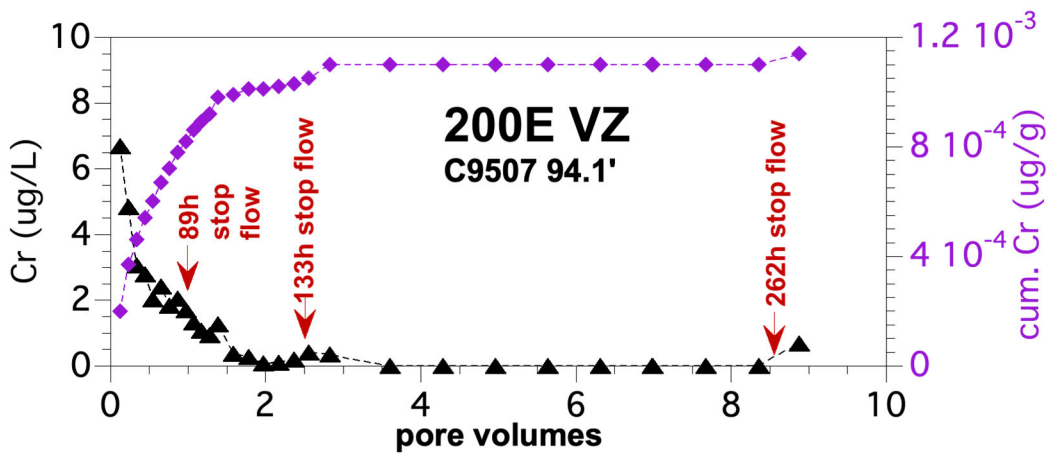


Figure A.5. Water-saturated Cr leach (S4) using artificial groundwater for sediment R22.

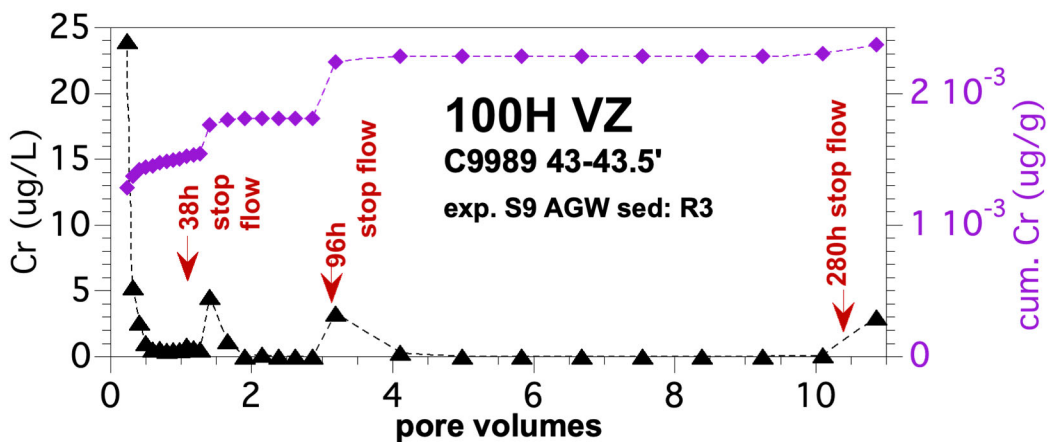


Figure A.6. Water-saturated Cr leach (S9) using artificial groundwater for sediment R3.

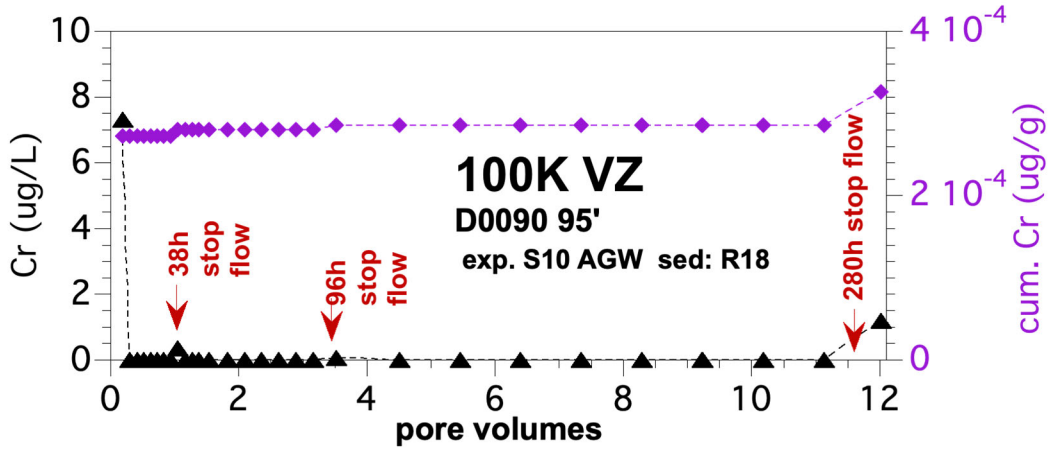


Figure A.7. Water-saturated Cr leach (S10) using artificial groundwater for sediment R18.

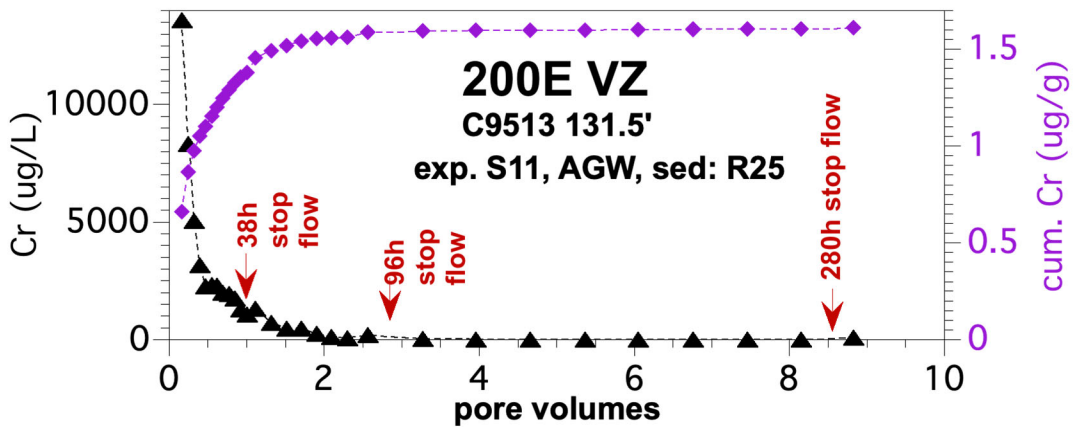


Figure A.8. Water-saturated Cr leach (S11) using artificial groundwater for sediment R25.

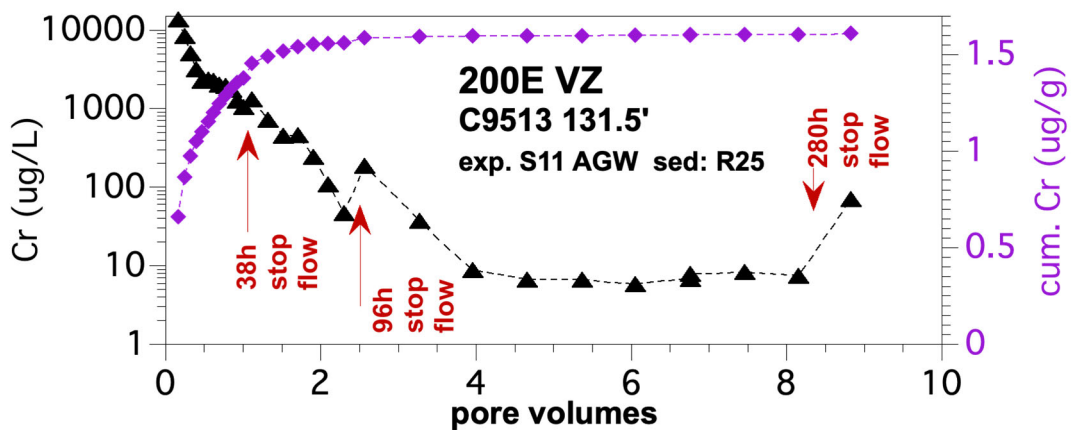


Figure A.9. Water-saturated Cr leach (S11) using artificial groundwater for sediment R25 (with log concentration scale).

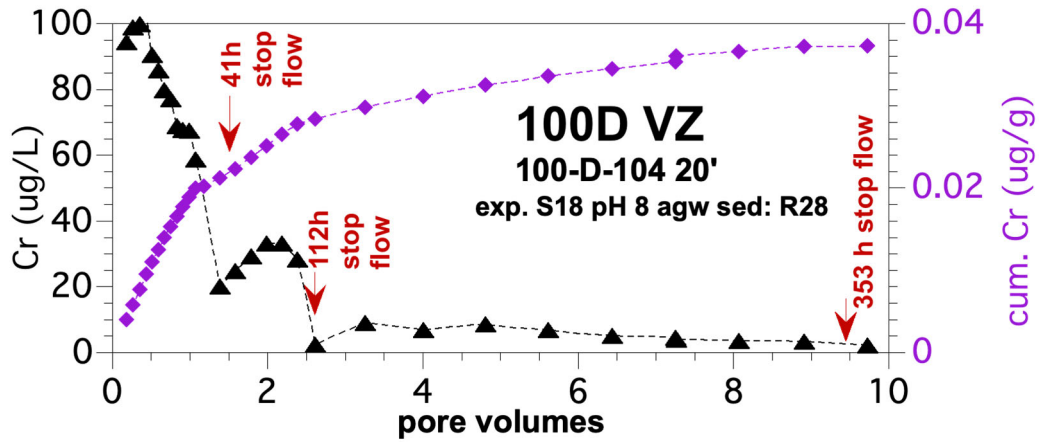


Figure A.10. Water-saturated Cr leach (S18) using artificial groundwater for sediment R28.

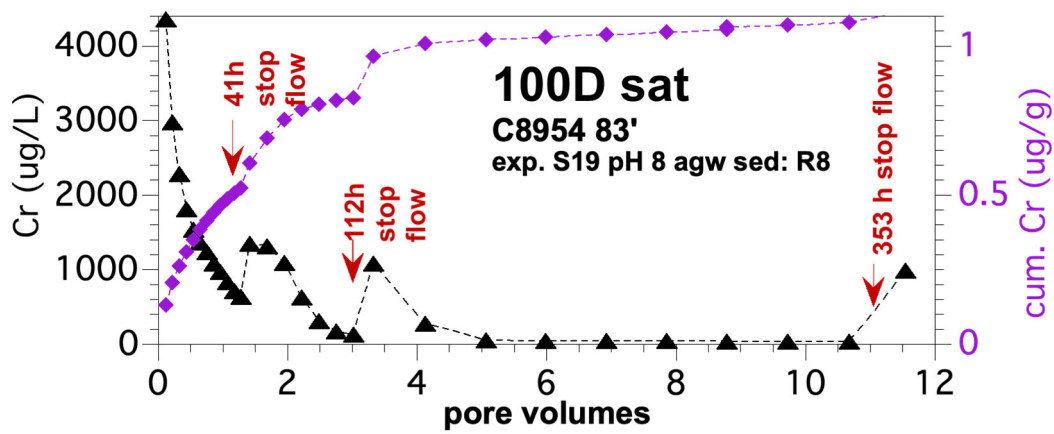


Figure A.11. Water-saturated Cr leach (S9) using artificial groundwater for sediment R8.

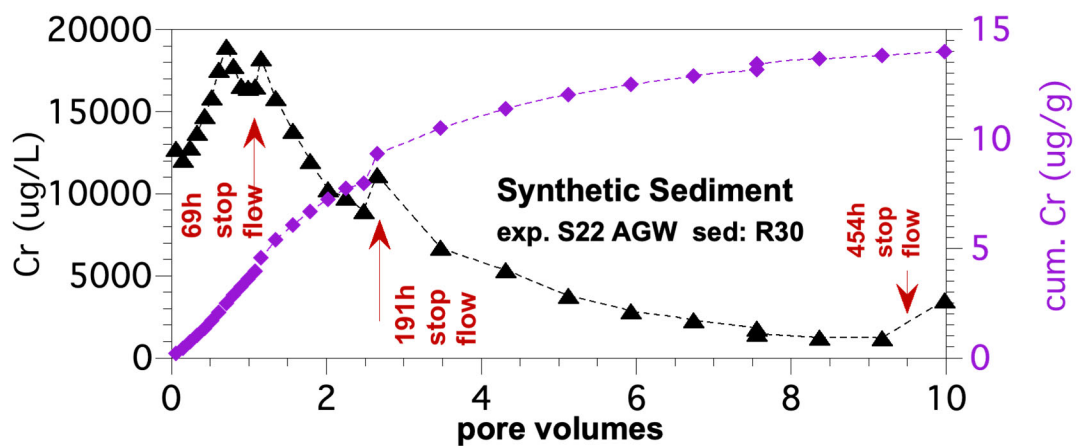


Figure A.12. Water-saturated Cr leach (S22) using artificial groundwater for sediment R30.

Appendix B – Cr Water-Saturated Leaching with Amendments

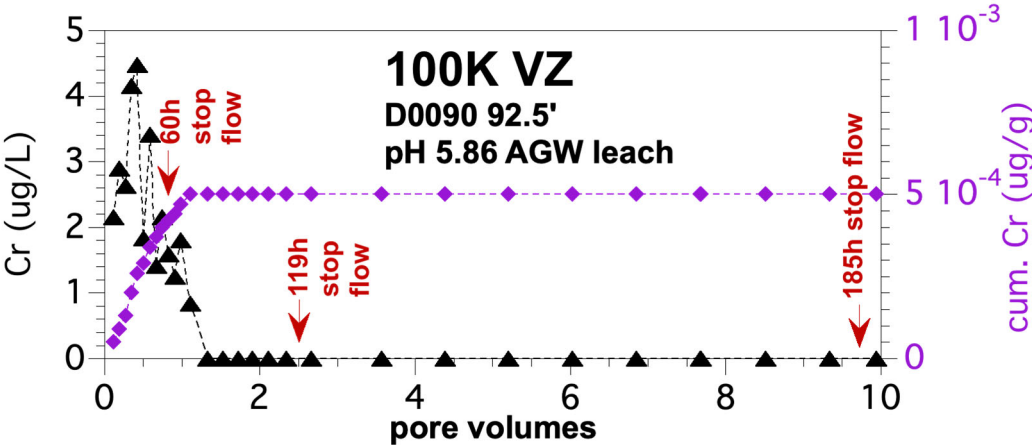


Figure B.1. Water-saturated Cr leach (S5) using pH 6 groundwater for sediment R17.

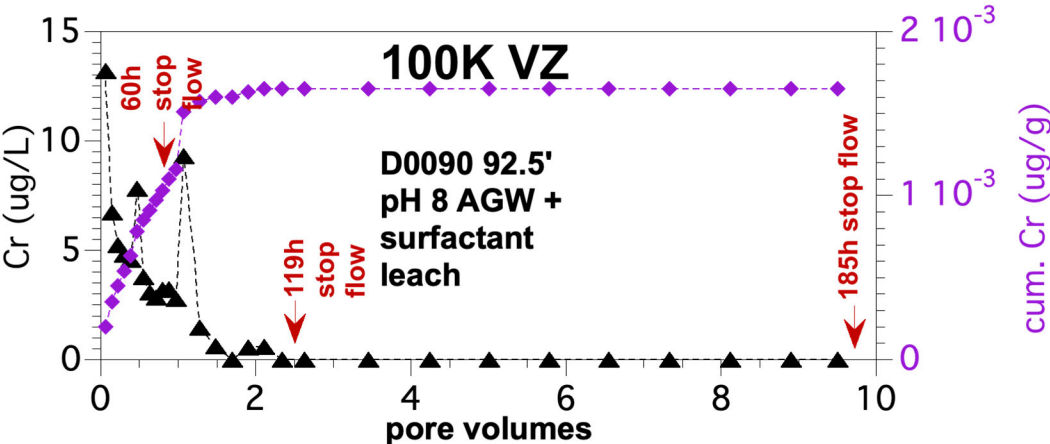


Figure B.2. Water-saturated Cr leach (S6) using a surfactant in groundwater for sediment R17.

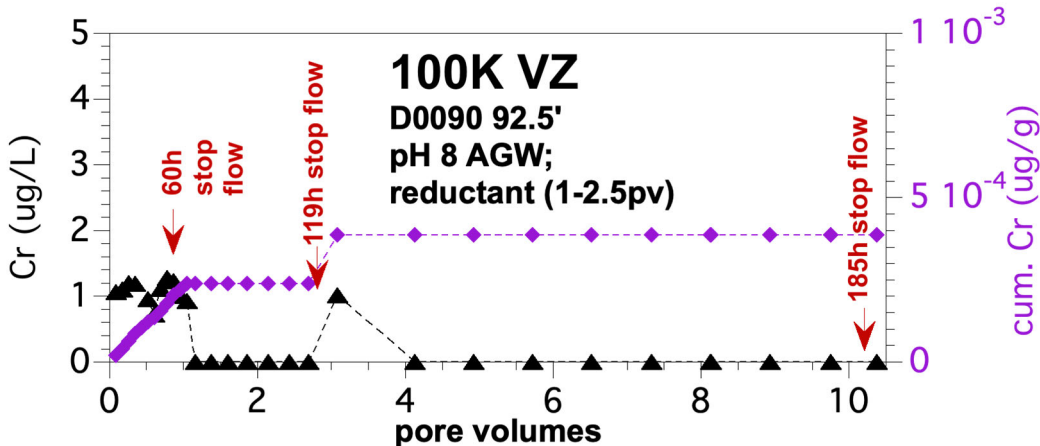


Figure B.3. Water-saturated Cr leach (S7) using a reductant for sediment R17.

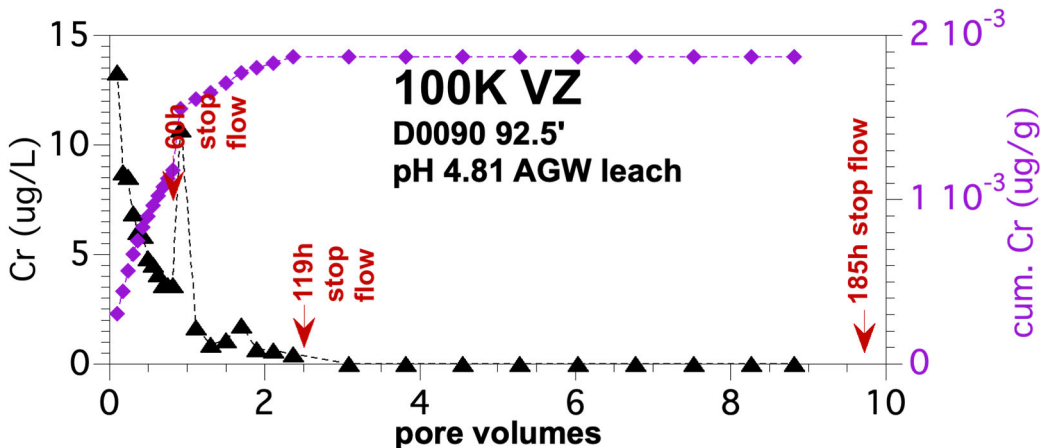


Figure B.4. Water-saturated Cr leach (S8) using pH 5 groundwater for sediment R17.

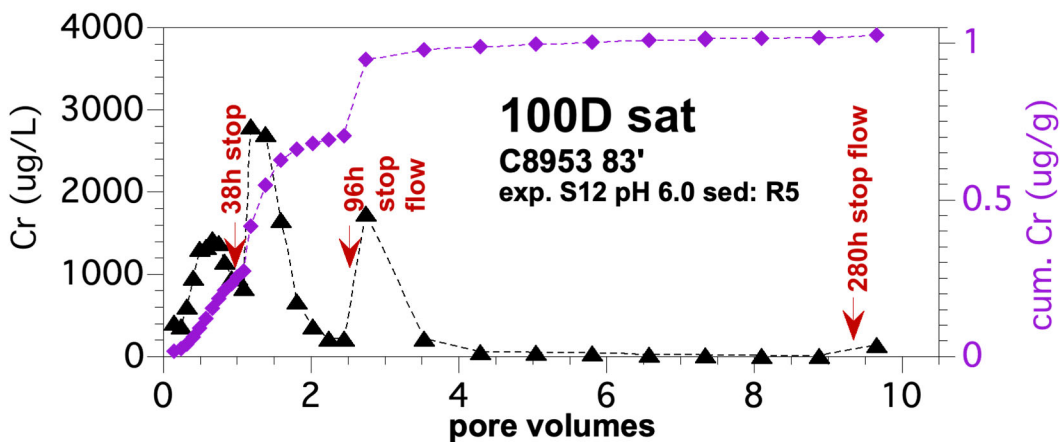


Figure B.5. Water-saturated Cr leach (S12) using pH 6 groundwater for sediment R5.

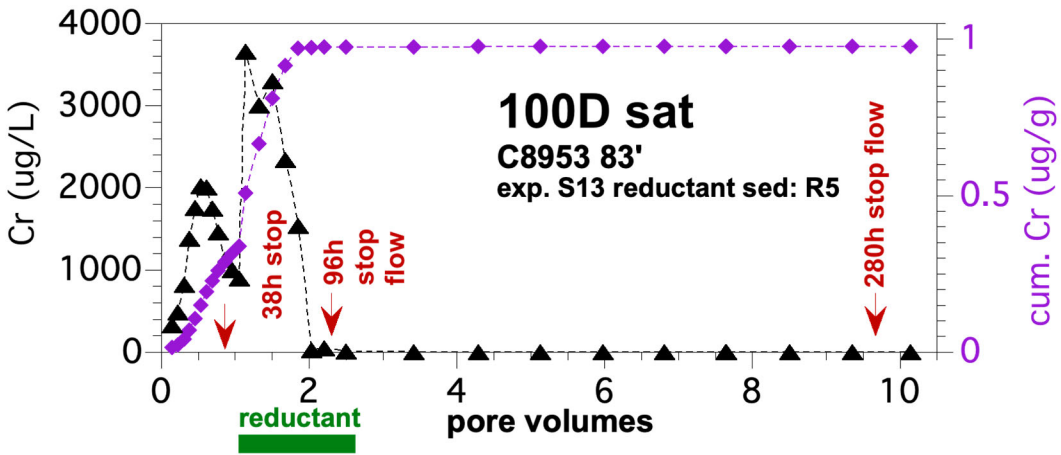


Figure B.6. Water-saturated Cr leach (S13) using a reductant for sediment R5.

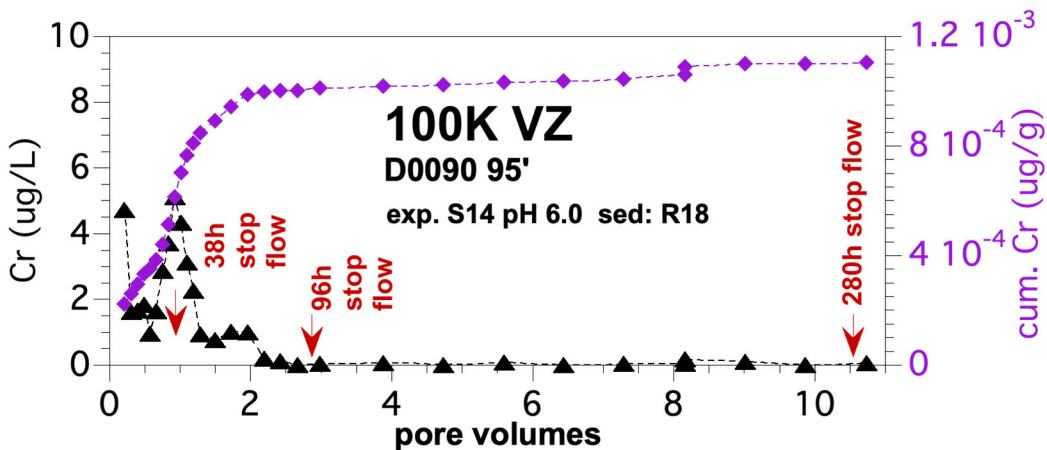


Figure B.7. Water-saturated Cr leach (S14) using pH 6 groundwater for sediment R18.

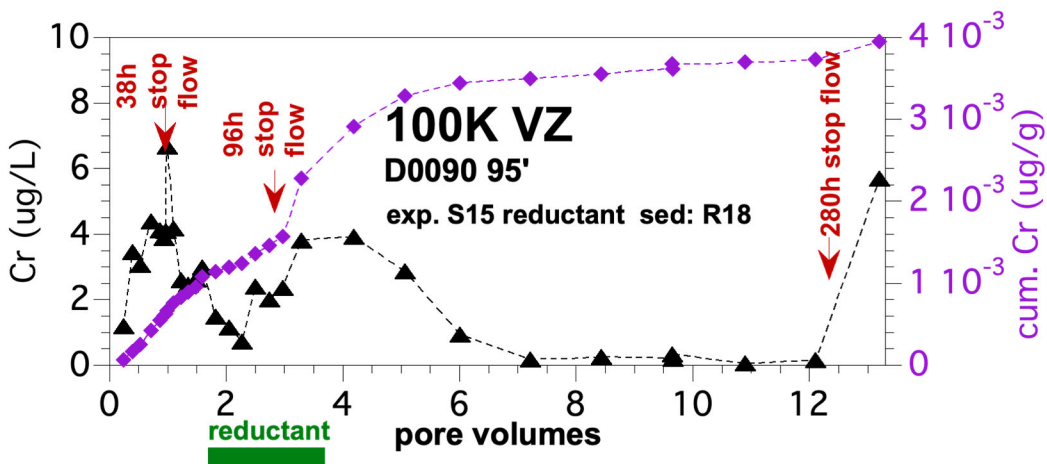


Figure B.8. Water-saturated Cr leach (S15) using a reductant for sediment R18.

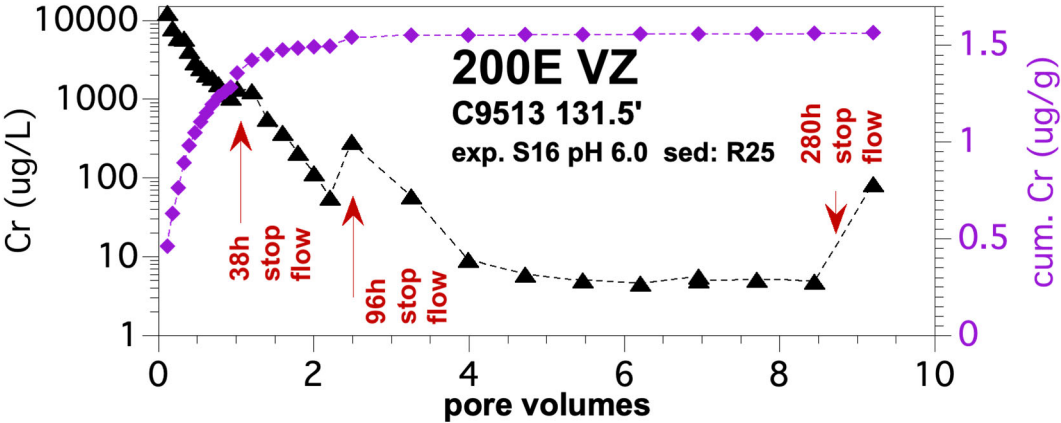


Figure B.9. Water-saturated Cr leach (S16) using a reductant for sediment R25.

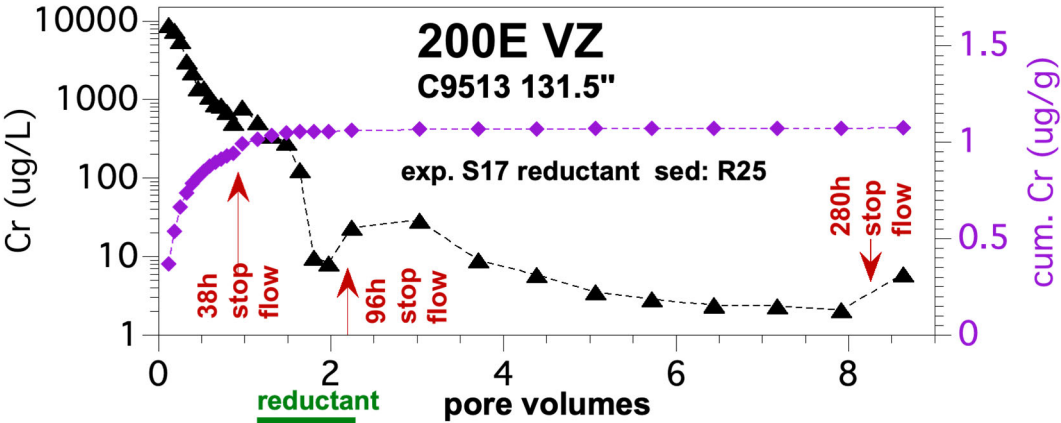


Figure B.10. Water-saturated Cr leach (S17) using a reductant for sediment R25.

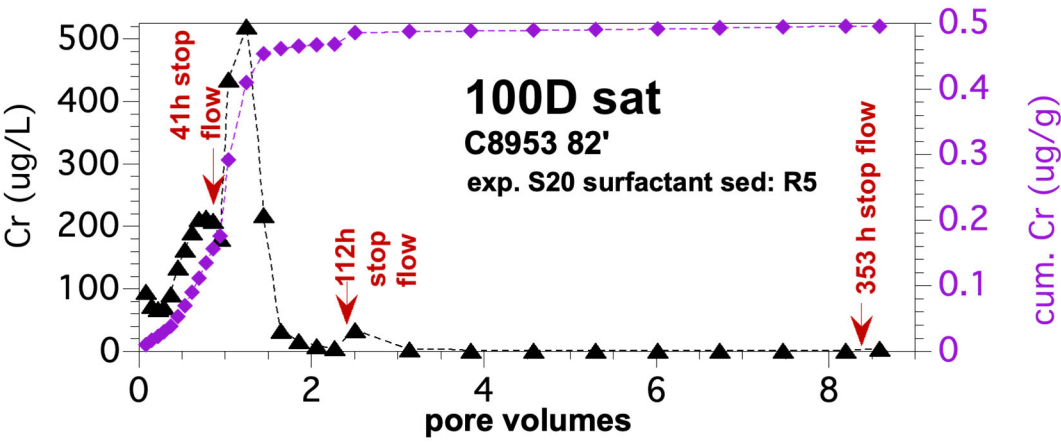


Figure B.11. Water-saturated Cr leach (S20) using a surfactant for sediment R5.

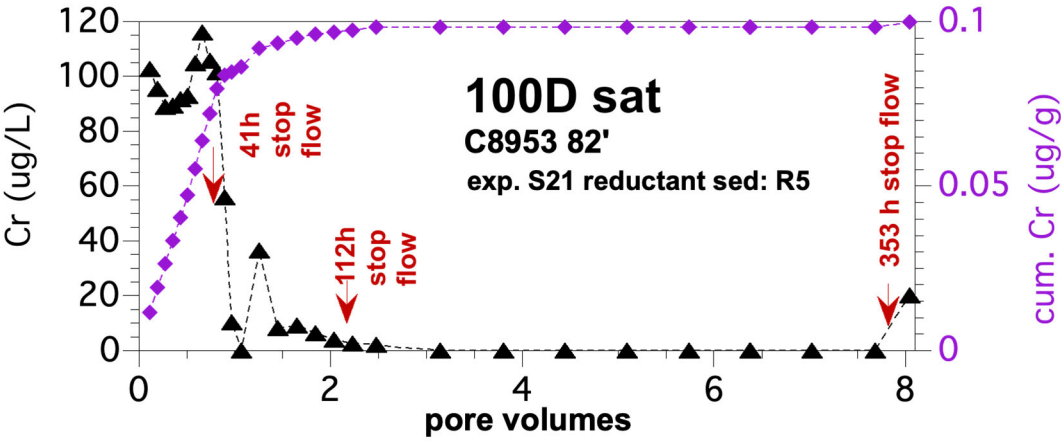


Figure B.12. Water-saturated Cr leach (S21) using a reductant for sediment R5.

Appendix C – Cr Sequential Extractions of Sediments: Pre- and Post-Leach

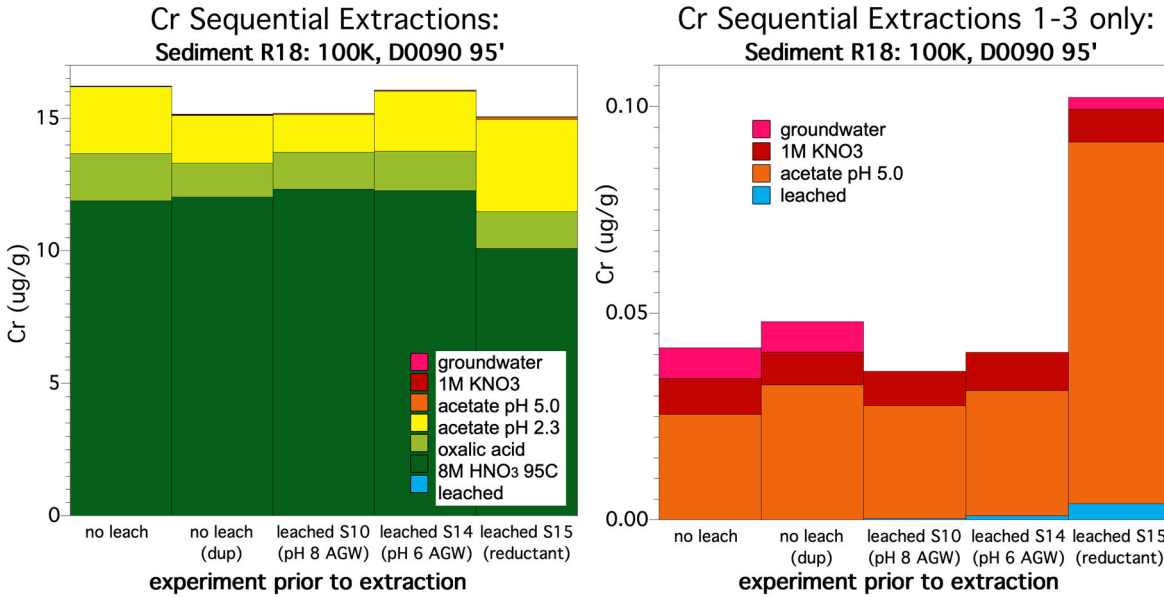


Figure C.1. Pre- and post-leach experiment sequential extractions for sediment R18.

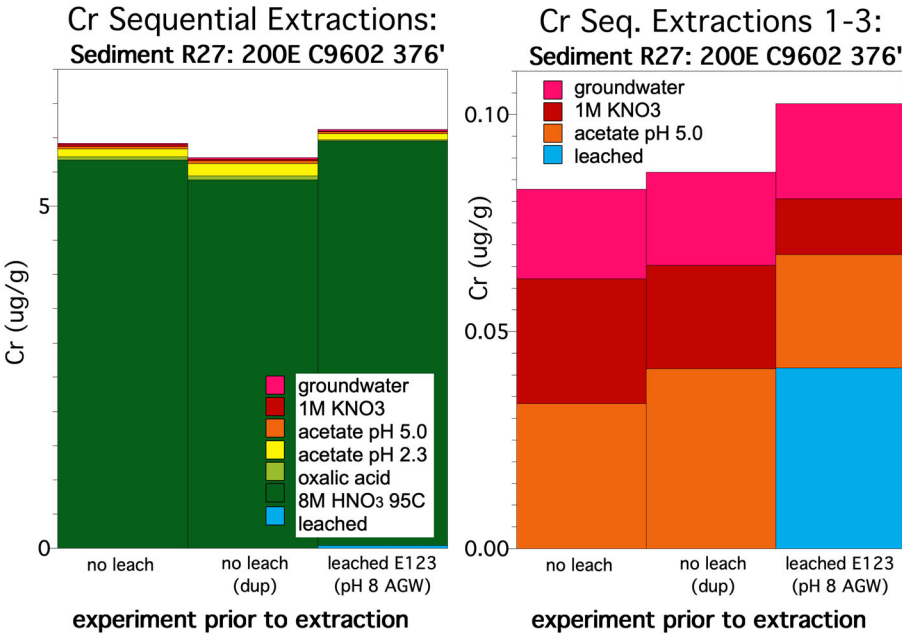


Figure C.2. Pre- and post-leach experiment sequential extractions for sediment R27.

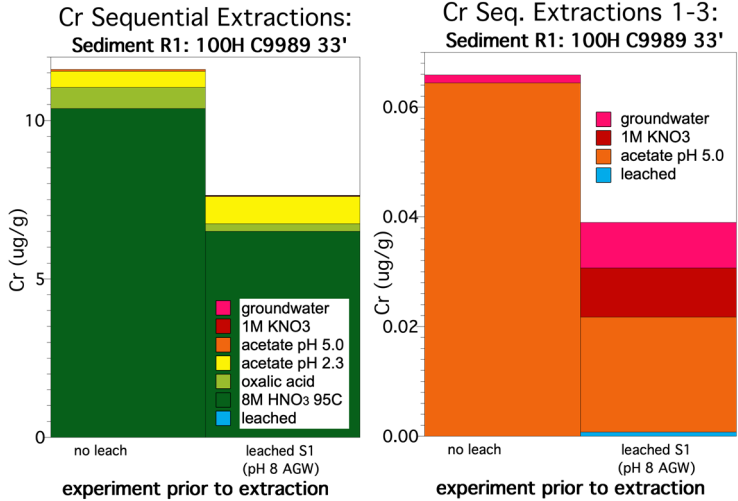


Figure C.3. Pre- and post-leach experiment sequential extractions for sediment R1.

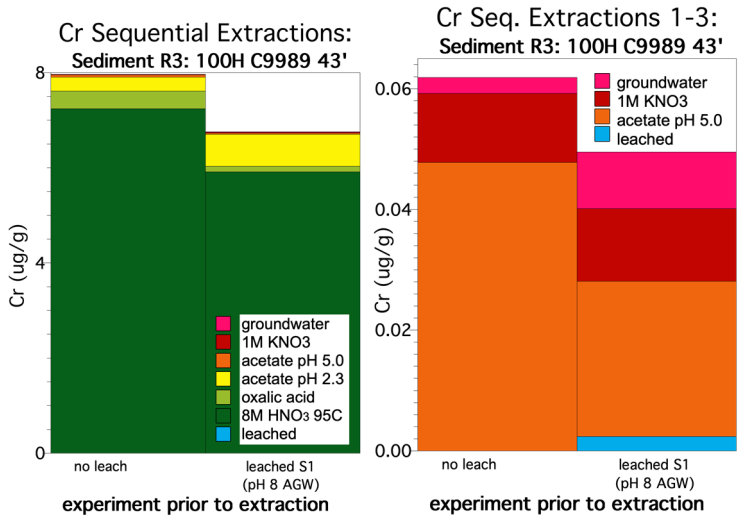


Figure C.4. Pre- and post-leach experiment sequential extractions for sediment R3.

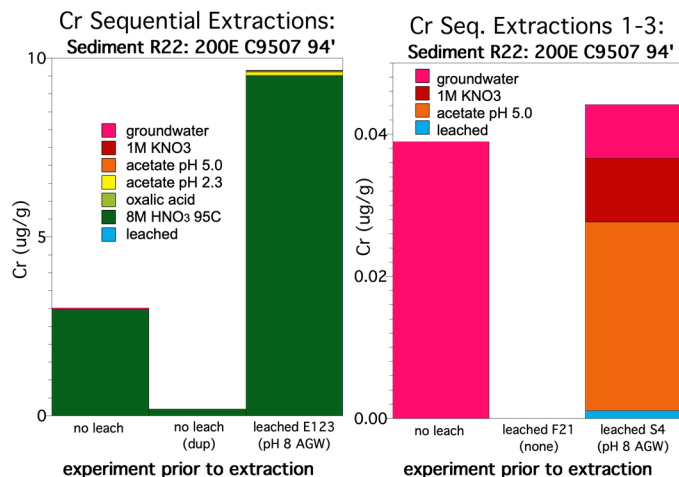


Figure C.5. Pre- and post-leach experiment sequential extractions for sediment R22.

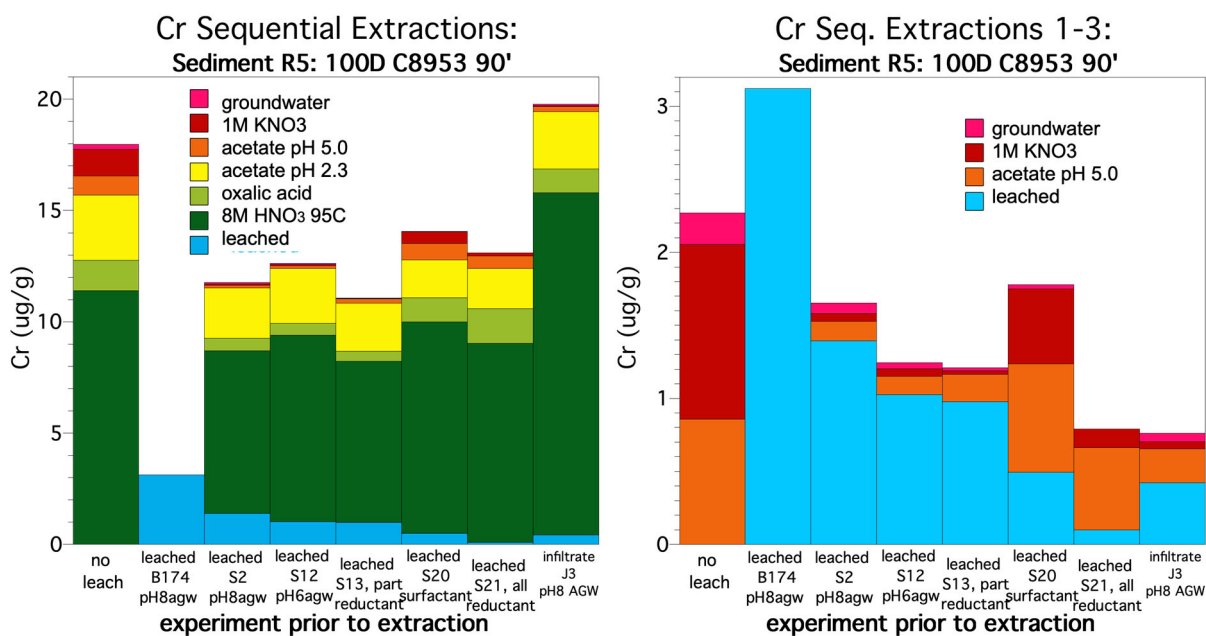


Figure C.6. Pre- and post-leach experiment sequential extractions for sediment R5.

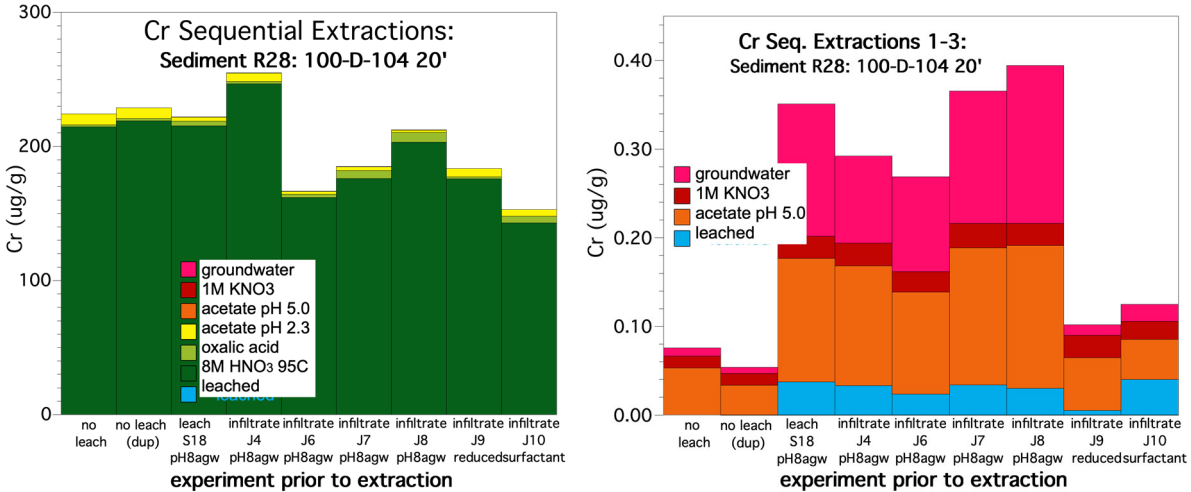


Figure C.7. Pre- and post-leach experiment sequential extractions for sediment R28.

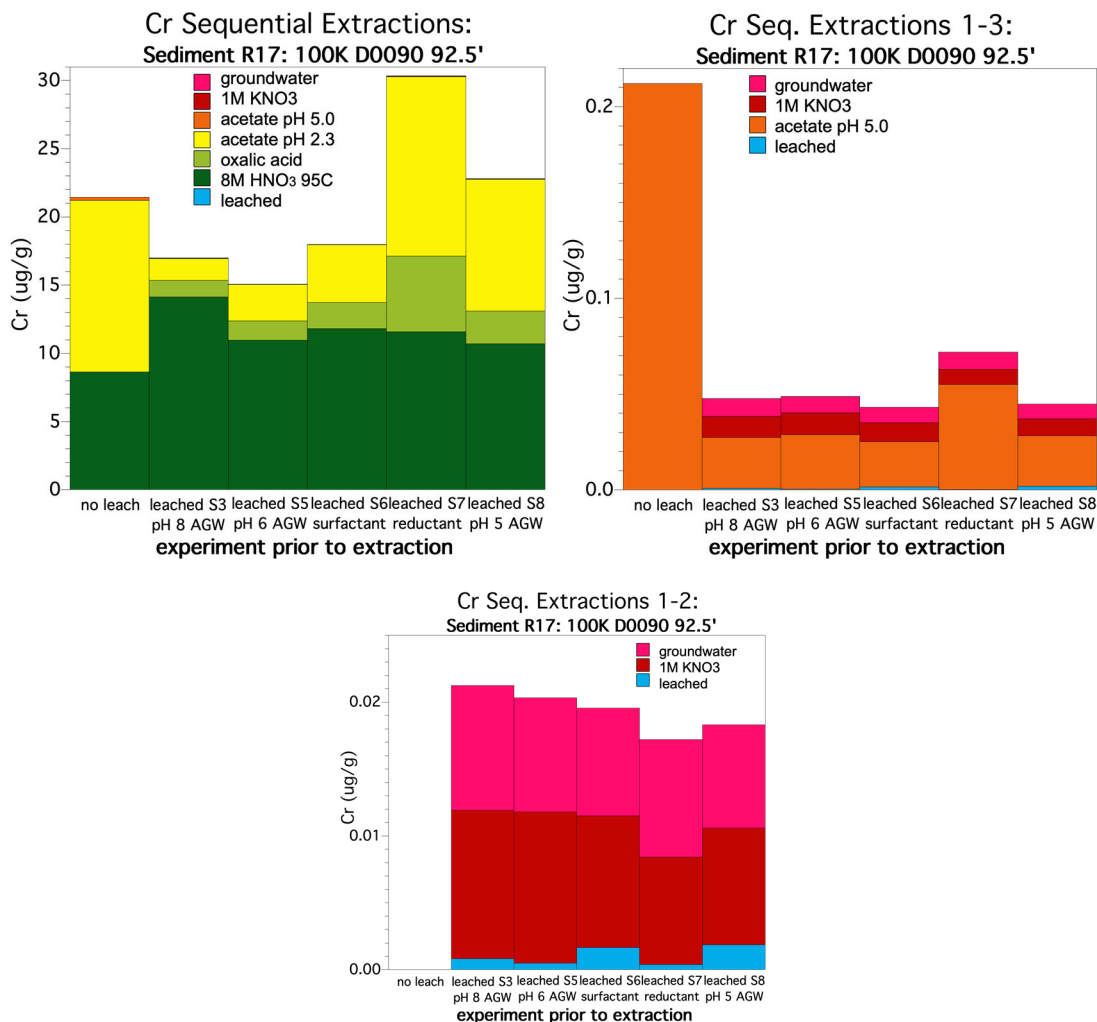


Figure C.8. Pre- and post-leach experiment sequential extractions for sediment R17.

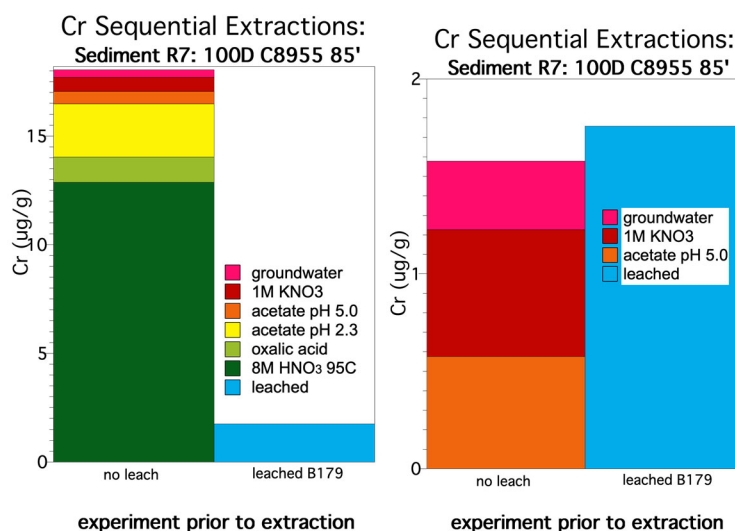


Figure C.9. Pre- and post-leach experiment sequential extractions for sediment R7.

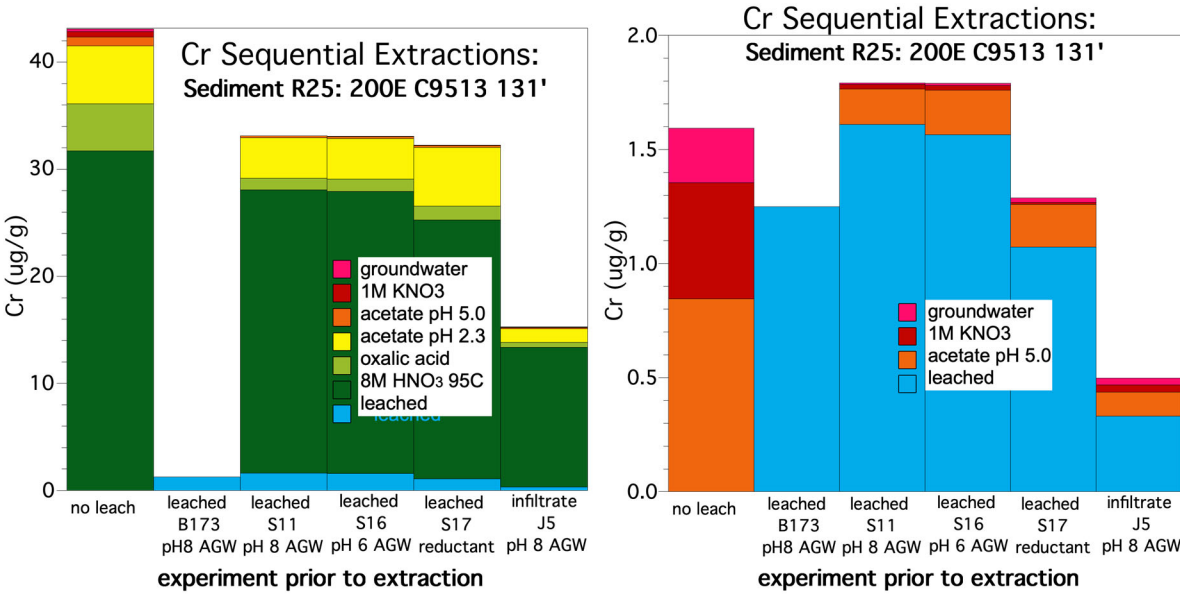


Figure C.10. Pre- and post-leach experiment sequential extractions for sediment R25.

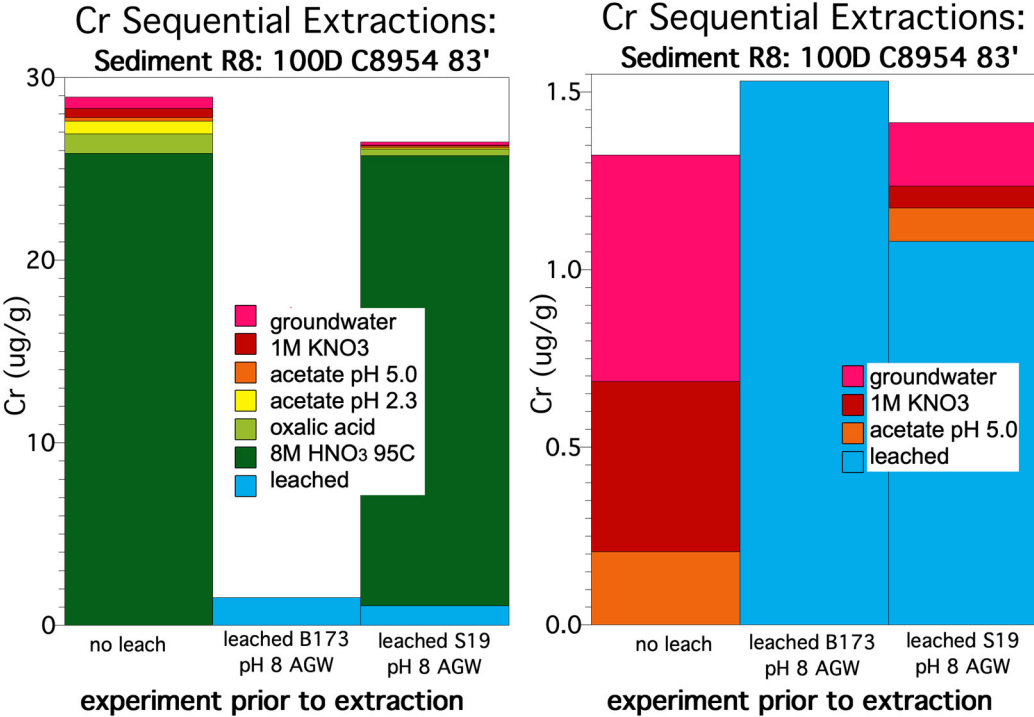


Figure C.11. Pre- and post-leach experiment sequential extractions for sediment R8.

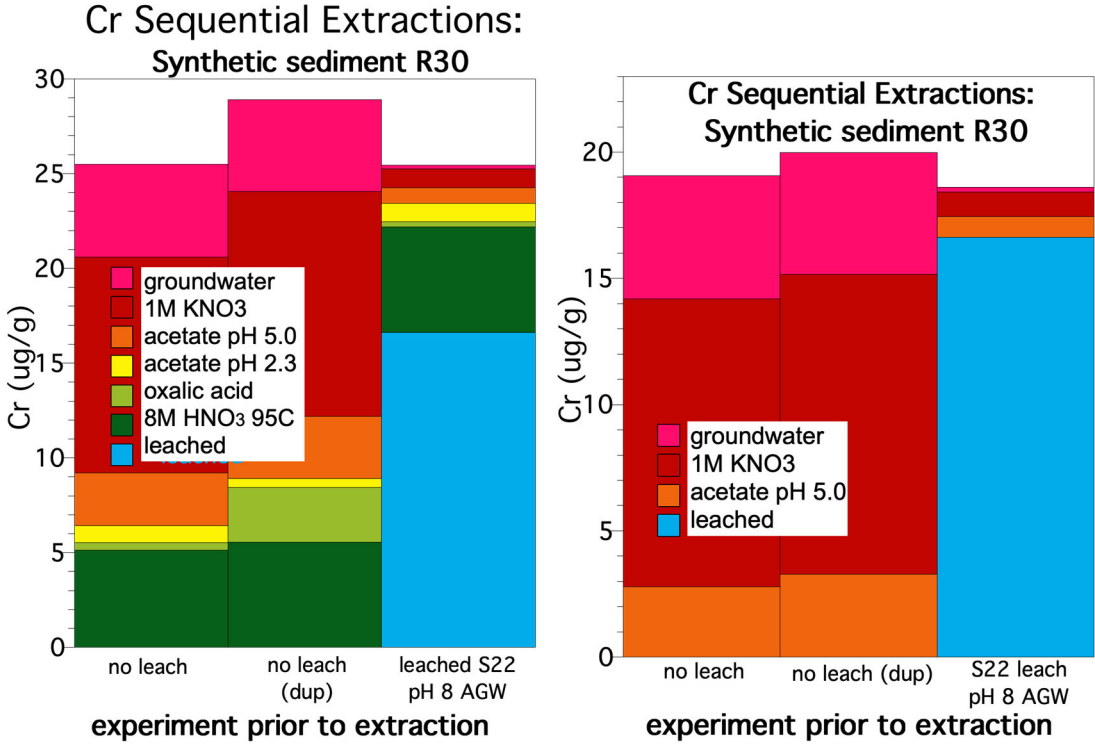


Figure C.12. Pre- and post-leach experiment sequential extractions for sediment R30.

Appendix D – Cr Unsaturated Leaching in Infiltration Experiments

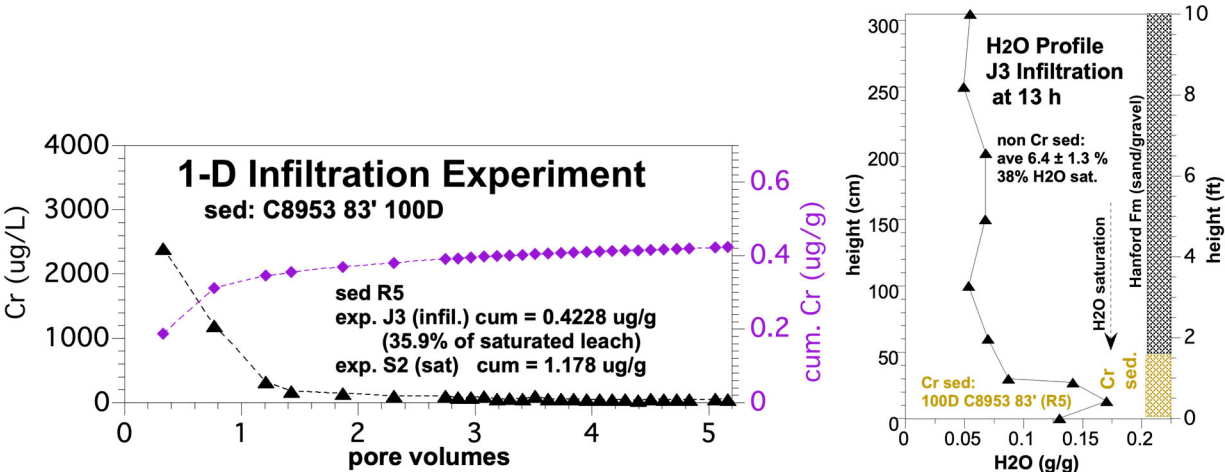


Figure D.1. 1-D infiltration experiment J3 with artificial groundwater for sediment R5 with Cr concentrations (left) and moisture profile at experiment end (right).

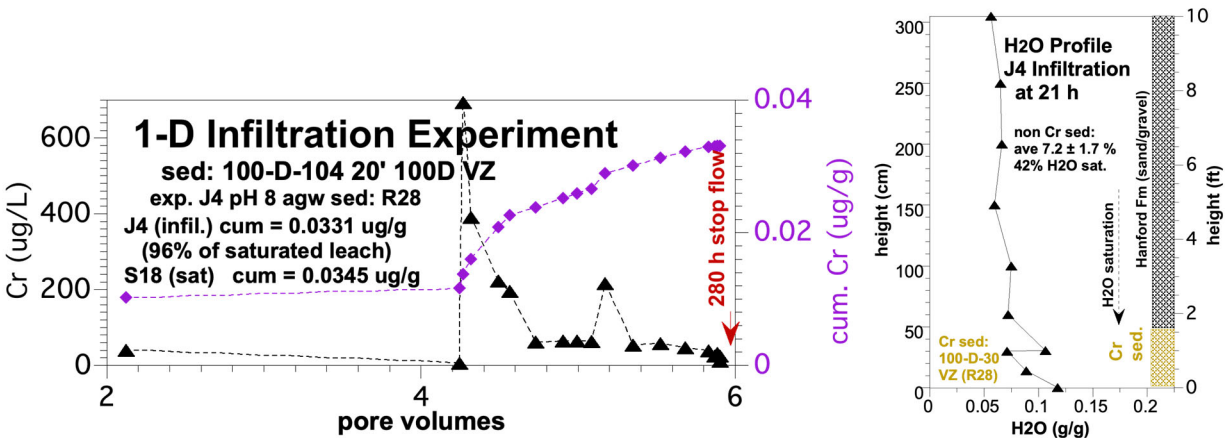


Figure D.2. 1-D infiltration experiment J4 with artificial groundwater for sediment R28 with Cr concentrations (left) and moisture profile at experiment end (right).

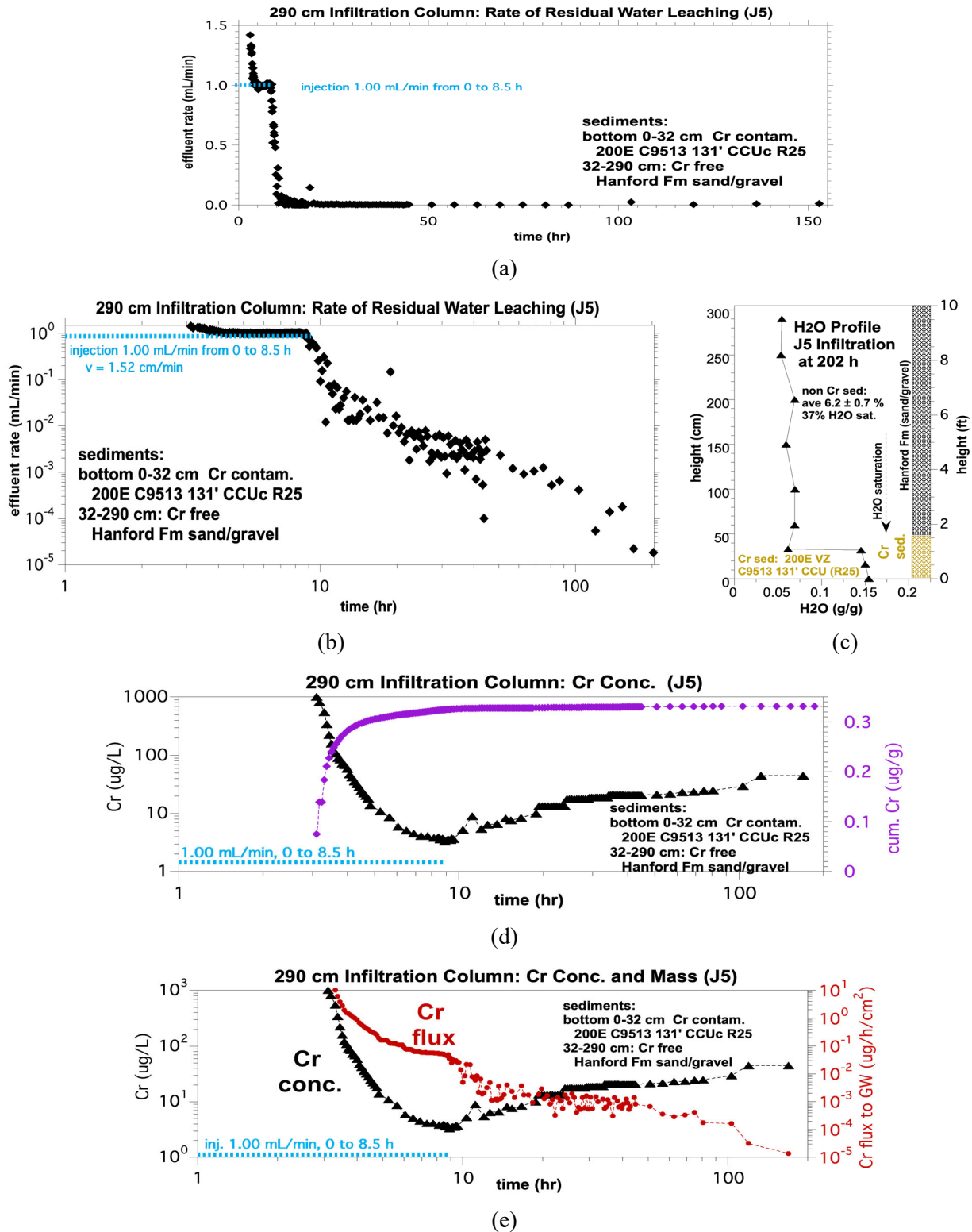


Figure D.3. 1-D infiltration experiment J5 with artificial groundwater for sediment R25 showing (a) water effluent rate, (b) water effluent rate on log scale, (c) moisture profile at experiment end, (d) Cr concentration, and (e) Cr concentration and flux.

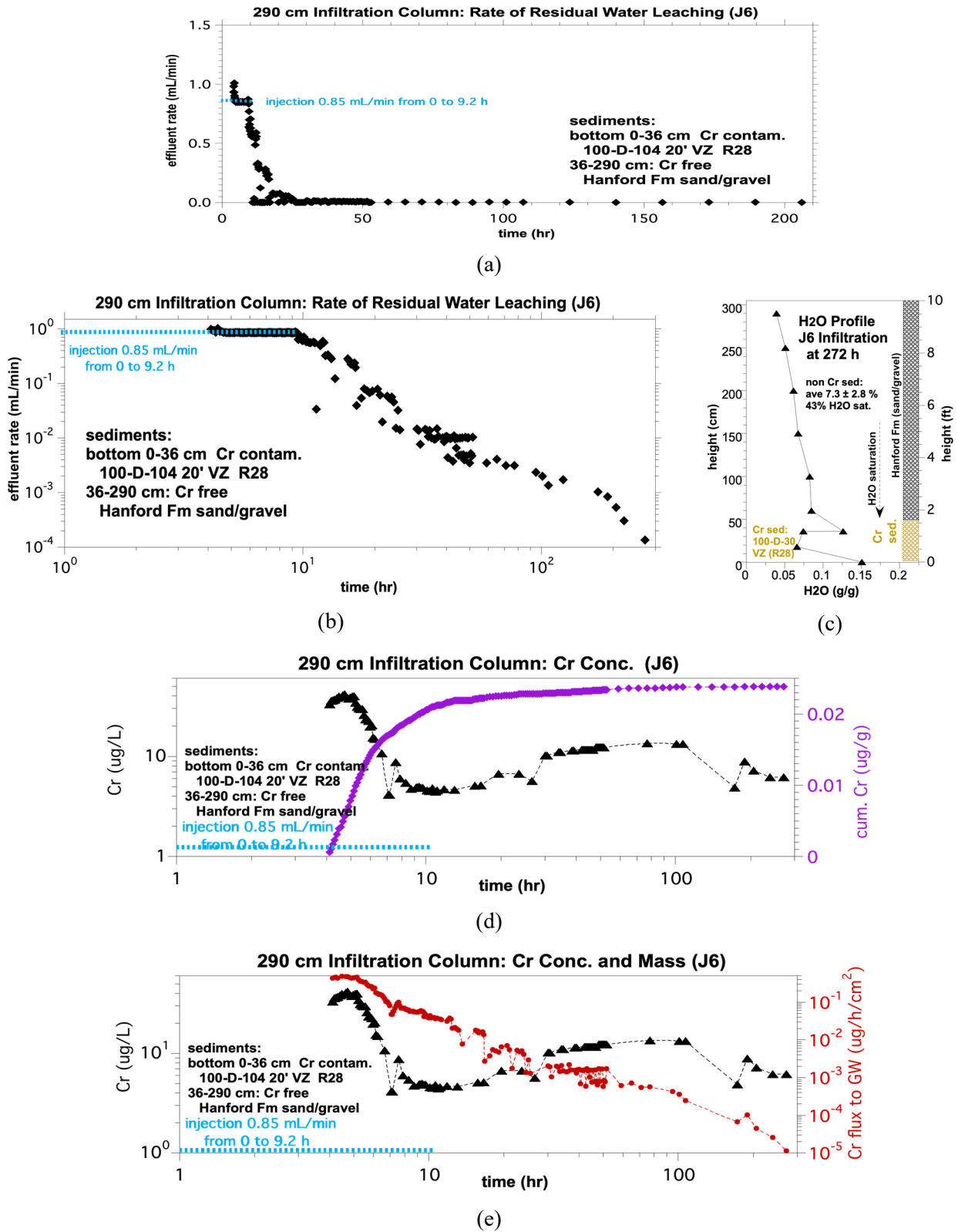


Figure D.4. 1-D infiltration experiment J6 with artificial groundwater for sediment R28 showing (a) water effluent rate, (b) water effluent rate on log scale, (c) moisture profile at experiment end, (d) Cr concentration, and (e) Cr concentration and flux.

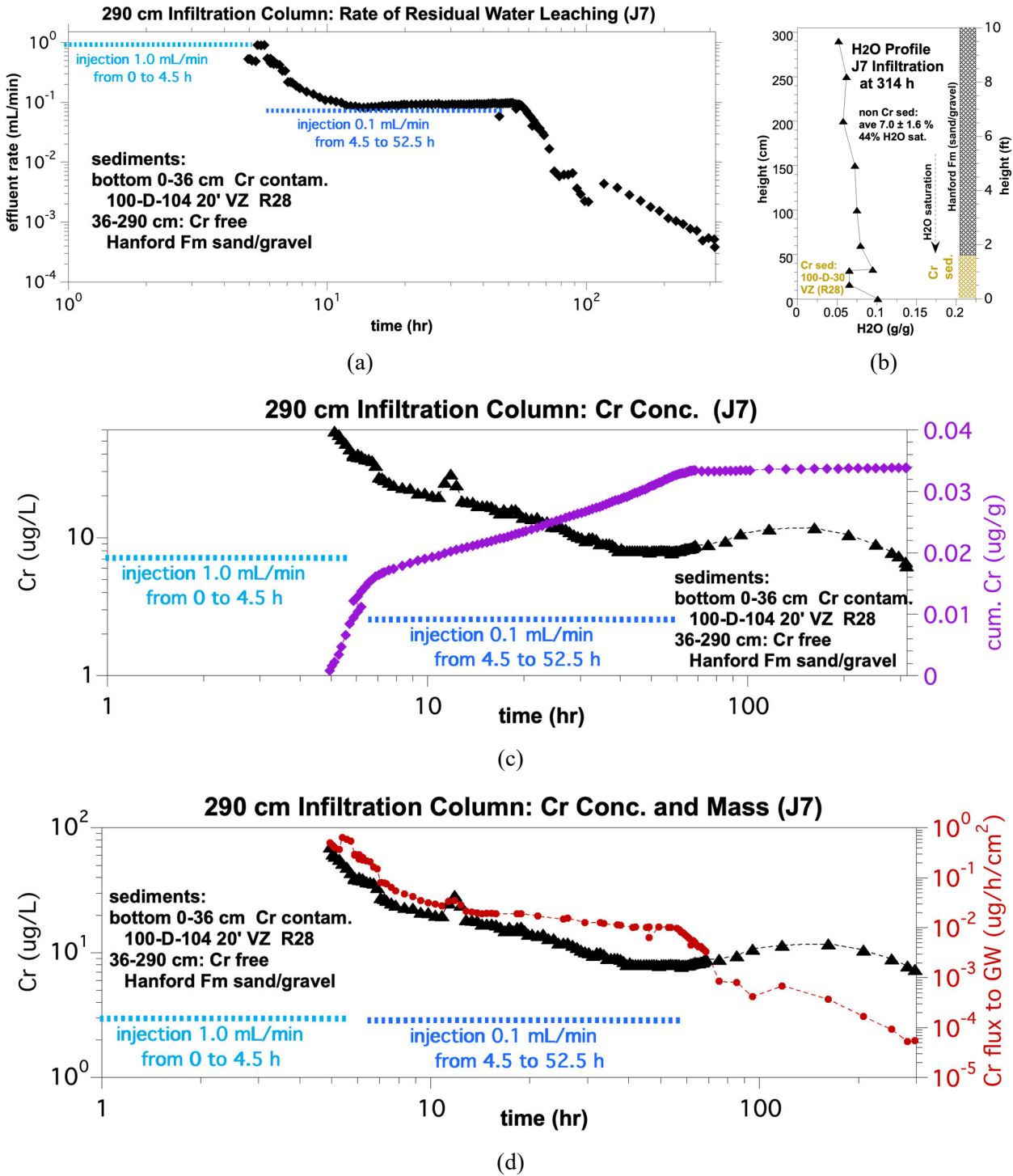


Figure D.5. 1-D infiltration experiment J7 with artificial groundwater for sediment R28 showing (a) water effluent rate, (b) moisture profile at experiment end, (c) Cr concentration, and (d) Cr concentration and flux.

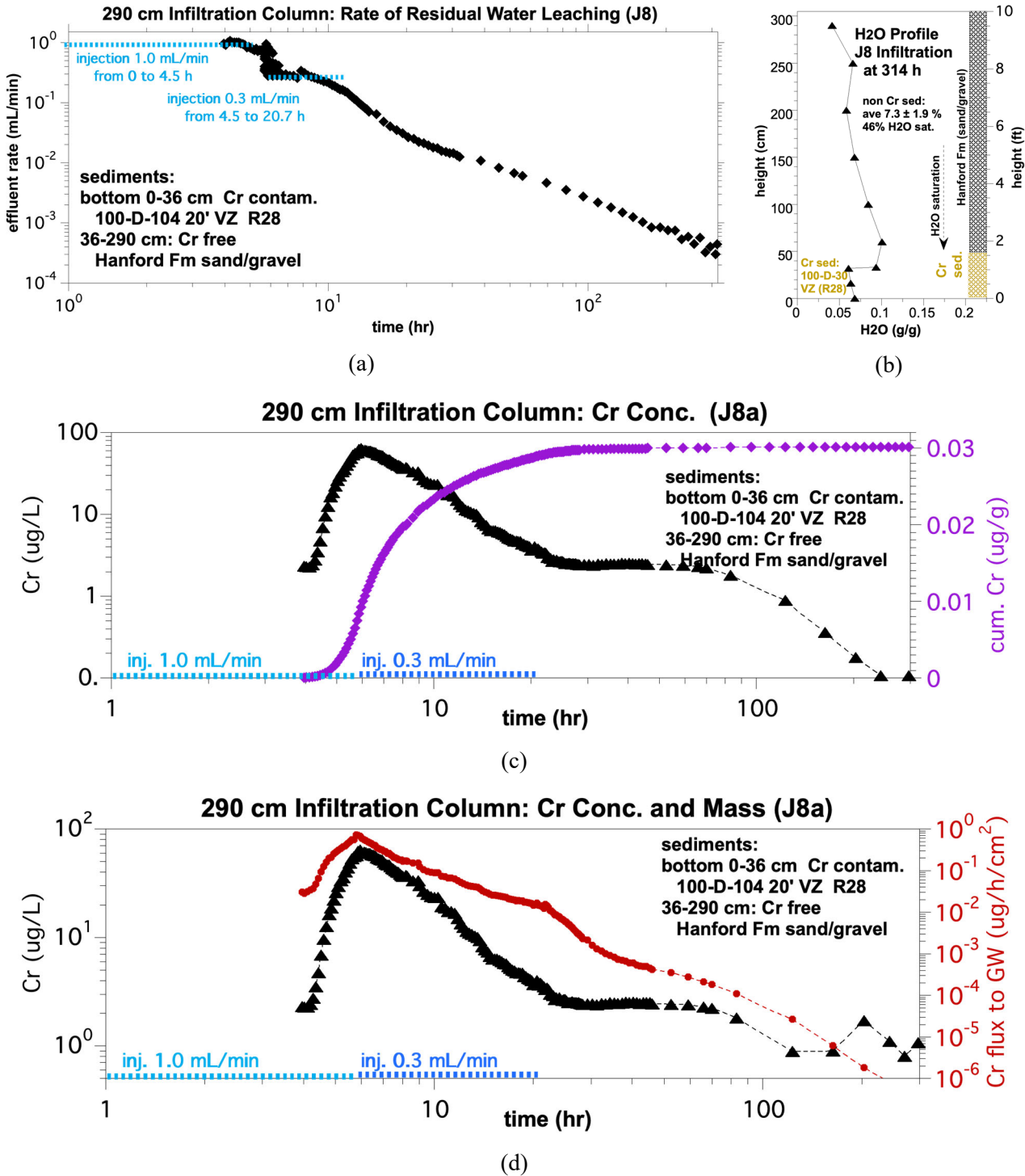


Figure D.6. 1-D infiltration experiment J8 with artificial groundwater for sediment R28 showing (a) water effluent rate, (b) moisture profile at experiment end, (c) Cr concentration, and (d) Cr concentration and flux.

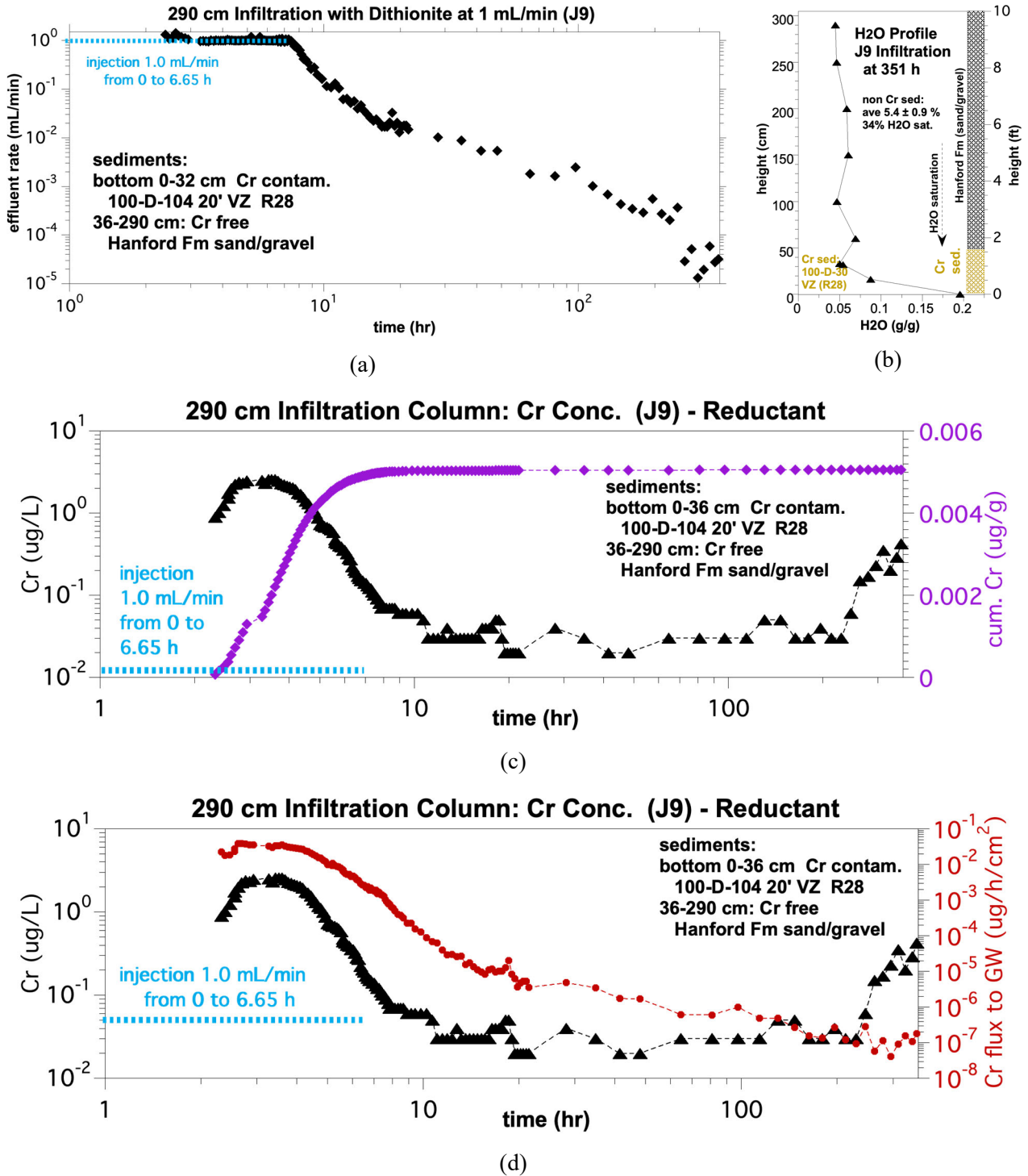


Figure D.7. 1-D infiltration experiment J9 with reductant injection for sediment R28 showing (a) water effluent rate, (b) moisture profile at experiment end, (c) Cr concentration, and (d) Cr concentration and flux.

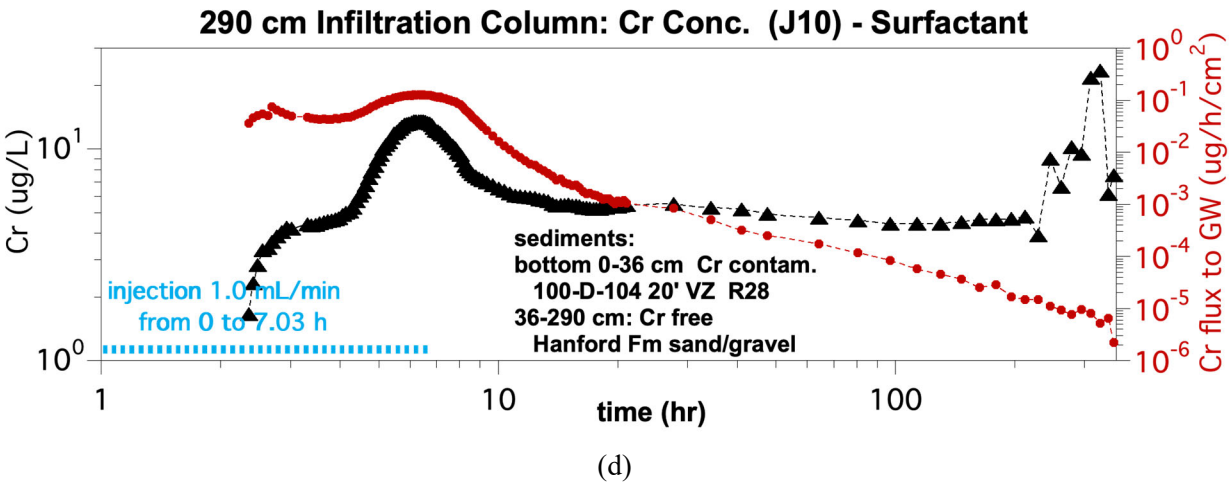
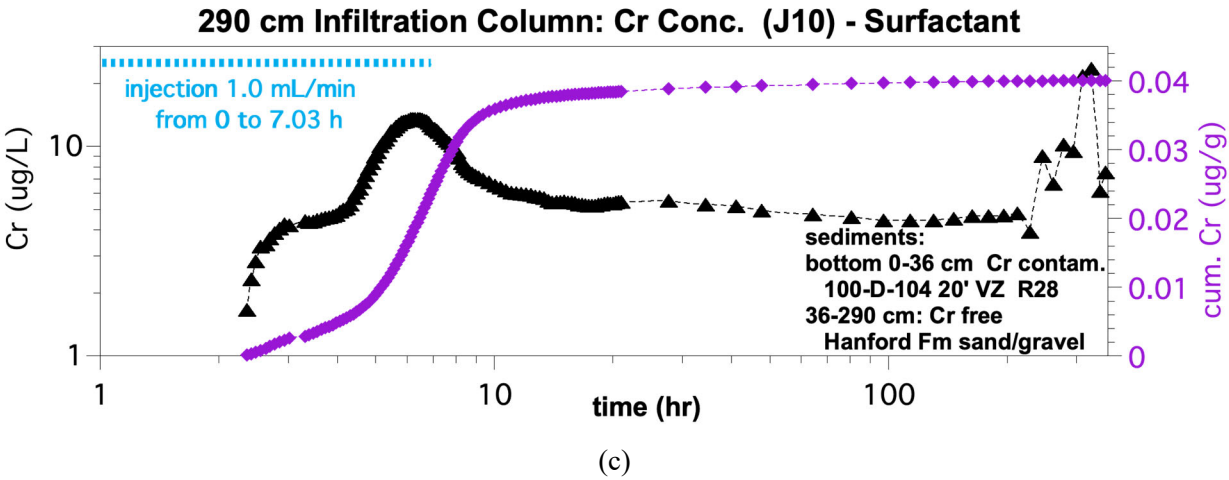


Figure D.8. 1-D infiltration experiment J9 with surfactant injection for sediment R28 showing (a) water effluent rate, (b) moisture profile at experiment end, (c) Cr concentration, and (d) Cr concentration and flux.

Appendix E – 2-D Infiltration Experiments

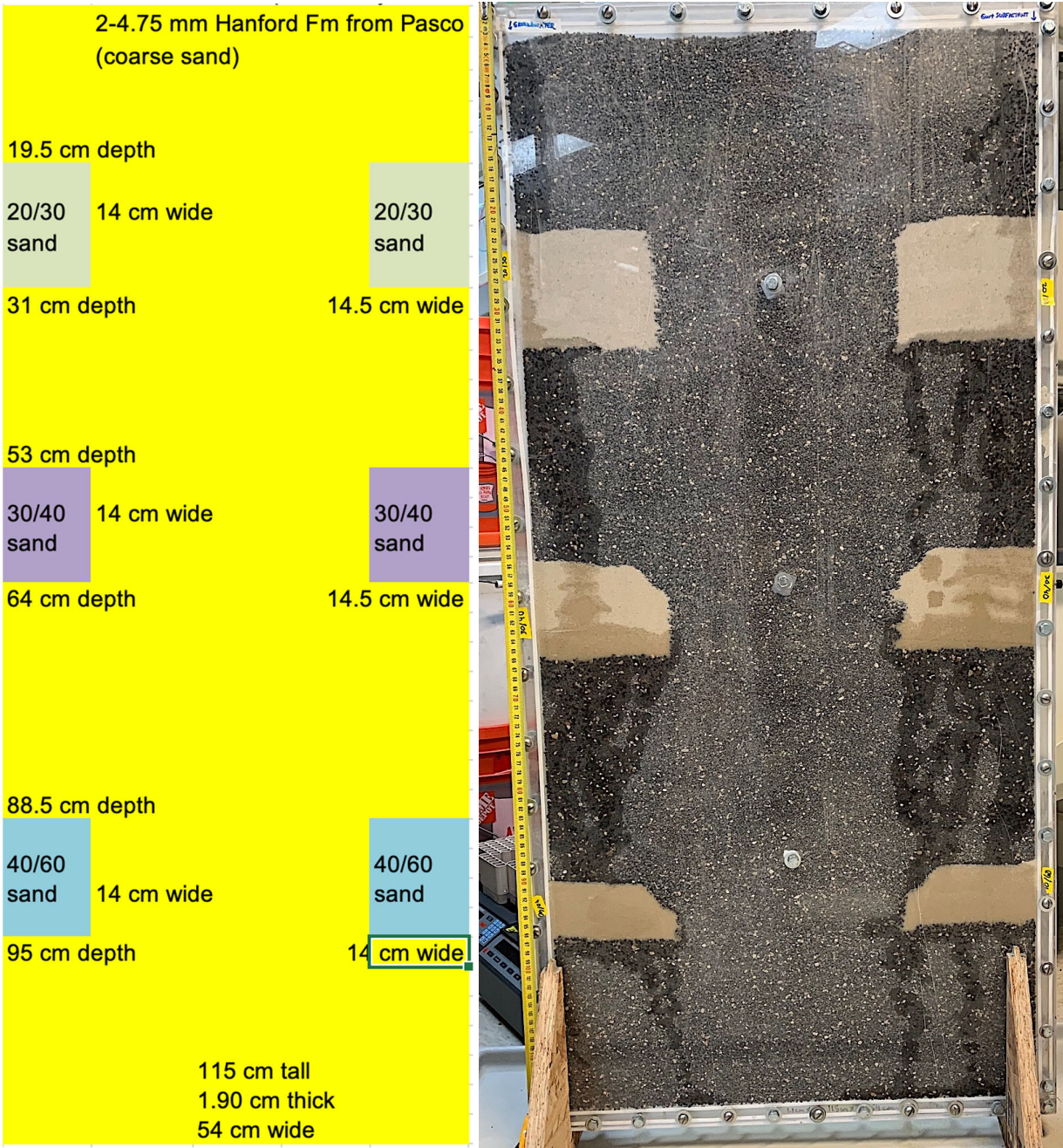


Figure E.1. 2-D infiltration experiment K1 with infiltration of artificial groundwater (left) and artificial groundwater with 400 mg/L surfactant (right) with fine sand low-K zones.



Figure E.2. 2-D infiltration experiment K2 with infiltration of artificial groundwater (left) and artificial groundwater with 400 mg/L surfactant (right) with fine sand low-K zones.

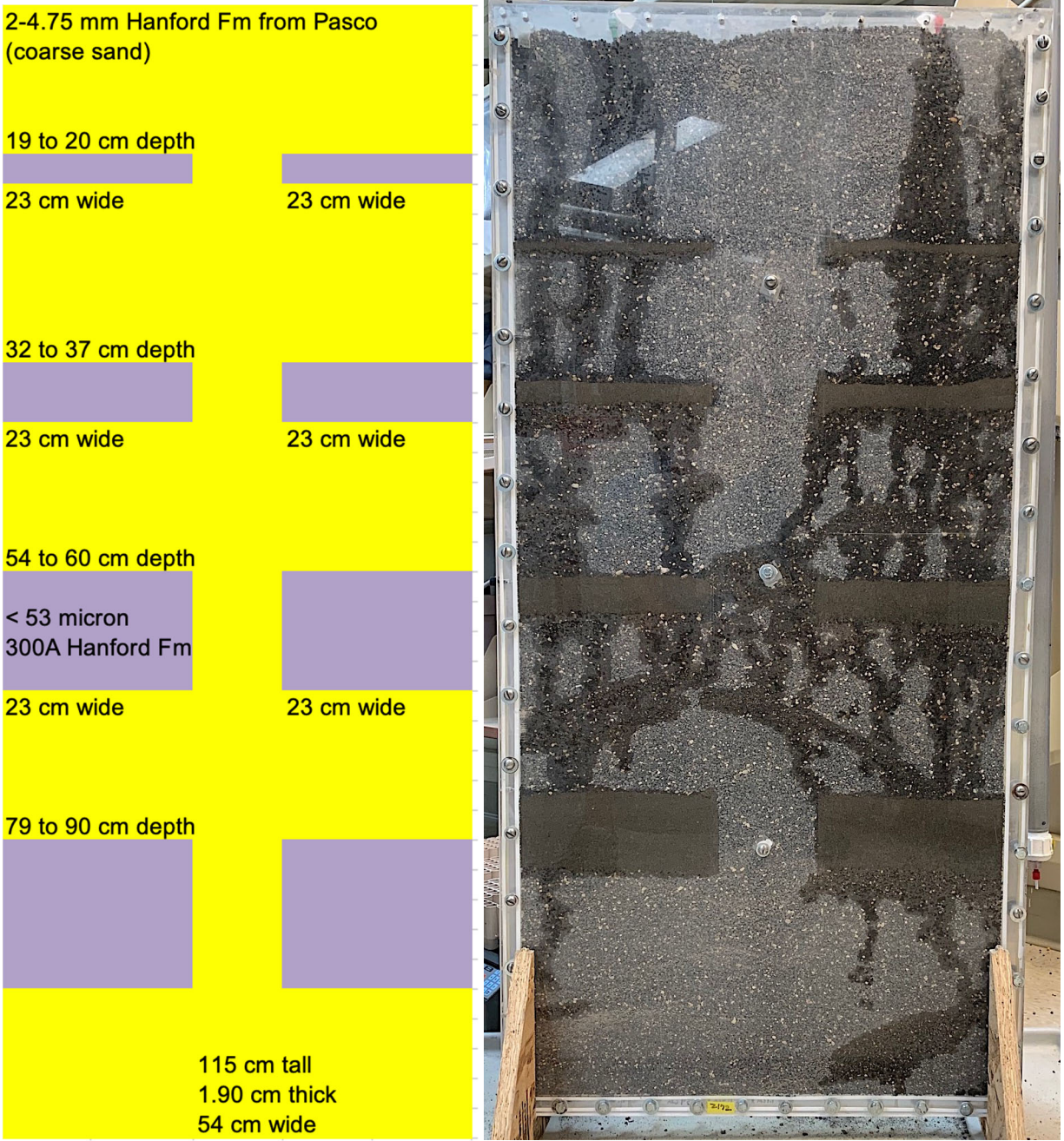


Figure E.3. 2-D infiltration experiment K3 with infiltration of artificial groundwater (left) and artificial groundwater with 400 mg/L surfactant (right) with silt low-K zones.

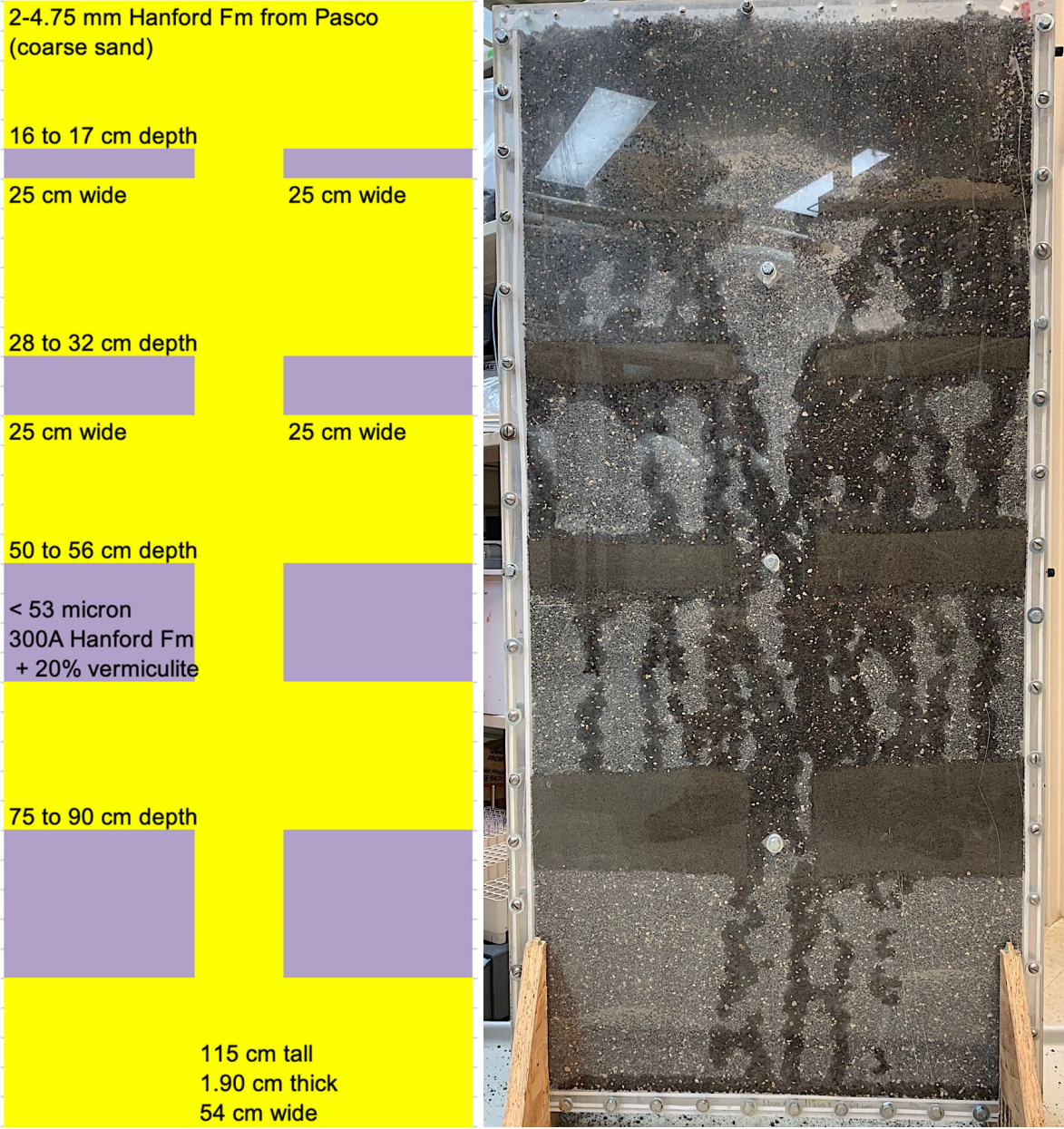


Figure E.4. 2-D infiltration experiment K4 with infiltration of artificial groundwater (left) and artificial groundwater with 400 mg/L surfactant (right) with silt/clay low-K zones.



Figure E.5. Early time image of 2-D infiltration experiment K4 illustrating groundwater is flowing around the low-K zone (upper left) whereas the surfactant solution is flowing through the low-K zone (upper right).

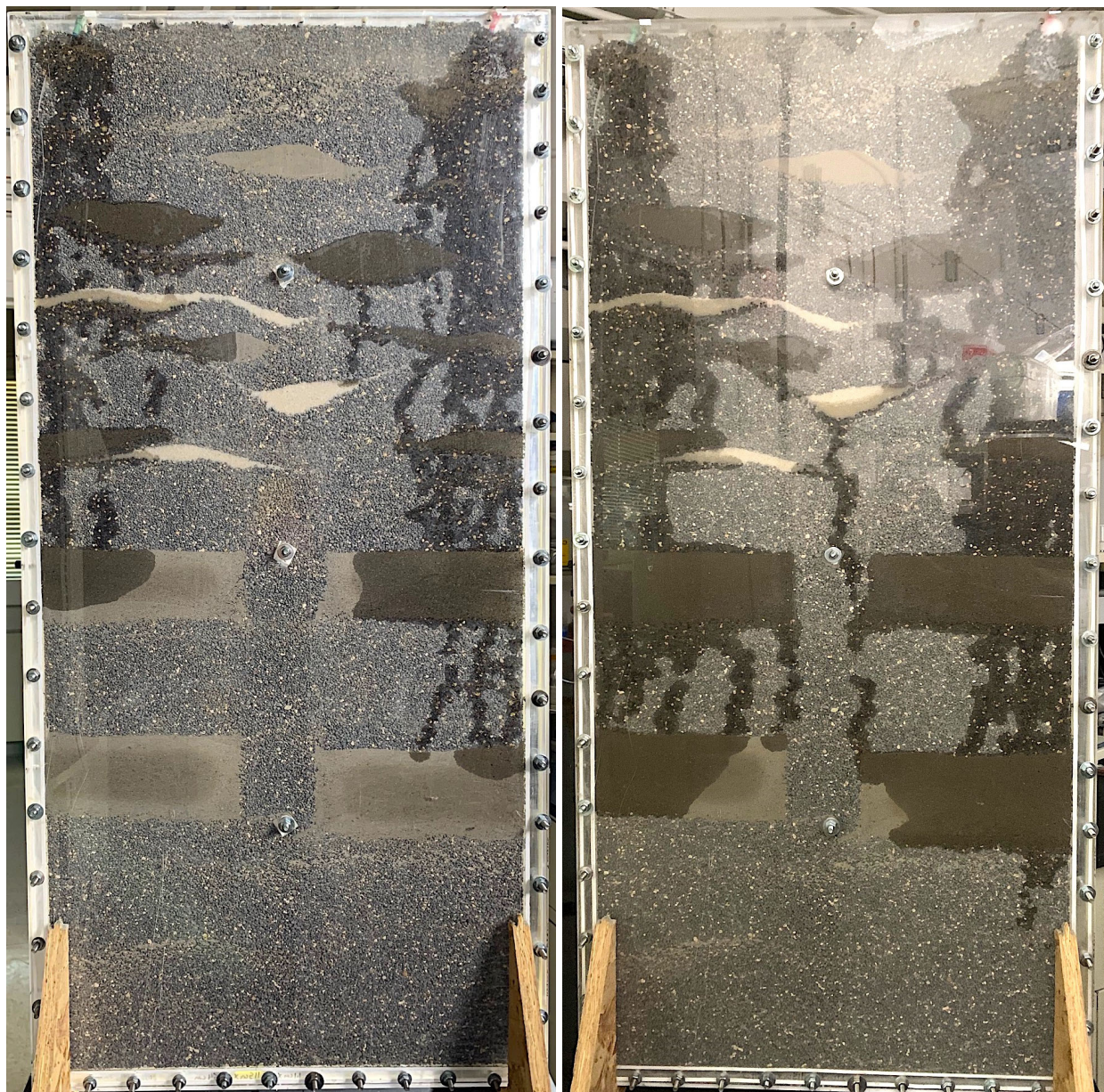


Figure E.6. 2-D infiltration experiment K5 with infiltration of artificial groundwater (left) and artificial groundwater with 400 mg/L surfactant (right) with silt/clay low-K zones. Note the more rapid flux of the surfactant solution through low-K zones.

Pacific Northwest National Laboratory

902 Battelle Boulevard
P.O. Box 999
Richland, WA 99354
1-888-375-PNNL (7665)

www.pnnl.gov